CONTRACT RESEARCH

GHD RESEARCH PROJECT NO. 7002

FINAL REPORT

REPEATED LOAD TEST EVALUATION OF BASE COURSE MATERIALS

DEPARTMENT OF TRANSPORTATION OF GEORGIA

SCHOOL OF CIVIL ENGINEERING
GEORGIA INSTITUTE OF TECHNOLOGY

1972

Contract Research

GHD Research Project No. 7002

Final Report

REPEATED LOAD TEST EVALUATION OF BASE COURSE MATERIALS

By

Richard D. Barksdale
Associate Professor
School of Civil Engineering
Georgia Institute of Technology

Contract with

Department of Transportation
State of Georgia

In cooperation with

U.S. Department of Transportation
Federal Highway Administration

May 1972

ACKNOWLEDGEMENT

The author would like to express his sincere appreciation to the Division of Materials and Tests, Highway Division, Georgia Department of Transportation, for their fine cooperation which helped to make possible the success of this research project. Although many individuals could be cited, specific acknolwedgement will only be given to Mr. T. D. Moreland and Mr. W. T. Stapler for their guidance in conducting this project and to Mr. Walt Doster for his assistance in obtaining the base course materials and for performing the routine tests on these materials. Acknowledgement is also given to Vulcan Materials Company for their aid in obtaining the materials used for the AASHO subbase and to Clemson University for supplying the AASHO base materials.

The author would like to express his sincere appreciation to Research Assistants C. M. Jackson, and W. Barlow and also to W. M. Webb (Civil Engineering Technologist, Division of Materials and Tests, Highway Division) for their help in performing the laboratory tests. Appropriate acknowledgement is also given to S. Kriengsiri, V. Pujals, and S. Broshek for their assistance in carrying out the analytical studies. The Figures were prepared by S. Kriengsiri.

ABSTRACT

Base course materials evaluated included sand, soil-aggregate, crushed stone and cement and asphalt stabilized bases. Required base course thickness was determined using a theoretical design procedure developed during this investigation. The procedure considers fatigue of stabilized layers and rutting in base and subgrade and was correlated with known performance of the AASHO Road Test. Base course coefficients for use in the AASHO INTERIM GUIDE TO THE DESIGN OF FLEXIBLE PAVEMENTS were determined for a selected number of equivalent 18 kip, single axle loadings. Properties of the base course materials were determined from results of repeated load triaxial and fatigue tests.

Cylindrical specimens of base course material were placed in conventional triaxial cells and subjected to 100,000 load repetitions. These tests were performed using a constant confining pressure and a triangular loading pulse having a duration of 0.10 seconds. Both elastic and plastic properties of materials were evaluated. All tests were performed with free drainage of specimens. Supplementary fatigue tests were performed on 18-1/2 inch diameter specimens of stabilized base materials.

The Rut Index proposed can be calculated using laboratory evaluated plastic responses. An evaluation of rutting characteristics of base materials studied was made using the Rut Index.

Key Words: AASHO Road Test, Base Course, Crushed Stone Base, Design, Dynamic Base Properties, Fatigue, Flexible Pavement, Repeated Load Triaxial Test, Rut Index, Rutting, Stabilized Base, Soil-Aggregate Base, Theoretical

TABLE OF CONTENTS

		Page
ACKNOWLEDGEMENT		ii
ABSTRACT		iii
LIST OF FIGURES		vi
LIST OF TABLES		xi
CHAPTER		
I.	INTRODUCTION	1
II.	BASE COURSE MATERIALS TESTED	4
III.	SAMPLE PREPARATION	9
	Soil Aggregate and Crushed Stone Triaxial Specimens	9
	Silty Sand and Soil-Cement Triaxial Specimens	10
	Asphalt Concrete Triaxial Specimens	10
	Fatigue Test Specimens	11
	Specimen Curing	13
IV.	TESTING PROCEDURE	15
	Repeated Load Triaxial Tests	15
	Fatigue Tests	19
V.	RESILIENT MODULUS TEST RESULTS	22
	Unstabilized Base Materials	23
	Stabilized Base Materials	36
	Discussion	36
VI.	PLASTIC STRAIN TEST RESULTS	38
	Summary of Test Results	38
	Effect of Unstabilized Base Type	40
	Effect of Aggregate Type and Fines	53
	Effect of Density	53
	Effect of Soaking	54
	Hyperbolic Plastic Stress-Strain Law	55
	Rut Depth Prediction	56
	Rut Index and Rut Potential	60

TABLE OF CONTENTS (Continued)

Page

Discussion of Plastic Response of Base Materials..... 63

VII. MECHANISTIC ANALYSIS OF AASHO TEST ROAD RESULTS 68

Pavement Temperatures and Traffic Loading..... 68
Nonlinear Layered System Analysis..... 70
Development of Fatigue Curves..... 76

VIII. DEVELOPMENT OF REQUIRED STRUCTURAL SECTIONS AND BASE COURSE COEFFICIENTS..... 84

Design Parameters..... 84
Temperature Prediction..... 85
Criteria for Limiting Subgrade Rutting..... 86
Required Structural Sections..... 92
Discussion..... 95

IX. RECOMMENDATIONS..... 102

X. ADDITIONAL RESEARCH..... 105

XI. GENERAL SUMMARY AND CONCLUSIONS..... 108

REFERENCES..... 112

APPENDIX A..... 115

APPENDIX B..... 119

LIST OF FIGURES

Figure		Page
1.	APPARATUS USED IN PREPARING THE ASPHALT CONCRETE FATIGUE SPECIMENS	12
2.	PNEUMATIC LOAD TESTING EQUIPMENT	12
3.	APPARATUS USED IN TESTING THE STABILIZED BASE MATERIALS (A. CLAMPS USED ON CEMENT STABILIZED BASES)	17
3.	TEST EQUIPMENT USED FOR STABILIZED BASE MATERIALS (B. TEST SET-UP FOR ASPHALT CONCRETE BASE SECTIONS)	17
4.	FATIGUE TEST APPARATUS	20
5.	INFLUENCE OF STRESS STATE ON RESILIENT MODULUS AFTER 10,000 REPETITIONS FOR A SILTY SAND-BASE 1	25
6.	EFFECT OF DEVIATOR STRESS ON RESILIENT MODULUS AFTER 10,000 REPETITIONS FOR A SILTY SAND-BASE 1	25
7.	INFLUENCE OF STRESS STATE ON RESILIENT MODULUS AFTER 10,000 REPETITIONS FOR A 40-60 BLEND SOIL AGGREGATE-BASE 2	26
8.	INFLUENCE OF STRESS STATE ON RESILIENT MODULUS AFTER 10,000 REPETITIONS FOR A 40-60 BLEND SOIL AGGREGATE-BASE 3	26
9.	INFLUENCE OF STRESS STATE ON RESILIENT MODULUS AFTER 10,000 REPETITIONS FOR A 17-83 BLEND SOIL AGGREGATE-BASE 4	27
10.	INFLUENCE OF STRESS STATE ON RESILIENT MODULUS AFTER 10,000 REPETITIONS FOR A 21-79 BLEND SOIL AGGREGATE-BASE 5	27
11.	COMPARISON OF RELATIONSHIP FOR RESILIENT MODULUS FOR SILTY SAND AND SOIL AGGREGATE BASES	28
12.	INFLUENCE OF STRESS STATE ON RESILIENT MODULUS AFTER 10,000 REPETITIONS IN A CRUSHED PORPHYRITIC GRANITE GNEISS WITH 3 PERCENT FINES-BASE 6	28

LIST OF FIGURES (Continued)

Figure		Page
13.	INFLUENCE OF STRESS STATE ON RESILIENT MODULUS AFTER 10,000 REPETITIONS IN A CRUSHED PORPHYRITIC GRANITE GNEISS WITH 3 PERCENT FINES AT 95% T-180 COMPACTION-BASE 6	29
14.	INFLUENCE OF STRESS STATE ON RESILIENT MODULUS AFTER 10,000 REPETITIONS FOR A PORPHYRITIC GRANITE GNEISS WITH 11.25 PERCENT FINES-BASE 7	29
15.	INFLUENCE OF STRESS STATE ON RESILIENT MODULUS AFTER 10,000 REPETITIONS IN A CRUSHED PORPHYRITIC GRANITE GNEISS WITH 11.25 PERCENT FINES AT 95% T-180 COMPACTION-BASE 7	30
16.	INFLUENCE OF STRESS STATE ON RESILIENT MODULUS AFTER 10,000 REPETITIONS IN A CRUSHED BIOTITE GRANITE GNEISS WITH 3 PERCENT FINES-BASE 8	33
17.	INFLUENCE OF STRESS STATE ON RESILIENT MODULUS AFTER 10,000 REPETITIONS FOR A CRUSHED BIOTITE GRANITE GNEISS WITH 11.25 PERCENT FINES-BASE 9	33
18.	INFLUENCE OF STRESS STATE ON RESILIENT MODULUS AFTER 10,000 REPETITIONS FOR A CRUSHED BIOTITE GRANITE GNEISS WITH 22 PERCENT FINES-BASE 10	34
19.	INFLUENCE OF FINES ON RESILIENT MODULUS FOR A CRUSHED BIOTITE GRANITE GNEISS	34
20.	COMPARISON OF RESILIENT MODULUS FOR SELECTED SOIL-AGGREGATE AND CRUSHED STONE BASES	20
21.	INFLUENCE OF STRESS STATE ON RESILIENT MODULUS OF SOIL-CEMENT (BASE 11) AND CEMENT STABILIZED SOIL-AGGREGATE (BASE 12)	37
22.	COMPARISON OF RESILIENT MODULUS FOR STABILIZED BASE MATERIALS	37
23.	INFLUENCE OF NUMBER OF LOAD REPETITIONS AND DEVIATOR STRESS RATIO ON PLASTIC STRAIN IN A PORPHYRITE GRANITE GNEISS-THREE PERCENT FINES	39
24.	INFLUENCE OF DEVIATOR STRESS AND CONFINING PRESSURE ON PLASTIC STRAIN AFTER 100,000 REPETITIONS IN A FINE SILTY SAND-BASE 1	39

LIST OF FIGURES (Continued)

Figure		Page
25.	EFFECT OF SOAKING AND DEGREE OF COMPACTION ON PLASTIC STRAIN IN A SILTY SAND-BASE 1.....	41
26.	INFLUENCE OF DEVIATOR STRESS AND CONFINING PRESSURE ON PLASTIC STRAIN AFTER 100,000 REPETITIONS IN A 40-60 BLEND SOIL AGGREGATE-BASE 2.....	41
27.	INFLUENCE OF DEVIATOR STRESS AND CONFINING PRESSURE ON PLASTIC STRAIN AFTER 1,000,000 REPETIRIONS IN A 40-60 BLEND SOIL AGGREGATE-BASE 3.....	42
28.	INFLUENCE OF SOAKING ON PLASTIC STRAIN IN A 40-60 BLEND SOIL AGGREGATE-BASE 3.....	42
29.	INFLUENCE OF DEVIATOR STRESS AND CONFINING PRESSURE ON PLASTIC STRAIN AFTER 100,000 REPETITIONS IN A 17-83 BLEND SOIL AGGREGATE-BASE 4.....	43
30.	INFLUENCE OF SOAKING AND 95 PERCENT COMPACTION ON PLASTIC STRAIN IN A 17-83 BLEND SOIL AGGREGATE-BASE 4.....	43
31.	INFLUENCE OF DEVIATOR STRESS AND CONFINING PRESSURE ON PLASTIC STRAIN AFTER 100,000 REPETITIONS IN A 21-79 BLEND SOIL AGGREGATE-BASE 5.....	44
32.	INFLUENCE OF SOAKING AND DEGREE OF COMPACTION OF PLASTIC STRAIN IN A 21-79 BLEND SOIL AGGREGATE-BASE 5.....	44
33.	INFLUENCE OF DEVIATOR STRESS AND CONFINING PRESSURE ON PLASTIC STRAIN AFTER 100,000 REPETITIONS IN A CRUSHED PORPHYRITE GRANITE GNEISS WITH 3 PERCENT FINES-BASE 6.....	45
34.	INFLUENCE OF SOAKING AND DEGREE OF COMPACTION ON PLASTIC STRAINS IN A CRUSHED PORPHYRITIC GRANITE GNEISS WITH 3 PERCENT FINES-BASE 6.....	45
35.	INFLUENCE OF DEVIATOR STRESS AND CONFINING PRESSURE ON PLASTIC STRAIN AFTER 100,000 REPETITIONS IN A PORPHYRITIC GRANITE GNEISS WITH 11.25 PERCENT FINES-BASE 7.....	46
36.	INFLUENCE OF SOAKING AND DEGREE OF COMPACTION ON PLASTIC STRAIN IN A PORPHYRITIC GRANITE GNEISS WITH 11.25 PERCENT FINES-BASE 7.....	46

LIST OF FIGURES (Continued)

Figure		Page
37.	INFLUENCE OF DEVIATOR STRESS AND CONFINING PRESSURE ON PLASTIC STRAIN AFTER 100,000 REPETITIONS IN A CRUSHED BIOTITE GRANITE GNEISS WITH 3 PERCENT FINES-BASE 8	47
38.	INFLUENCE OF DEVIATOR STRESS AND CONFINING PRESSURE ON PLASTIC STRAIN AFTER 100,000 REPETITIONS IN A CRUSHED BIOTITE GRANITE GNEISS WITH 11.25 PERCENT FINES-BASE 9	47
39.	INFLUENCE OF DEVIATOR STRESS AND CONFINING PRESSURE ON PLASTIC STRAIN AFTER 100,000 REPETITIONS IN A CRUSHED BIOTITE GRANITE GNEISS WITH 22 PERCENT FINES-BASE 10	48
40.	SUMMARY OF PLASTIC STRESS-STRAIN CHARACTERISTICS AT 100,000 LOAD REPETITIONS AND A CONFINING PRESSURE OF 10 PSI	49
41.	INFLUENCE OF DEVIATOR STRESS AND CONFINING PRESSURE ON PLASTIC STRAIN AFTER 100,000 REPETITIONS IN A SILTY SAND STABILIZED WITH 6 PERCENT CEMENT-BASE 11	50
42.	INFLUENCE OF DEVIATOR STRESS AND CONFINING PRESSURE ON PLASTIC STRAIN IN A 40-60 BLEND SOIL AGGREGATE STABILIZED WITH 2.73 PERCENT CEMENT-BASE 12	50
43.	EFFECT OF STRESS STATE AND TEMPERATURE ON PLASTIC STRAINS IN AN ASPHALT CONCRETE-BASE 13	51
44.	INFLUENCE OF FINES AND DEVIATOR STRESS RATIO ON THE PLASTIC STRAINS IN A CRUSHED GRANITE GNEISS BASE AFTER 100,000 LOAD REPETITIONS	51
45.	COMPARISON OF PLASTIC STRAIN RESPONSE OF STABILIZED BASE MATERIALS	52
46.	COMPARISON OF CALCULATED HYPERBOLIC PLASTIC STRAIN WITH EXPERIMENTAL CURVES FOR A 21-79 SOIL AGGREGATE-BASE 5	57
47.	IDEALIZATION OF LAYERED PAVEMENT STRUCTURE FOR CALCULATING RUT DEPTH	57
48.	VARIATION OF RUT INDEX WITH PERCENT FINES FOR CRUSHED GRANITE GNEISS BASES AFTER 100,000 LOAD REPETITIONS	66

LIST OF FIGURES (Continued)

Figure		Page
49.	RELATIONSHIP BETWEEN APPLIED LOADING AND TEMPERATURE IN THE ASPHALT CONCRETE FOR THREE SELECTED MONTHS-EXPERIMENTAL DATA FROM THE AASHO ROAD TEST	71
50.	VARIATION OF MODULUS OF ELASTICITY OF ASPHALT CONCRETE WITH TEMPERATURE FOR A LOADING FREQUENCY OF APPROXIMATELY 14 CPS	75
51.	COMPARISON OF MEASURED AND CALCULATED SURFACE DEFLECTIONS-LOOP 4, SECTION 625 AASHO ROAD TEST	75
52.	VARIATION OF MAXIMUM TENSILE STRAIN IN ASPHALT CONCRETE WITH TEMPERATURE AND SEASON	77
53.	VARIATION OF MAXIMUM TENSILE STRAIN IN ASPHALT CONCRETE WITH TEMPERATURE AND SEASON	77
54.	VARIATION OF MAXIMUM TENSILE STRAIN IN CEMENT STABILIZED GRAVEL WITH TEMPERATURE AND SEASON	78
55.	FATIGUE CURVES FOR PSI OF 2.5 IN A CRUSHED STONE BASE PAVEMENT-AASHO ROAD TEST	81
56.	FATIGUE CURVES FOR PSI OF 2.5 IN AN ASPHALT CONCRETE BASE PAVEMENT-AASHO ROAD TEST	81
57.	FATIGUE CURVE FOR PSI OF 2.5 IN A CEMENT STABILIZED BASE PAVEMENT-AASHO ROAD TEST	82
58.	INFLUENCE OF ASPHALT CONCRETE THICKNESS ON TENSLE STRAIN REQUIRED TO CAUSE FAILURE	82
59.	COMPARISON OF PLASTIC RESPONSE OF AASHO CLAY SUBGRADE AND A SILTY SAND SUBGRADE AFTER 10,000 REPETITIONS	89
60.	ALLOWABLE INCREASE IN VERTICAL SUBGRADE STRESS ON MICACEOUS SILTY SAND SUBGRADE FOR 180,000 REPETITIONS OF AN 18 KIP AXLE LOADING	91
61.	DESIGN RELATIONSHIP FOR RESILIENT MODULUS OF PIEDMONT MICACEOUS SILTY SAND SUBGRADE	91
62.	EFFECT OF BASE THICKNESS ON PAVEMENT LIFE FOR SELECTED BASE TYPES-3 IN. A.C. SURFACE AND 4 IN. SUBBASE	100

LIST OF TABLES

Table		Page
1.	MATERIAL CHARACTERISTIC OF BASES INVESTIGATED.....	5
2.	SUMMARY OF PHYSICAL PROPERTIES OF CRUSHED STONE BASE MATERIALS.....	6
3.	GRADATION OF CRUSHED STONE USED IN SOIL-AGGREGATE BASES.....	7
4.	SUMMARY OF CHARACTERISTICS OF SOIL USED IN SOIL AGGREGATE BASES.....	7
5.	ASPHALT CONCRETE BASE MIX DESIGN.....	8
6.	SUMMARY OF ELASTIC AND PLASTIC BASE CHARACTERISTICS EVALUATED FROM REPEATED LOAD TRIAXIAL TESTS.....	24
7.	SUMMARY OF MATERIAL CHARACTERISTICS USED IN THE ANALYSIS OF THE AASHO ROAD TEST.....	73
8.	LONG TERM CLIMATOGICAL WEATHER DATA FOR ATLANTA, GEORGIA.....	87
9.	PROPERTIES OF THE ASPHALT CONCRETE USED IN THE THERMAL ANALYSIS.....	86
10.	REQUIRED BASE THICKNESS AND SUBGRADE STRESS TO MINIMIZE RUTTING IN THE AASHO SUBGRADE FOR A 22.4 KIP SINGLE AXLE LOADING.....	89
11.	SUMMARY OF REQUIRED STRUCTURAL SECTIONS AND BASE COURSE COEFFICIENTS FOR 18 KIP AXLE LOADING AND 20 YEAR DESIGN LIFE.....	96
12.	SUPPLEMENTARY FATIGUE TEST RESULTS FOR STABILIZED BASE MATERIALS.....	97

CHAPTER I

INTRODUCTION

In recent years an important trend has been established toward the use of heavier highway wheel loadings. To accommodate this traffic new types of construction are being used, such as deep strength and full depth asphalt concrete pavements, and new materials are being developed such as glass and epoxy asphalts. The engineer must design these new pavements without having had extensive previous experience with similar pavement structures upon which to rely. These technological changes have further intensified the need for developing new methods of designing pavements to withstand rutting and cracking. The base course of a pavement constitutes a very important part of this problem and is given detailed attention in this report.

An acceptable base course should have sufficient rigidity or depth to spread the load out in order to reduce to an acceptable level the magnitude of cumulative rutting in the subgrade, and eliminate the possibility of a bearing capacity failure. The base should also be compacted to a sufficient density so that it will not undergo excessive permanent deformations. Finally, the overall pavement system must act in such a way so as to prevent fatigue type of failure from prematurely occurring in the asphaltic concrete surfacing due to the repeated flexing that occurs as large numbers of wheel loads move over the pavement system [1][1]. Fatigue failure results in cracking of the bound layers, and a resulting loss of load spreading capability of the pavement system. Fatigue failures can also eventually contribute to the occurrence of

---

1. The numbers in brackets refer to the references given at the end of this report.

serious rutting in the base and subgrade. Fatigue failure is particularly likely to occur in pavement systems constructed over highly micaceous, silty sand and sandy silt subgrade soils such as those commonly found in the Piedmont Province of Georgia due to their high resilience.

In the past static tests such as the CBR, Hveen Stabilometer, or the static triaxial test have been usually used to evaluate the characteristics of highway materials subjected in the field to large numbers of repeated load application. To more realistically simulate the stress conditions that exist in the field a confined specimen can be subjected to repeated axial loads using the repeated load triaxial test. This type of dynamic test has the following important advantages over the conventionally used type of static test:

1. A dynamic load can be applied having approximately the same duration as that occurring in the field.
2. The stress state occurring beneath the pavement at a desired point can be simulated using this test.
3. Both elastic and plastic material properties are obtained from the test.
4. The effect of large numbers of repetitive loadings can be studied.

The objective of this study is to evaluate the relative performance of seven different types of base course materials used by the State Highway Department of Georgia in pavement systems constructed on the micaceous subgrade soils of the Piedmont Province of Georgia. This objective is accomplished primarily by studying the behavior of these base course materials in the laboratory using the repeated load triaxial test. A limited number of fatigue tests were also performed on the stabilized materials to aid in the overall evaluation. Fatigue curves and rutting criteria for use in Georgia were established from the observed performance of the AASHO Road Test using nonlinear layered theory together with measured material properties. Using the developed criterion the

experimentally measured material properties for Georgia base course materials were then theoretically analyzed to develop required base course thicknesses and base course coefficients. Georgia's environmental and subgrade conditions were considered in this evaluation.

A Glossary of Terms used frequently in this report is given in Appendix A.

CHAPTER II

BASE COURSE MATERIALS TESTED

Repeated load triaxial tests were performed on the following unstabilized base course materials: (1) a silty sand, (2) four soil-aggregate mixtures, and (3) five crushed stone base materials. Cement stabilized specimens of silty sand and soil-aggregate, and an asphalt concrete base were tested in both the repeated load triaxial apparatus and also in flexure using a fatigue apparatus. All base materials used in the testing program were used by the State Highway Department of Georgia on construction projects except Bases 8 through 11, and 13 (Table 1); these materials were also typical of those used on state projects and met all applicable material specifications.

A general description and a summary of the properties of the base course materials tested is given in Table 1. The source, description and physical properties of the crushed stone used in these bases is given in Table 2. The gradation of crushed stone and the properties of the soil used in the soil-aggregate bases are summarized in Table 3 and 4, respectively. The mix design for the dense graded asphalt concrete base is summarized in Table 5.

TABLE 1. MATERIAL CHARACTERISTICS OF BASES INVESTIGATED[1]

Base	Description	Grain Size Distribution										Maximum Density			Atterberg Properties		Volume Change (%)			Project
		Percent Passing					Percent Passing No. 10 Sieve					Method[2]	γ_d (pcf)	W opt. (%)	L.L.	P.I.	Swell	Shrinkage	Total	
		2	1-1/2	3/4	10	40	10	60	200	silt	clay									
1	Orange-tan, slightly clayey, silty sand	100	100	100	100	88	100	63	40	30	10	GHD-7	115.4	13.0	22	6	3.8	3.4	7.2	Fulton-Forsyth Counties APD-056-1(13)
2	A blend of 40% silty fine sand and 60% No. 467 stone.	100	98.8	85.0	42.4	28.8	100	60	31	15	16	GHD-49 T-180C	138.2 141.1	4.2 6.5	SIC	N.P.	.7	2.0	2.7	Bibb County I-75-1(59)
3	A blend of approximately 40% silty sand and 60% No. 467 stone	100	100	72	39	29	100	59	28	11	17	T-180C	138.0	6.6	SIC	N.P.	2.5	1.6	4.1	Henry County S-HG-2673(1)
4	A blend of approximately 17% silty sand and 83% crushed Biotite Granite Gneiss	100	95	60	30	-	100	43	27	10	17	GHD-49 T-180C	143.0 141.6	4.6 5.9	SIC	N.P.	2.0	3.5	5.5	DeKalb-Gwinette Counties F-10401[2]
5	A blend of 21% sandy silt and 79% crushed Biotite Granite Gneiss	100	97	77.5	40	-	100	70	37	17	20	GHD-49 T-180C	140.2 140.0	6.0 6.3	SIC	N.P.	6.1	3.1	9.2	DeKalb-Gwinette Counties F-10401[2]
6	Crushed Porphyritic Granite Gneiss-3% fines; Source A	100	100	60	25	13	100	36	12	8	4	GHD-49 T-180C	136.0 137.4	3.7 6.5	-	-	2.1	0.4	2.5	Coweta County I-85-1(39)46
7	Crushed Porphyritic Granite Gneiss-11.2% fines; Source B	100	100	90	45	31	100	60	25	18	7	GHD-49 T-180C	135.0 135.0	5.7 6.0	-	-	9.4	0.5	9.9	Coweta County I-85-1(39)46
8	Crushed Biotite Granite Gneiss-3% fines; Source B	100	100	60	25	13	100	36	12	-	-	T-180C	137.4	6.5	-	-				-
9	Crushed Biotite Granite Gneiss-11.2% fines; Source B	100	100	90	45	31	100	60	25	19	6	T-180C	135.0	6.0	-	-	6.3	0.5	6.8	-
10	Crushed Biotite Granite Gneiss-22% fines; Source B	100	100	90	45		100	60	49	40.6	8.4	T-180C	132.9	6.1	-	-	7.3	0.4	7.7	-
11	Cement Stabilized silty sand-6% cement			100	93	73	100	60	31	15	16	GHD-7	124.0	10.0	SIC	N.P.	0.7	2.0	2.7	Bibb County I-75-1(59)
12	Cement Stabilized 40% silty sand and 60% No. 467 stone, 2.73% cement	100	100	72	39	29	100	59	28	11	17	T-180C	138.0	7.5	SIC	N.P.	2.5	1.6	4.1	Henry County S-HG-2673(1)
13	Asphalt concrete base-5% asphalt	See Table 5 For Mix Design																		Standard A Binder Design

1. All tests were performed in accordance with STATE HIGHWAY DEPARTMENT OF GEORGIA SAMPLING, TESTING AND INSPECTION MANUAL.

2. This soil-aggregate base was fabricated from the materials used on Project F-10401. The soil gradation and percent soil used is not the same as used on Project F-10401.

TABLE 2. SUMMARY OF PHYSICAL PROPERTIES OF CRUSHED STONE BASE MATERIALS(1)

Base	Description	Aggregate Producer	Specific Gravities			Absorp. (%)	Wear (%)	Class	Magnesium Sulfate Soundness Loss, (%)
			Bulk	S.S.D.	Apparent				
2	Granite Gneiss	I-75-1 (59)160 Ct. 1 Palmer Station Bibb County	2.64	2.65	2.65	.40	45	A	1.21
3,12	Biotite Gneiss	Vulcan Materials Co. Stockbridge, Georgia	2.64	2.66	2.68	.44	39	A	.95
4,5	Biotite Granite Gneiss	Southeastern Highway Contracting Co. Peachtree-DeKalb Quarry DeKalb County	2.69	2.71	2.74	.69	34	A	2.00
6,7	Porphyritic Granite Gneiss	Southeastern Highway Contracting Co., McCollum Quarry, Newnan, Georgia	2.67	2.68	2.71	.64	47	A	1.95
8,9, 10	Biotite Granite Gneiss	Vulcan Materials Co. Norcross, Georgia	2.68	2.69	2.72	.59	52	B	1.00

1. Aggregate characteristics taken from State Highway Department of Georgia, Laboratory Memorandum No. 102-8, Coarse Aggregate Sources.

TABLE 3. GRADATION OF CRUSHED STONE USED IN SOIL-AGGREGATE BASES

Base	Source[1]	GRAIN SIZE DISTRIBUTION								Comments
		% Passing					% Passing No. 10 Sieve			
		2	1-1/2	3/4	10	40	10	60	200	
2	1	100	98	75	0	0				No. 467 Stone
3,12	2	-	-	-	-					No. 467 Stone
4	3	100	94	52	16	2	0	0	0	
5	3	100	96	72	25	17	100	80	34	

1. Refer to Table 2

TABLE 4. SUMMARY OF CHARACTERISTICS OF SOIL USED IN SOIL-AGGREGATE BASES

Base	Soil Description	Soil Classification	Atterberg Limits		GRADATION								COMPACTION			VOLUME CHANGE			S.G.
					% Passing			% Passing #10											
			LL	PI	3/4	10	40	10	60	200	silt	clay	Test	(pcf)	(%)	%	%	Total	
2,11	Grey, silty fine sand	A-2-4(0); SM	SIC	N.P.	100	93	73	100	60	31	15	16	GHD-7	124	10	0.7	2.0	2.7	2.66
3,12	Light Brn. Silty fine Sand	A-2-4(0); SM	SIC	N.P.	100	97	75	100	59	24	12	12	GHD-7	125	9	1.7	0.8	2.5	2.65
4	Slightly micaceous, brn. clayey sand silt	A-6(5); ML	35	20	100	100	100	100	75	52	-	-							2.71
5	Slightly micaceous, brn. clayey sandy silt	A-6(5); ML	35	20	100	100	100	100	82	52	-	-							2.71

1. Slid in liquid limit cup during test.

TABLE 5. ASPHALT CONCRETE BASE MIX DESIGN

DESCRIPTION: A dense graded Asphalt Concrete Base having 5 percent of an 85-100 penetration grade asphalt

PROJECT: Standard A Binder Design

AGGREGATE COMBINATION: 50% No. 57 size stone and 50% Stone Screenings

MIX DESIGN:

A.C. %	Theoretical Sp. Gr.	Actual Sp. Gr.	Voids in Mix %	Mix Density Lbs/Cu. Ft.	Stability Lbs.	Flow	Agg. Voids Filled %	VMA
4.0	2.518	2.347	6.8	146.5	2757	9.0	57.2	14.6
4.5	2.500	2.375	5.0	148.2	2711	9.0	67.5	14.0
5.0	2.481	2.380	4.1	148.5	2627	10.0	73.7	14.3
5.5	2.463	2.414	2.0	150.6	2378	12.0	86.6	13.6

AGGREGATE GRADATION OF MIXTURE: Total Percent Aggregate Passing by Weight

1-1/2"	1"	3/4"	1/2"	3/8"	No. 4	No. 8	No. 16	No. 50	No. 100	No. 200
100	97	86	67	57	41	32	25	14	8	5

AGGREGATE GRADATION AND SPECIFIC GRAVITY:

Sieve Size (% Passing)	Coarse Aggregate (No. 57 stone)	Fine Aggregate (Screenings)
1-1/2"	100	
1"	94	
1/4"	72	
1/2"	33	
3/8"	14	100
No. 4	3	78
No. 8	2	62
No. 16		50
No. 50		27
No. 100		15
No. 200		10
Apparent Sp. Gr.	2.68	2.68
Bulk Sp. Gr.	2.64	2.64

ASPHALT PROPERTIES:

Penetration, 77° F(mm): 85-100
Kinematic Viscosity
140° F (Poises)(1) 1500
275° F (Centistokes) 416
325° F (Centistokes) 139

1. Saybolt Furol Viscosity

SOURCE OF COARSE AND FINE AGGREGATE: Vulcan Materials Company, Red Oak, Georgia

SOURCE OF ASPHALT: Shell Oil Company, Atlanta, Georgia

CHAPTER III

SAMPLE PREPARATION

Sample preparation is an extremely important phase of any laboratory investigation. The preparation of specimens having up to 1-3/4 inch diameter aggregates and also the preparation of soil-aggregate mixtures added to the usual problems involved in obtaining uniform, reproducible specimens. The sample preparation methods that were developed during this project were found to give satisfactory specimens without expending excessive time and effort for preparation.

Specimens 2.8 inches in diameter and 6 inches high of silty sand and soil-cement base materials were prepared for testing in the repeated load triaxial test apparatus. Asphalt concrete specimens tested in the repeated load triaxial apparatus were 4 inches in diameter and 8 inches high. All stabilized and unstabilized soil-aggregate and crushed stone specimens tested in the repeated load triaxial apparatus were 6 inches in diameter and 12 inches in height. Fatigue specimens were 2-1/2 inches thick and 18-1/2 inches in diameter.

Soil Aggregate and Crushed Stone Triaxial Specimens

Cylindrical specimens 6 inches in diameter and 12 inches high of Bases 2 through 10 and 12 were prepared directly on the base of the triaxial cell. This method of preparation was found to be necessary since movement after specimen preparation from a separate mold to the base of the triaxial cell was found to be almost impossible without at least some amount of damage occurring to the specimen.

The aggregate greater in size than the #10 sieve used in Bases 4 through 10 and Base 12 was first soaked in water overnight and then carefully dried in order to achieve a

saturated, surface dry aggregate condition before specimen compaction. The material to be compacted was mixed by hand in a large pan. A filter paper was placed over the porous stone on the base, and a steel mold split in three equal segments was clamped around the base of the cell.

The specimens were compacted in the mold in 2 inch thick layers using on the average approximately 50 blows from a 5.5 pound standard Proctor hammer dropped through a height of 12 inches. Before beginning compaction, the correct amount of material for each layer was weighed out and stored in plastic bags until needed in order to prevent moisture loss. The compactive effort used was varied for each material and level of density in order to give the required layer thickness. The specimens were prepared about 1/16 inches greater than the desired height of 12 inches and while still in the mold, they were compressed in a testing machine to the desired height. The mold was then removed after tapping it lightly with a hammer to break it loose from the specimens.

Silty Sand and Soil-Cement Triaxial Specimens

Specimens 2.8 inches in diameter and 6 inches in height were prepared for the silty sand and soil-cement materials (Bases 1 and 11). After thoroughly mixing these materials with water in a metal pan, the proper amount of material for four 1-1/2 inch thick layers was weighed out and stored in plastic bags. Each layer was compacted to the required thickness using a standard Proctor hammer. The specimens were initially compacted to a height slightly greater than 6 inches and then compressed in a testing machine to the desired height and extruded from the steel mold. A filter paper was placed on the base of the triaxial cell before positioning the compacted specimen in the cell.

Asphalt Concrete Triaxial Specimens

Cylindrical specimens 4 inches in diameter and 8 inches

in height were prepared using a kneading compactor. The specimens were compacted in a steel mold in three layers, and extruded from the mold after cooling. After placing the material in each layer the asphalt was carefully troweled and partially compacted with a Proctor hammer to eliminate any large voids around the sides of the specimens. The asphalt concrete was mixed using standard State Highway Department of Georgia procedures.

Fatigue Test Specimens

Fatigue test specimens of the stabilized bases 18-1/2 inches in diameter and 2-1/2 inches thick were prepared in the heavy steel mold shown in Figure 1. The base of the mold was surface ground in order to assure as nearly a perfectly flat base as possible. The specimens were compacted in two layers using a standard Proctor hammer weighing 5.5 pounds and dropped through a height of 12 inches. The proper amounts of stabilizing agent, water, and base material were thoroughly mixed by hand.

One quarter of the cement stabilized material required for each layer was weighed out and sealed in plastic bags to prevent moisture loss. Before compaction of each layer began the mold was divided into quarters, and a bag of soil was placed in the center of each segment. The material was carefully spread out, leveled and then each quarter segment was first compacted with 10 blows and thereafter 15 blows. After each quarter of the specimen had been compacted with one sequence of blows, the layer thickness was checked by means of the wood template also shown in Figure 1. After achieving a thickness of 1.25 inches a new layer was placed in a manner similarly to that just described and the compaction sequence was repeated until a thickness of 2-1/2 inches was obtained.

After compacting both layers, the specimen was then compressed to the required thickness by loading in a 450,000

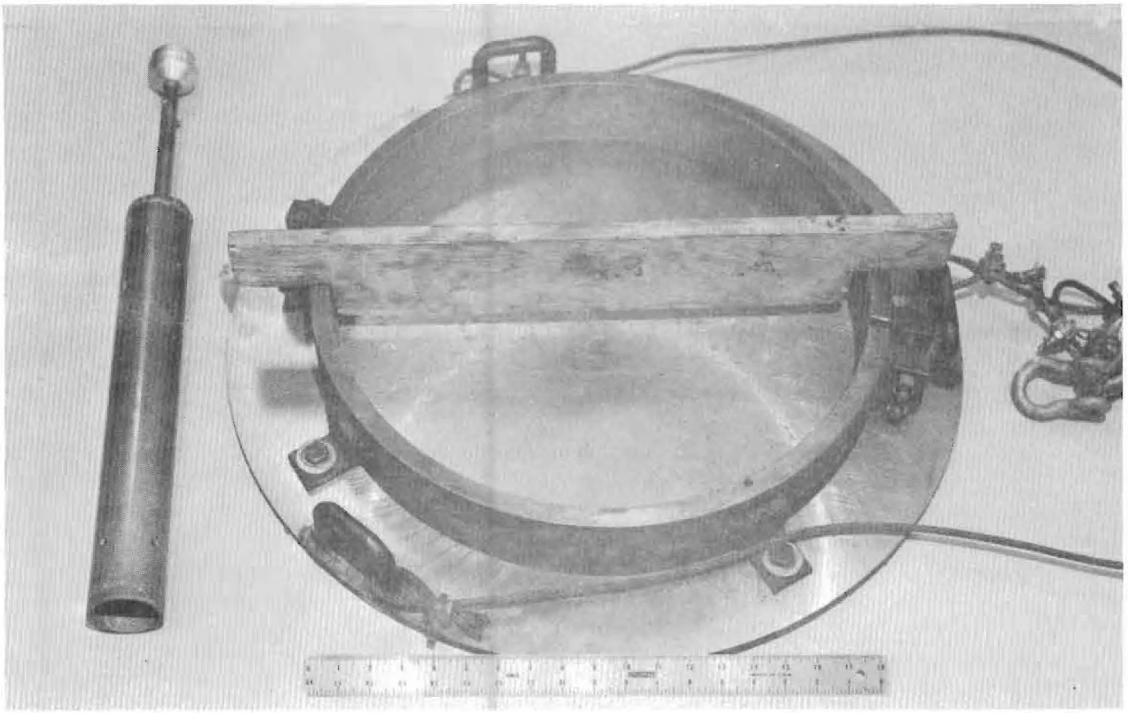

FIGURE 1. APPARATUS USED IN PREPARING THE ASPHALT CONCRETE FATIGUE SPECIMENS

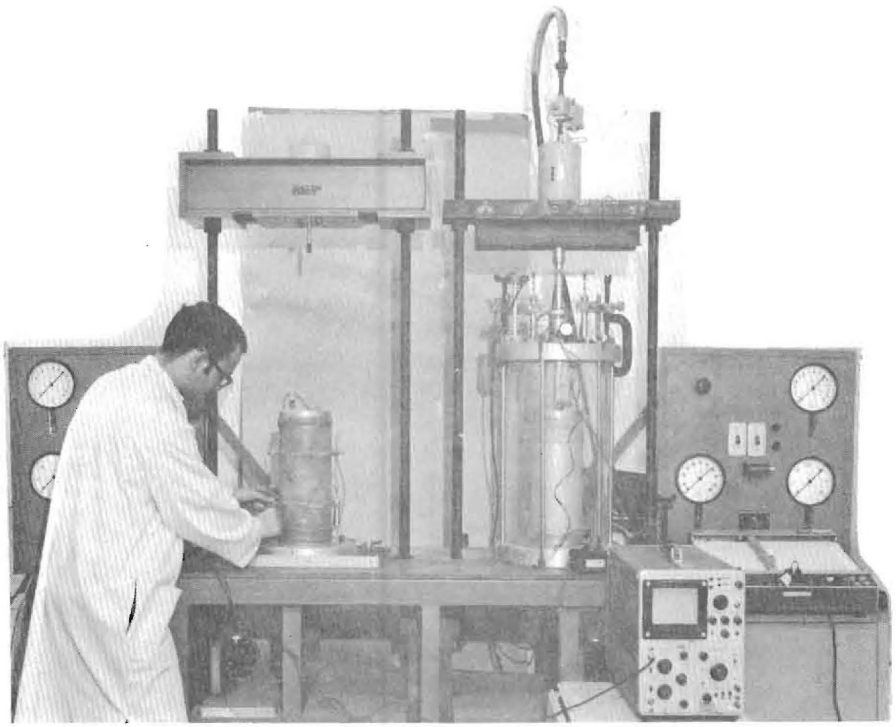

FIGURE 2. PNEUMATIC LOAD TESTING EQUIPMENT

pound testing machine. The purpose of loading the specimen in the testing machine was to obtain a sample of the required thickness having a smooth, level surface. Because of the 450,000 pound capacity of the testing machine, the following procedure was used. Initially, a 6 inch diameter steel plate was placed in the center of the specimen and loaded in the testing machine to give the required sample thickness. The small plate was then removed and an 18-1/2 inch diameter plate was placed in the mold and loaded in order to compress the outside portion of the specimen.

The asphalt concrete mix was prepared as described elsewhere [28]. The prepared asphalt concrete was placed in the mold and compacted in a manner similar to that described above. To prevent excessive heat loss from the asphalt concrete during preparation, the mold and loading plates were first heated in a steam bath. During preparation the mold was then placed on a hot plate.

Specimen Curing

All unstabilized cylindrical specimens were tested in the triaxial cell shortly after sample preparation. The cement stabilized triaxial specimens were left in the mold after compaction for approximately 24 hours in order to prevent slumping of the specimen. During this time the specimens remained covered with a plastic bag and wet cloth towels to prevent moisture loss. After removal from the mold, the soil cement (Base 11) and cement stabilized soil aggregate (Base 12) specimens were placed in plastic bags and stored in a moisture room for 21 days. The asphalt concrete base specimens were stored in the natural environment for approximately 3 months before testing.

One cement stabilized graded aggregate triaxial specimen (Base 12) was subjected to six wet-dry cycles before testing in the repeated load triaxial apparatus in order to approximately evaluate in the laboratory the effects of field

weathering. Each cycle consisted of drying at 105° C for approximately 24 hours, and then storing the uncovered specimen in a moisture room for another 24 hours. No visually noticeable deterioration of the specimen occurred during this period.

The 18-1/2 inch diameter fatigue test specimens stabilized with cement were left in the steel mold after compaction for approximately 24 hours. During curing the specimens were covered with a plastic bag and a layer of wet towels to prevent moisture loss. After the specimens were removed from the mold they were placed on surface ground steel plates and covered with a plastic bag and a layer of wet towels which were moistened periodically. Results from previous investigations indicate that the full fatigue strength of the cement stabilized bases would not be expected to be developed until about 60 to 70 days after curing. Sufficient time was not available to allow all of the specimens to cure for this length of time. The specimens for the main series of fatigue tests were therefore cured at room temperature and humidity for 14 days before testing. Fatigue tests were also performed on two soil-cement specimens after a curing period of 150 days to obtain an indication of the effect of curing time on fatigue response.

CHAPTER IV

TESTING PROCEDURE

Descriptions of the procedure developed for performing the repeated load triaxial tests and also the fatigue tests on the stabilized materials are given in this chapter.

Repeated Load Triaxial Tests

All repeated load triaxial tests were performed using a constant cell pressure and a repeated axial deviator stress applied by a pneumatic loading system. The pneumatic system consisted of a rolling diaphragm type piston, quick release valve and a microswitch-cam arrangement operated by a variable speed motor. The equipment and test set-up used to perform these tests is shown in Figure 2.

Each specimen tested was subjected to thirty load pulses per minute. The pulse used had a triangular shape and a duration of 0.10 seconds. This load pulse duration corresponds to a vehicle speed of approximately 30 mph [2]. Specimens were tested to an average of 100,000 load repetitions using confining pressures of 3,5 and 10 psi. Deviator stresses varying from approximately 1 to 6 times the confining pressure were used in the repeated load tests.

Permanent axial deformations occurring throughout the entire height of the specimens were measured by means of a pair of linear variable differential transducers (LVDT's). A horizontal plexiglass plate was clamped to the portion of the piston protruding out of the triaxial cell. The probes of the LVDT's were positioned vertically with the tip of the probe resting on leveling screws located on each side of the plexiglass plate. The LVDT's were located an equal distance from the piston. The electrical signals from the transducers

were added together and the combined output was recorded on a Moseley Model 7004 X-Y recorder.

Test results on the cement stabilized bases indicated that deformations in the piston, the top cap, and base of the cell became quite important when measuring the resilient modulus[1] of these quite rigid materials. Therefore, to eliminate these end effects plexiglass clamps were attached to approximately the quarter points of the specimen. The deformation between the clamps was measured by a pair of LVDT's as shown in Figure 3a. Inside clamps were used for the cement stabilized specimens and also for a limited number of non-stabilized specimens. The resilient modulus given for the stabilized materials was measured using inside clamps while those given for nonstabilized materials was obtained from deformation measurements outside the cell.

The repeated load triaxial tests on the asphalt concrete base were performed inside a constant temperature box (Figure 3b) whose temperature could be controlled to within $\pm$ 1° F. The resilient modulus was measured using two 3 inch long SR-4 strain gages attached to the specimens. The strain gages were orientated axially on the specimens and wired together to give an average axial strain. Permanent deformations were measured using a pair of transducers as previously described for the other base materials.

The use of inside clamps attached directly to the specimen was found to work nicely when measuring the elastic deformation (bounce) of the specimens. However, scatter in the permanent axial deformations was observed at large numbers of load repetitions when the inside clamps were used. Due to this problem, a pair of transducers were always used on the outside of the cell to measure the permanent displacement occurring throughout the entire specimen height.

---

1. The resilient modulus is equal to the repeated deviator stress applied to the specimen divided by the resilient strain. The resilient strain is the elastic "bounce" of the specimen after a given number of repetitions divided by the distance over which the bounce is measured.

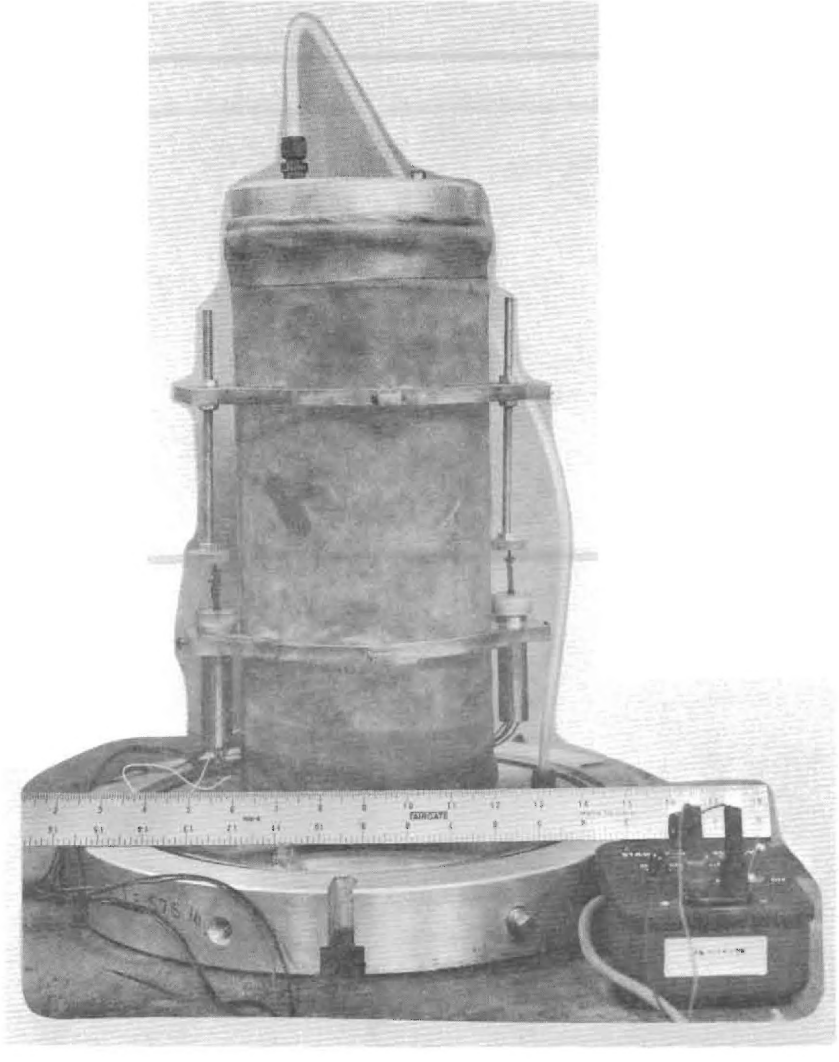

FIGURE 3(A). CLAMPS USED ON CEMENT STABILIZED BASES

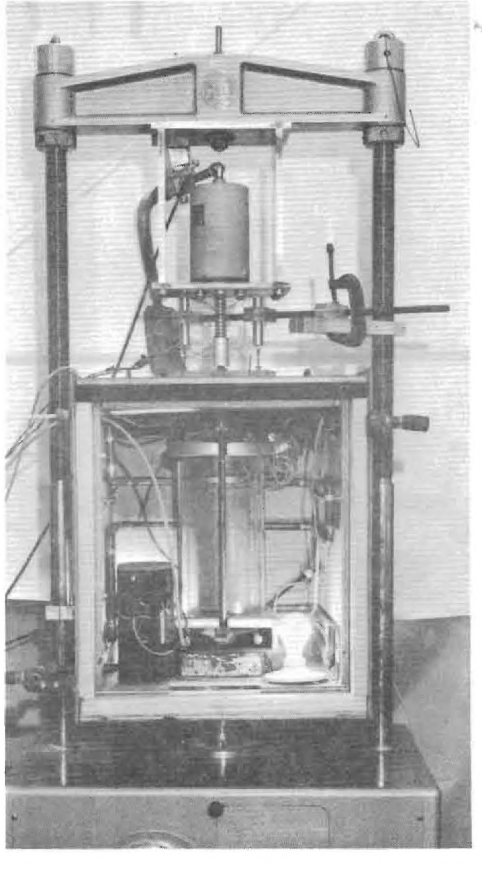

FIGURE 3(B). TEST SET-UP FOR ASPHALT

FIGURE 3. TEST EQUIPMENT USED FOR STABILIZED BASE MATERIALS

After all transducers were positioned properly, the confining pressure was applied to the specimen and it was then allowed to consolidate isotropically until the reduction in sample height with time became negligible. During the test, elastic and plastic deformation readings on the outside transducers were taken continuously from zero to 10 load repetitions. Thereafter, deformation readings were taken on the outside transducers, and also the inside transducers when used, at approximately 100, 1000, 10,000 and 100,000 applications which corresponds to each logarithmic interval of load repetition.

To obtain plastic strain properties of the materials, the confining pressure was maintained at a constant value throughout the test except for a very few cycles of loading at logarithmic intervals of load application. The confining pressure and deviator stress at these intervals were temporarily reduced in a number of the tests for a few repetitions to obtain elastic deformation of the materials at different stress states in order to better define the resilient modulus. In order to not ruin the plastic strain data, care was taken not to stress the specimens at the reduced confining pressure more critically than during the remainder of the test. At the end of the test a StrainSert load cell and oscilloscope were used to accurately check the axial load pulse applied to the specimen.

All transducer-recorder systems were periodically calibrated using a calibration stand by mechanically displacing the two probes of each pair of transducers simultaneously through a range of known displacements and measuring the corresponding displacement of the recorder pen. As an additional check on the operation of the displacement recording system, 0.030 inch calibration blocks were inserted beneath the probes of the transducers just before beginning a test, and the corresponding displacement of the recorder pen was measured. The calibration constants obtained using the calibration blocks were then compared to standard calibration constants to determine if the

system was working properly. All tests were performed with the drainage lines to the inside of the sample left open. Therefore, an appreciable build up in pore pressure would not be expected to have occurred within the sample during the test. Selected unstabilized specimens were soaked by applying a cell pressure of about 3 psi to the specimen and then a 2.5 psi back pressure to the water reservoir leading to the inside of the sample. The back pressure was left on until water was flowing freely through the inside of the specimen. To simulate a continued wet condition, once a day the tests involving the soaked specimens were stopped, and the specimens were resoaked using the above described procedure. A brief description of the sample condition for each series of tests on each soil is given in Table 6.

Fatigue Tests

The general test set-up used in the fatigue tests is shown in Figure 4. The support and reaction assembly consisted of a steel layout table which was fastened to a heavy steel reaction frame. A layout table was used since its top is surface ground which insures a uniform bearing surface. Two 18-1/2 inch diameter circular rubber pads which were 1.95 inches thick were placed on top of the layout table to simulate a soil subgrade. The static modulus of elasticity of the rubber pad was approximately 800 psi and the corresponding theoretical modulus of subgrade reaction for an 18 inch diameter, rigid plate resting on the surface of a continuous, semi-infinite medium was calculated to be 100 pci.

A repeated load was applied through a rigid 6 inch diameter plate to the specimen using the same type pneumatic system as was used in the repeated load triaxial tests. A thin layer of fine sand was placed between the plate and the specimen to insure application of load over the entire area. The main series of tests were conducted using a repeated load of 1200 pounds in addition to a small seating load which was maintained

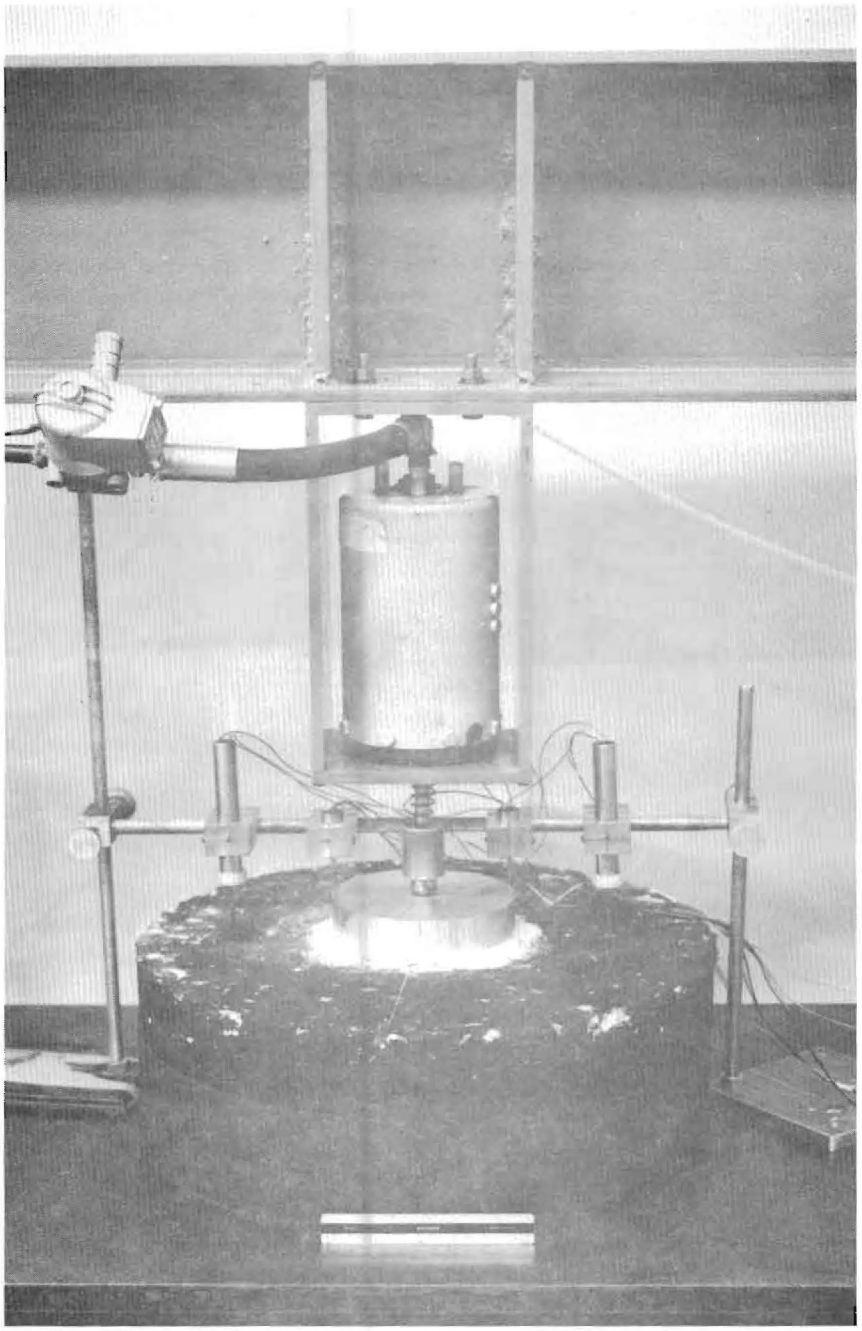

FIGURE 4. FATIGUE TEST APPARATUS

on the specimen throughout the test. Two tests were performed using a 1440 pound repeated loading.

Vertical surface displacements were measured using LVDT's along a diameter of the specimen on each side of the center at three different radii. The transducers were calibrated in a manner similar to that used to calibrate the transducer-recorder system used in the repeated load triaxial tests. Continuous deflection readings were taken until failure of the specimen occurred. At this point the deflection increased rapidly and radial cracks developed on the surface of the specimens.

CHAPTER V

RESILIENT MODULUS TEST RESULTS

The resilient modulus of the layers of the pavement system determine the recoverable deformations and strains which will occur in a pavement structure when subjected to loadings. Fatigue cracking of stabilized layers is influenced by the tensile strain level in the stabilized layer, the temperature and thickness of the layer, and the magnitude and number of wheel load repetitions. Since the value of the resilient modulus has an important influence on the tensile strain in the stabilized layers, it also has an important affect on the fatigue life and hence the performance of the pavement.

The resilient modulus, E_r, is defined as the repeated axial deviator stress applied to the repeated load triaxial test specimens divided by the strain associated with the recoverable bounce. The recoverable bounce is the deformation in the specimen which occurs as the axial deviator stress placed on the sample is removed. The resulting strain is the recoverable bounce divided by the distance over which the bounce occurs. From this definition it follows that the resilient modulus corresponds to a secant modulus of elasticity of the material. An increase in resilient modulus would in general cause a decrease in deflections, stresses and strains and hence increase the fatigue life of the pavement structure.

The relationship between the resilient modulus and the sum of the principal stresses for all base materials tested was found for the stress conditions used to give approximately a straight line relationship on a log-log plot which is in

agreement with the results obtained by other investigators [3]. This relationship can be expressed as

$$E_r = \bar{K}\ \sigma_\theta^{\bar{n}} \quad \ldots\ldots\ldots\ldots\ldots\ldots\ldots \quad (1)$$

Where

E_r = resilient modulus of the material (psi)
σ_θ = sum of principal stress, $\sigma_1+\sigma_2+\sigma_3$ (psi)
$\bar{n}$ = slope of the line on a log-log plot
$\bar{K}$ = a constant defining the vertical position of the line

The straight line curve fits to the experimental resilient moduli data were determined by a linear regression analysis of the data. The correlation coefficients, standard error and the values of $\bar{K}$ and $\bar{n}$ obtained from the regression analysis are tabulated in Table 6, which gives a general summary of the laboratory test results.

The experimental relationships found using the repeated load triaxial test between the resilient modulus, E_r and the sum of the principal stresses, σ_θ acting on the triaxial test specimens are shown in Figure 5 and Figures 7 through 22. Figure 6 shows the relationship between deviator stress and resilient modulus for the silty sand base material tested. All of the test results shown in these figures are for 10,000 load repetitions. The relationship for the modulus of the specimen in both the as compacted and soaked conditions is shown on the same figure for most materials. The resilient modulus test results are summarized in Figures 11, 19, 20 and 22 which give comparisons of the experimentally evaluated elastic response for selected materials and gradations.

Unstabilized Base Materials

As would be expected, the silty sand (Base 1) exhibited the lowest resilient modulus as shown in Figures 5 and 11. Furthermore, the resilient modulus of the silty sand base

TABLE 6. SUMMARY OF ELASTIC AND PLASTIC BASE CHARACTERISTICS EVALUATED FROM REPEATED LOAD TRIAXIAL TESTS

CHARACTERISTICS EVALUATED FROM REPEATED LOAD TRIAXIAL TESTS

BASE	BASE DESCRIPTION	SAMPLE CONDITION	RESILIENT MODULUS, E_r (PSI) 10,000 LOAD APPLICATIONS				PLASTIC STRAIN (%)x10^2 (σ_3 = 0 PSI) DEVIATOR STRESS RATIO @ 100,000 REPETITIONS			RUTTING CHARACTERISTICS	
			$\bar{K}$	$\bar{n}$	Corr. Coeff.	Standard Error (log-log)	2.5	3.5	6.0(1)	RUT INDEX 100,000 REP.	RUT POTENTIAL 1,000,000 REP.
1	Silty Fine Sand	100% GHD-7 Soaked	1855.6 3126.2	0.606 0.371	0.85 0.93	0.080 0.048	114	00	00	Very Large	----
2	Soil Aggregate 40-60 Blend	100% GHD-49 Soaked	2507.1 3825.7	0.624 0.459	0.95 0.98	0.064 0.029	128 128	270 270	780 ---	1050 (extrapolated)	1130
3	Soil Aggregate 40-60 Blend	100% T-180C Soaked	1791.5 3902.6	0.802 0.529	0.92 0.94	0.088 0.059	58 90	120 190	285 ---	405	467
4	Soil Aggregate 17-83 Blend	100% GHD-49 Soaked	3835.5 3145.0	0.534 0.552	0.94 0.98	0.057 0.049	30 36	82 --	250 ---	332	371
5	Soil Aggregate 21-79 Blend	100% GHD-49 Soaked	4982.6 5938.9	0.450 0.365	0.93 1.00	0.048 0.002	30 40	44 64	120 ---	164	202
6	Crushed Porphyrite Granite Gneiss - Source A 3% fines	100% T-180C 95% T-180C Soaked	3746.1 2145.8 2857.5	0.532 0.703 0.632	0.93 0.98 0.99	0.054 0.062 0.032	38 50 70	56 76 114	120 170 ---	176	254
7	Crushed Porphyritic Granite Gneiss - Source A 11.25% fines	100% T-180C 95% T-180C Soaked	1976.9 3359.2 2414.5	0.681 0.539 0.619	0.92 0.96 0.99	0.077 0.059 0.028	38 126 170	72 large large	226 --- ---	298	360
8	Crushed Biotite Granite Gneiss - Source B 3% fines	100% T-180C	1986.7	0.682	0.94	0.095	36	78	100	258	292
9	Crushed Biotite Granite Gneiss - Source B 11.25% fines	100% T-180C	1494.8	0.718	0.91	0.111	46	105	280	385	630
10	Crushed Biotite Granite Gneiss - Source B 22% fines	101.4%T-180C	1491.8	0.731	0.98	0.045	46	105	314	419	520
11	Silty Sand Stabilized with 60% Cement	100% GHD-7	2.51x10^6	-0.444	-0.82	0.096	2	4	36	40	
12	40-60 Blend Soil-Aggregate Stabilized with 2.73% Cement	100% T-180	0.303x 10^6	0.399	0.63	0.1[illegible]	3	5	19	29	
13	Asphalt Concrete A Binder Base - 89° F 72° F	-					27 7	52 12	00 59	Very Large 71	

Note: 1. These values were in most instances extrapolated from laboratory test data.

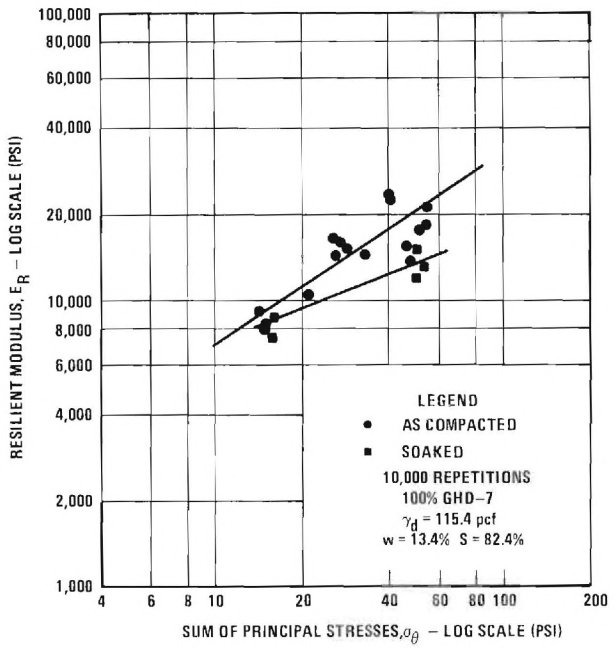

FIGURE 5. INFLUENCE OF STRESS STATE ON RESILIENT MODULUS AFTER 10,000 REPETITIONS FOR A SILTY SAND-BASE 1

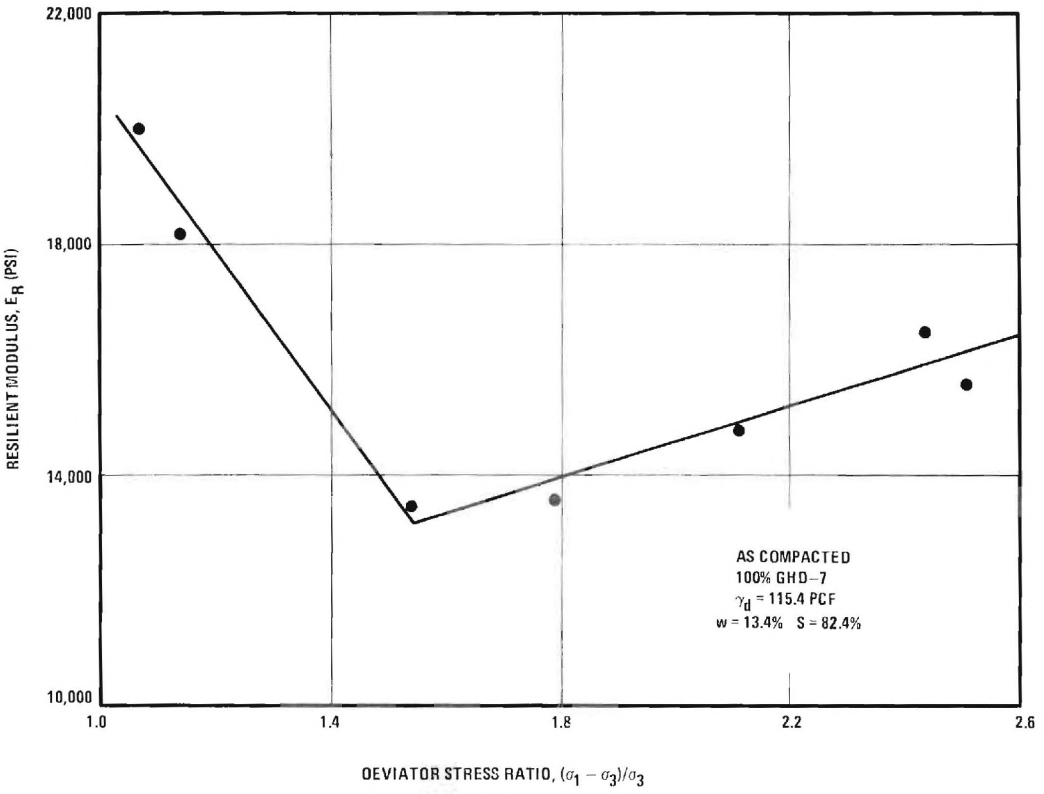

FIGURE 6. EFFECT OF DEVIATOR STRESS ON RESILIENT MODULUS AFTER 10,000 REPETITIONS FOR A SILTY SAND-BASE 1

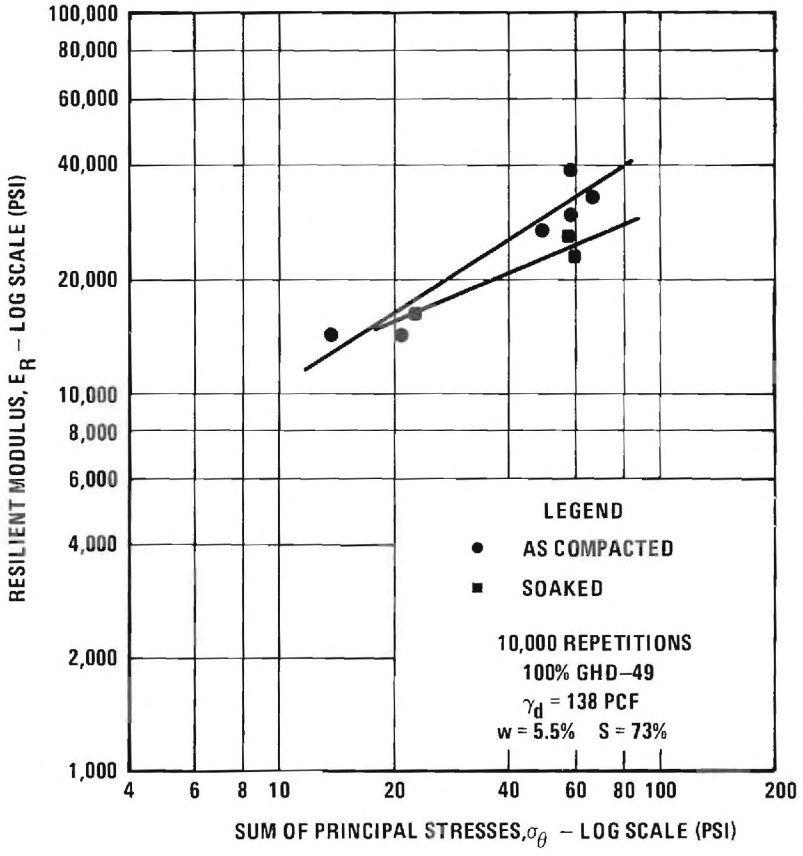

FIGURE 7. INFLUENCE OF STRESS STATE ON RESILIENT MODULUS AFTER 10,000 REPETITIONS FOR A 40–60 BLEND SOIL AGGREGATE–BASE 2

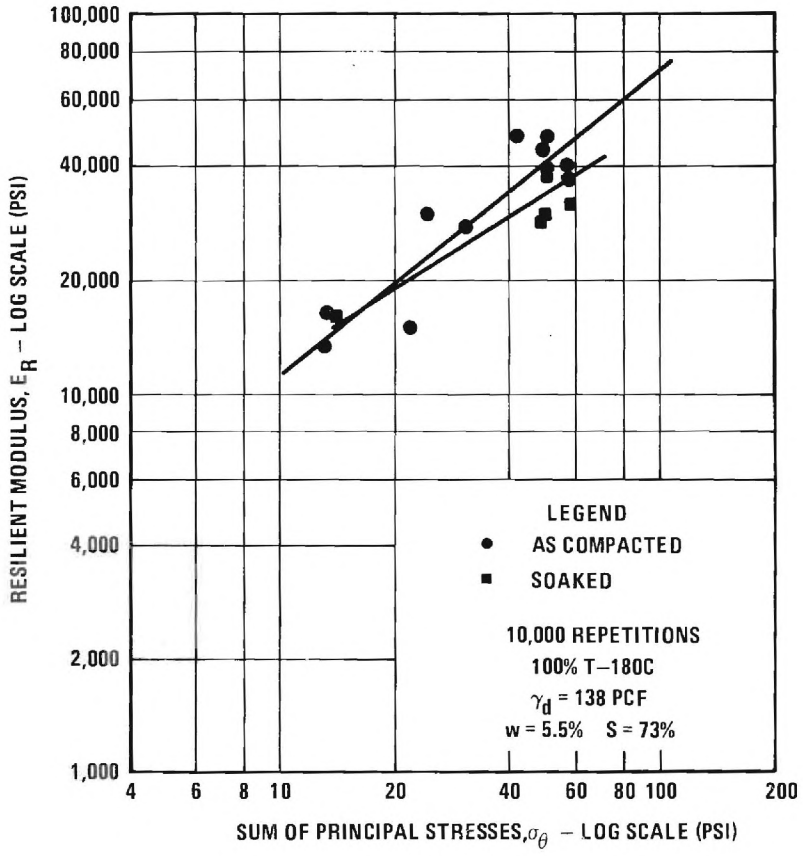

FIGURE 8. INFLUENCE OF STRESS STATE ON RESILIENT MODULUS AFTER 10,000 REPETITIONS FOR A 40–60 BLEND SOIL AGGREGATE–BASE 3

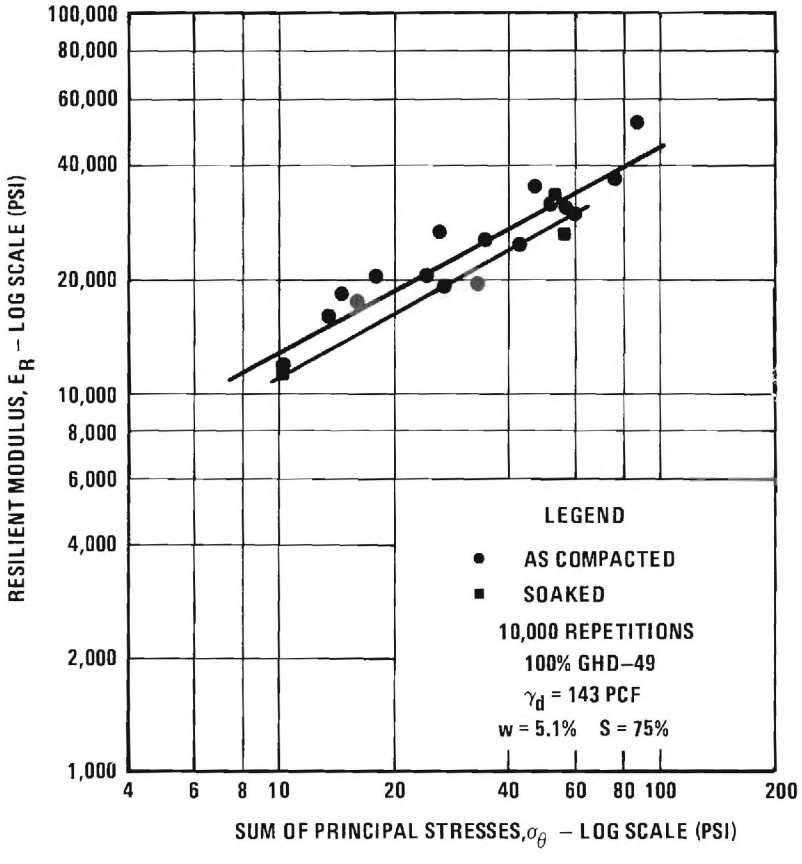

FIGURE 9. INFLUENCE OF STRESS STATE ON RESILIENT MODULUS AFTER 10,000 REPETITIONS FOR A 17–83 BLEND SOIL AGGREGATE–BASE 4

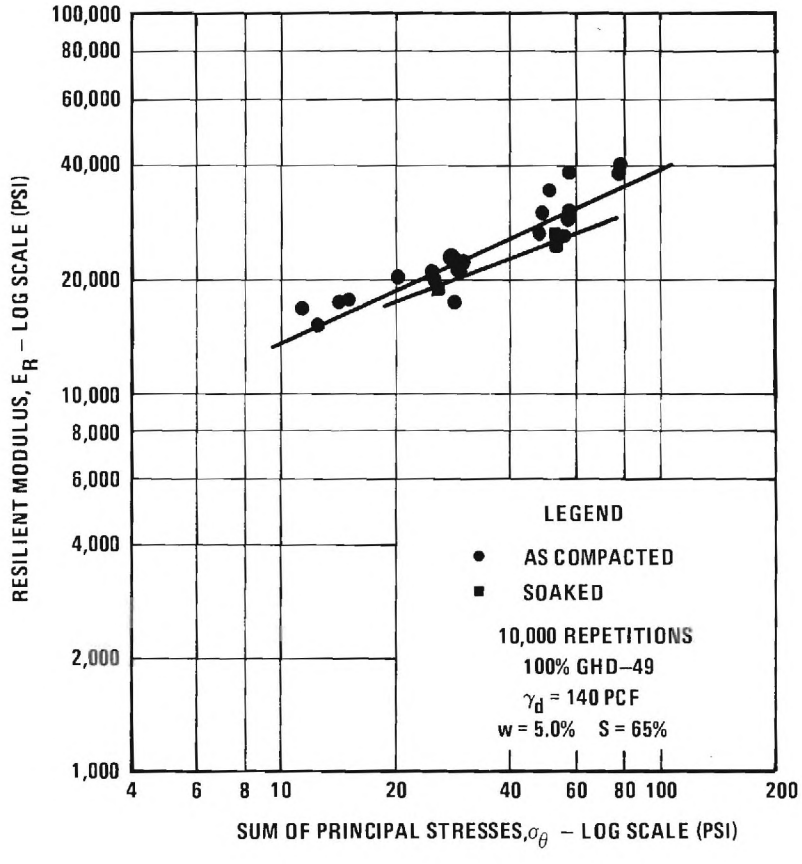

FIGURE 10. INFLUENCE OF STRESS STATE ON RESILIENT MODULUS AFTER 10,000 REPETITIONS FOR A 21–79 BLEND SOIL AGGREGATE–BASE 5

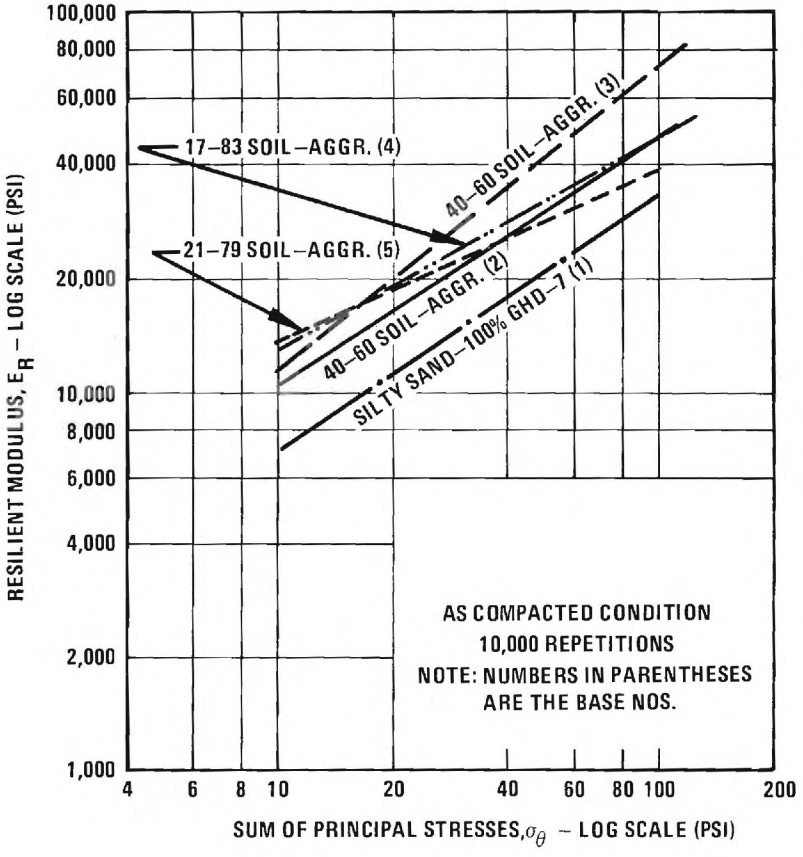

FIGURE 11. COMPARISON OF RELATIONSHIP FOR RESILIENT MODULI FOR SILTY SAND AND SOIL AGGREGATE BASES

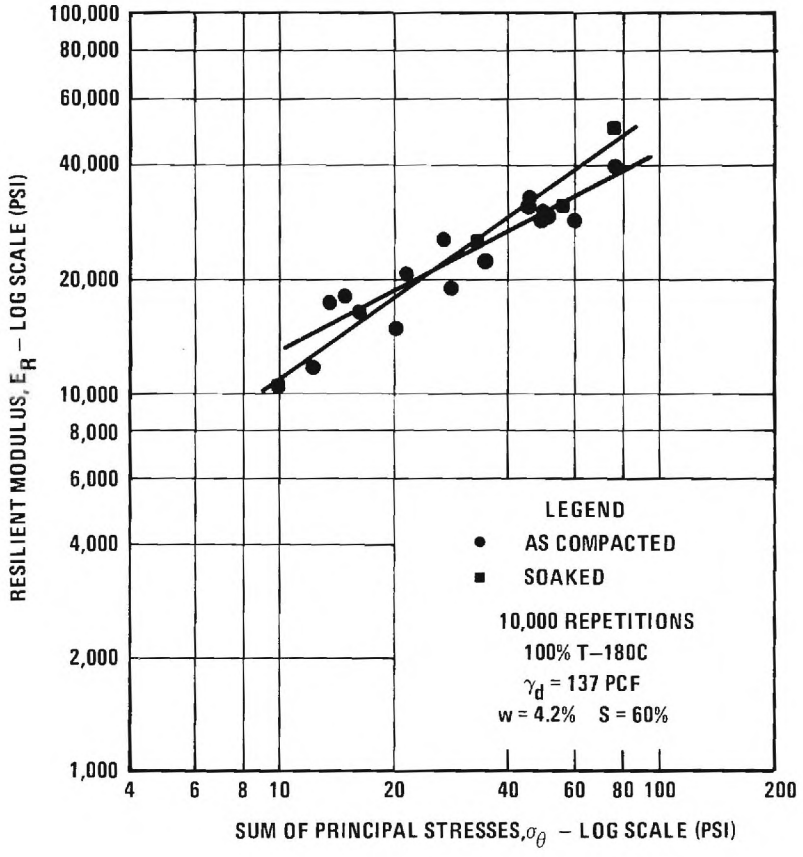

FIGURE 12. INFLUENCE OF STRESS STATE ON RESILIENT MODULUS AFTER 10,000 REPETITIONS IN A CRUSHED PORPHYRITIC GRANITE GNEISS WITH 3 PERCENT FINES–BASE 6

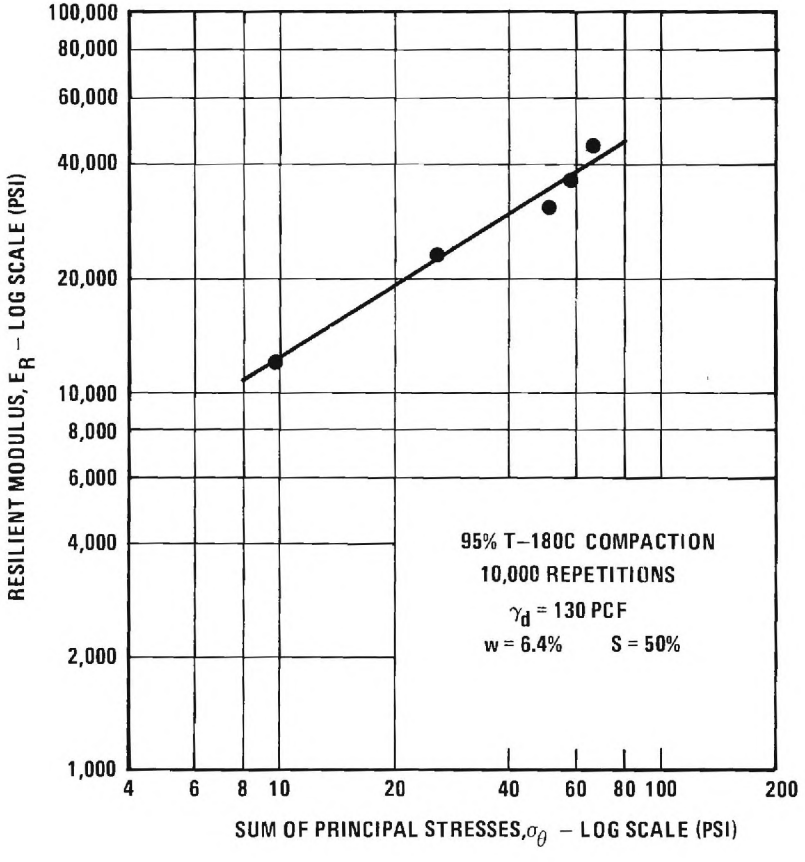

FIGURE 13. INFLUENCE OF STRESS STATE ON RESILIENT MODULUS AFTER 10,000 REPETITIONS IN A CRUSHED PORPHYRITIC GRANITE GNEISS WITH 3 PERCENT FINES AT 95% T–180 COMPACTION–BASE 6

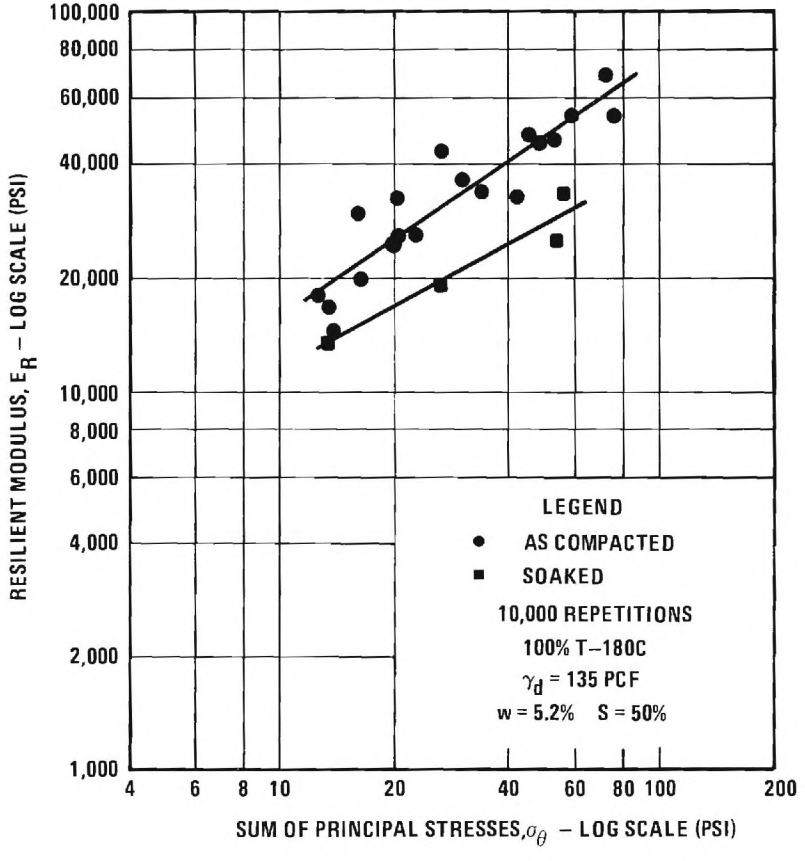

FIGURE 14. INFLUENCE OF STRESS STATE ON RESILIENT MODULUS AFTER 10,000 REPETITIONS FOR A PORPHYRITIC GRANITE GNEISS WITH 11.25 PERCENT FINES–BASE 7

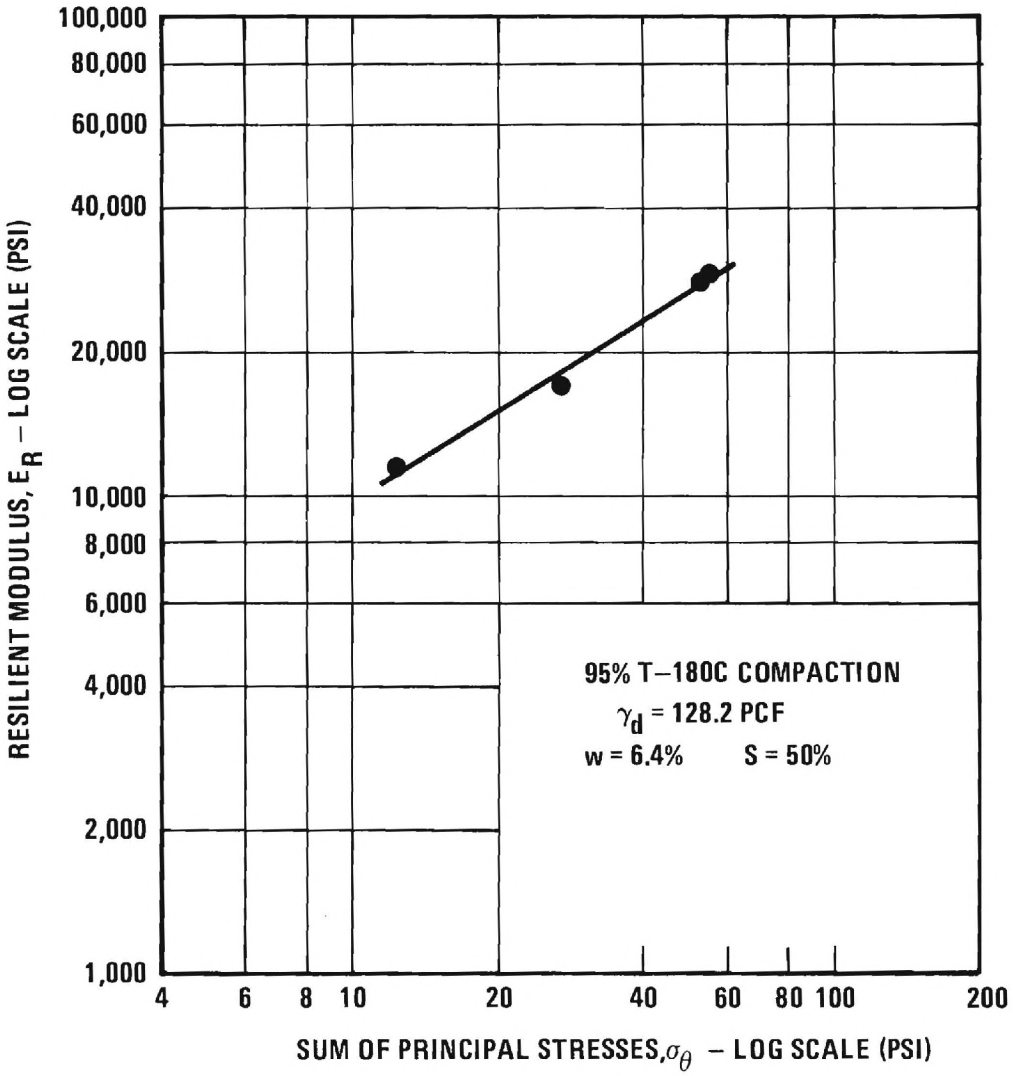

FIGURE 15. INFLUENCE OF STRESS STATE ON RESILIENT MODULUS AFTER 10,000 REPETITIONS IN A CRUSHED PORPHYRITIC GRANITE GNEISS WITH 11.25 PERCENT FINES AT 95% T-180 COMPACTION-BASE 7

underwent the greatest reduction of all base types studied after soaking (Figure 5). This base had the largest percentage of fines and thus should have had the lowest permeability. As a result, under the application of a rapidly applied load pulse, there probably was a larger pore pressure buildup in the silty sand specimens than in the other base materials tested.

The effect of soaking on the resilient modulus E_r of the soil-aggregate bases (Figures 7 through 10) was to significantly reduce its value at higher stress states. As the sum of the principal stresses decreased the effect of soaking became progressively less until at very low stress states which are more representative of the insitu conditions the as compacted and soaked moduli were very nearly the same. An exception to this occurred in Base 4 (Figure 9) which exhibited in the soaked condition a E_r-σ_θ relationship on the log-log plot that was almost parallel but somewhat lower than the as compacted relationship.

A summary comparison of the resilient behavior of the silty sand and soil-aggregate bases for specimens tested in the as compacted condition is given in Figure 11. The silty sand, as would be expected, exhibited the lowest resilient moduli characteristics for all stress states tested. At the lower values of stress state, σ_θ the nominal 20-80 soil-aggregate bases gave higher values of E_r and hence performed slightly better than did the 40-60 blend soil aggregate bases probably due to the greater influence of friction in the 20-80 blend bases. Since moderate to relatively low stress states are probably more typical of the stress conditions in a base, the 20-80 soil-aggregate bases would be expected to exhibit slightly higher resilient moduli than would the 40-60 blends tested. At higher stress states the 40-60 blends resulted in larger resilient moduli probably due to an increase in the influence of cohesion and viscous effects at the greater values of σ_θ.

The modulus relationships obtained for the crushed stone bases are presented in Figures 12 through 19. The test results on the soaked granular bases showed that as the percent fines increased, the resilient modulus in the soaked condition progressively decreased below the value observed for the as compacted condition. For example, the granular base tested having only three percent fines showed very little effect of soaking on the resilient modulus (Figure 12), but with 11.25 percent fines the effect of soaking had become considerably greater (Figure 14).

A comparison of the effect on resilient modulus of an increase in fines in a crushed biotite granite gneiss is shown in Figure 19 for the as compacted condition. An important reduction in resilient modulus was found to occur as the fines were increased from 3 to 11.25 percent. With a further increase in fines from 11.25 to 22 percent a slight increase was observed in the resilient modulus. This increase was probably a result of the greater density of the specimens having 22 percent fines (101.4% T-180) instead of 100 percent for the other specimens.

The comparisons shown in Figures 11 and 20 indicate that in general the resilient characteristics of the soil-aggregate bases in the as compacted condition are on the average slightly superior to the crushed stone bases. The resilient moduli of the crushed porphyritic granite gneiss (Stone A) was found to be greater than that of a crushed biotite granite gneiss (Stone B) at the same stress state for both 3 and 11.25 percent fines (compare Figures 12 and 14 with Figures 16 and 17). The greatest difference in moduli occurred in the specimens having 3 percent fines at lower values of the sum of the principal stresses. One reason for this difference was a result of the crushed porphyritic granite gneiss being more angular and having a rougher surface texture than did the biotite granite gneiss. Furthermore, although the same gradations were

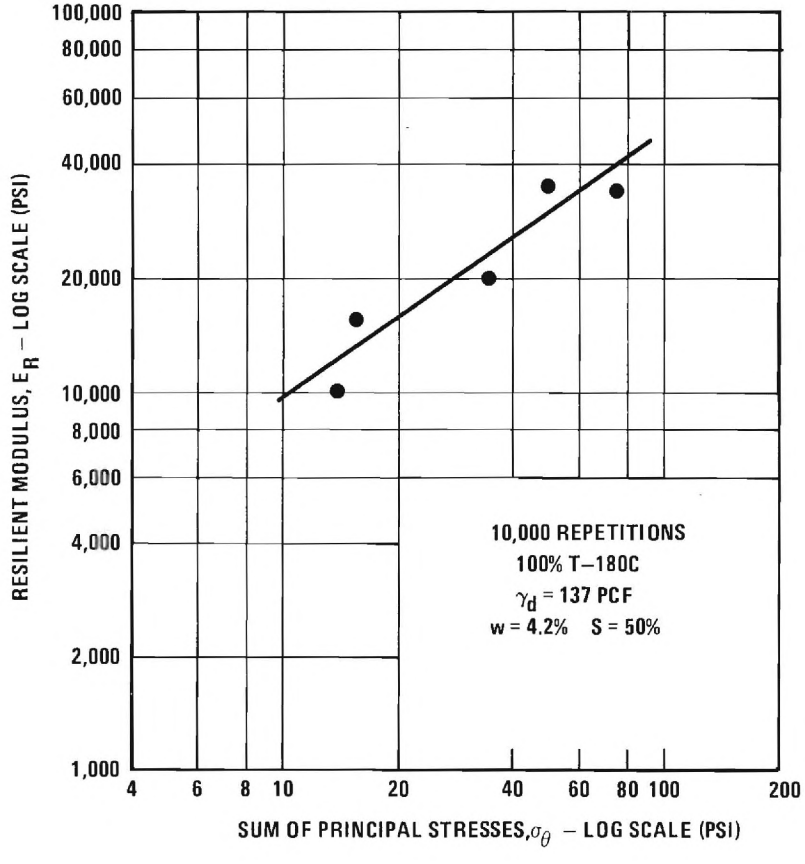

FIGURE 16. INFLUENCE OF STRESS STATE ON RESILIENT MODULUS AFTER 10,000 REPETITIONS IN A CRUSHED BIOTITE GRANITE GNEISS WITH 3 PERCENT FINES–BASE 8

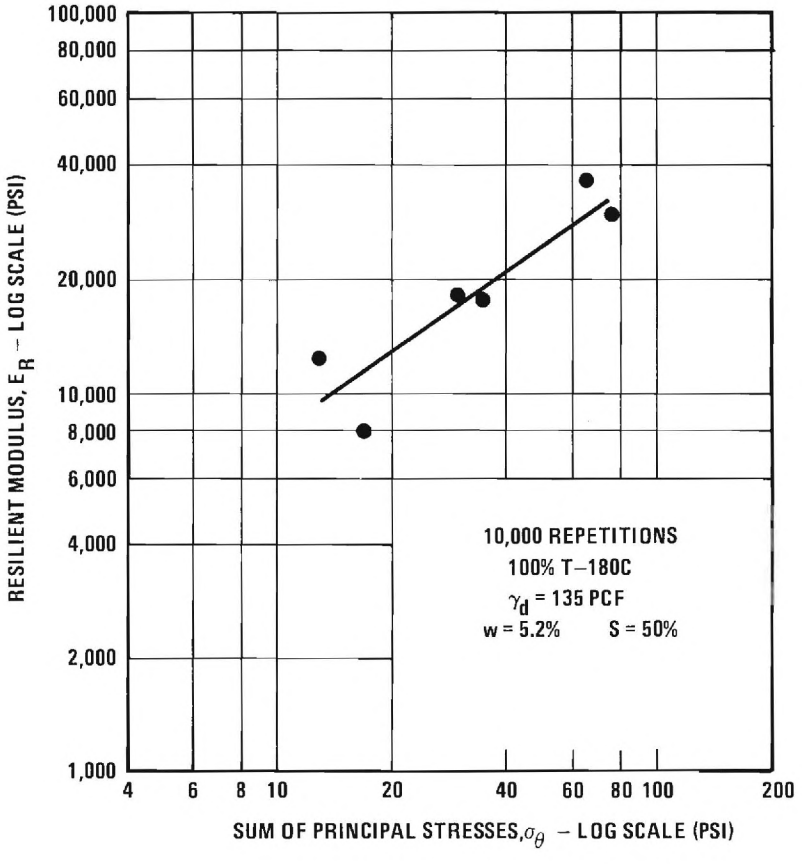

FIGURE 17. INFLUENCE OF STRESS STATE ON RESILIENT MODULUS AFTER 10,000 REPETITIONS FOR A CRUSHED BIOTITE GRANITE GNEISS WITH 11.25 PERCENT FINES–BASE 9

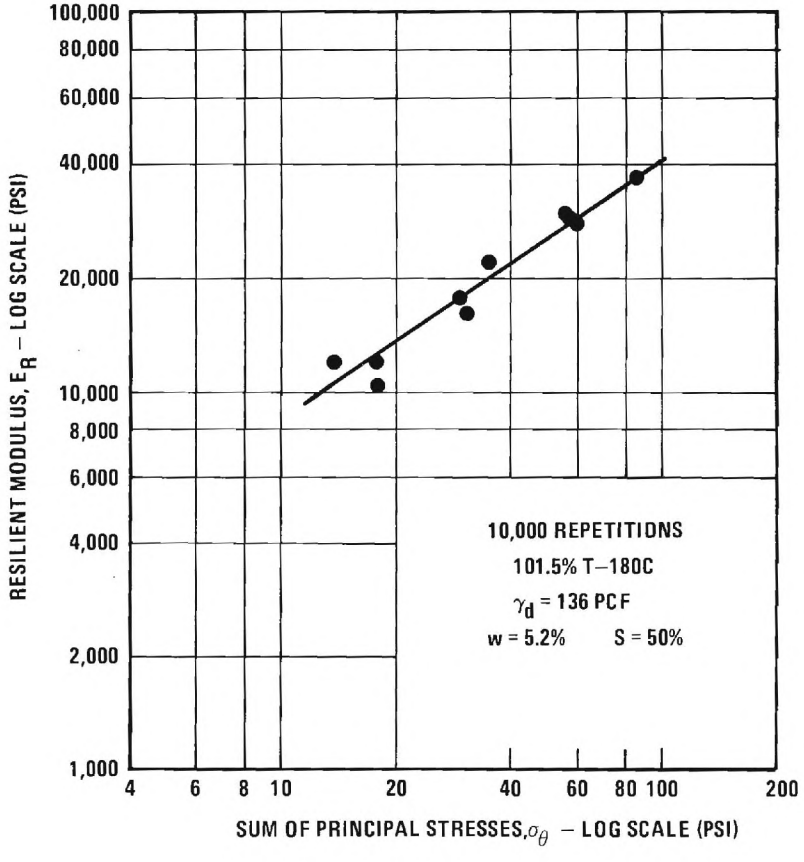

FIGURE 18. INFLUENCE OF STRESS STATE ON RESILIENT MODULUS AFTER 10,000 REPETITIONS FOR A CRUSHED BIOTITE GRANITE GNEISS WITH 22 PERCENT FINES–BASE 10

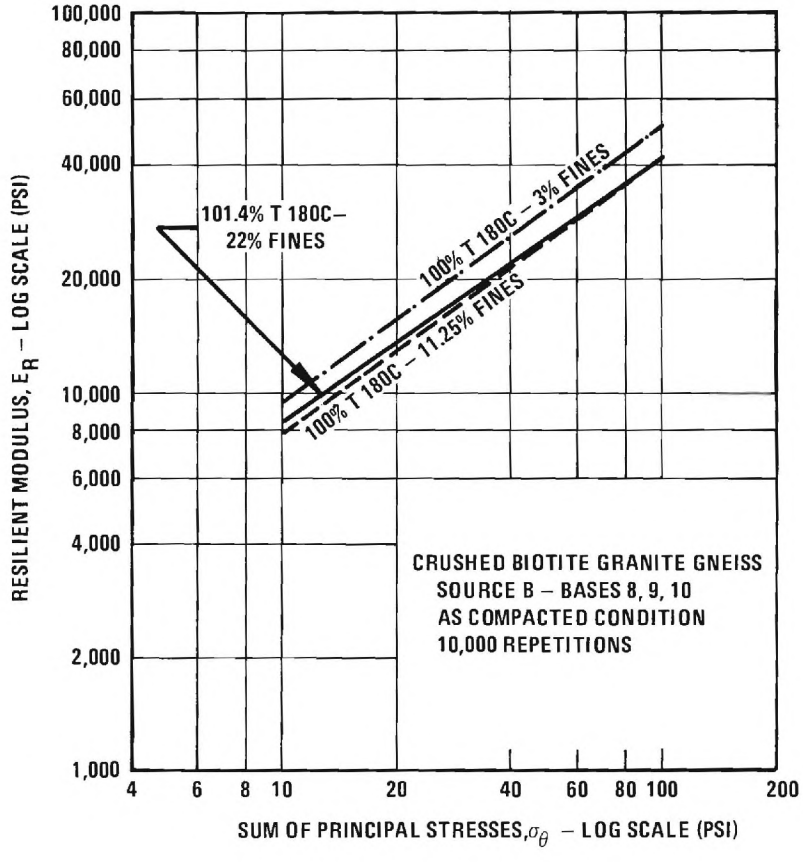

FIGURE 19. INFLUENCE OF FINES ON RESILIENT MODULI FOR A CRUSHED BIOTITE GRANITE GNEISS

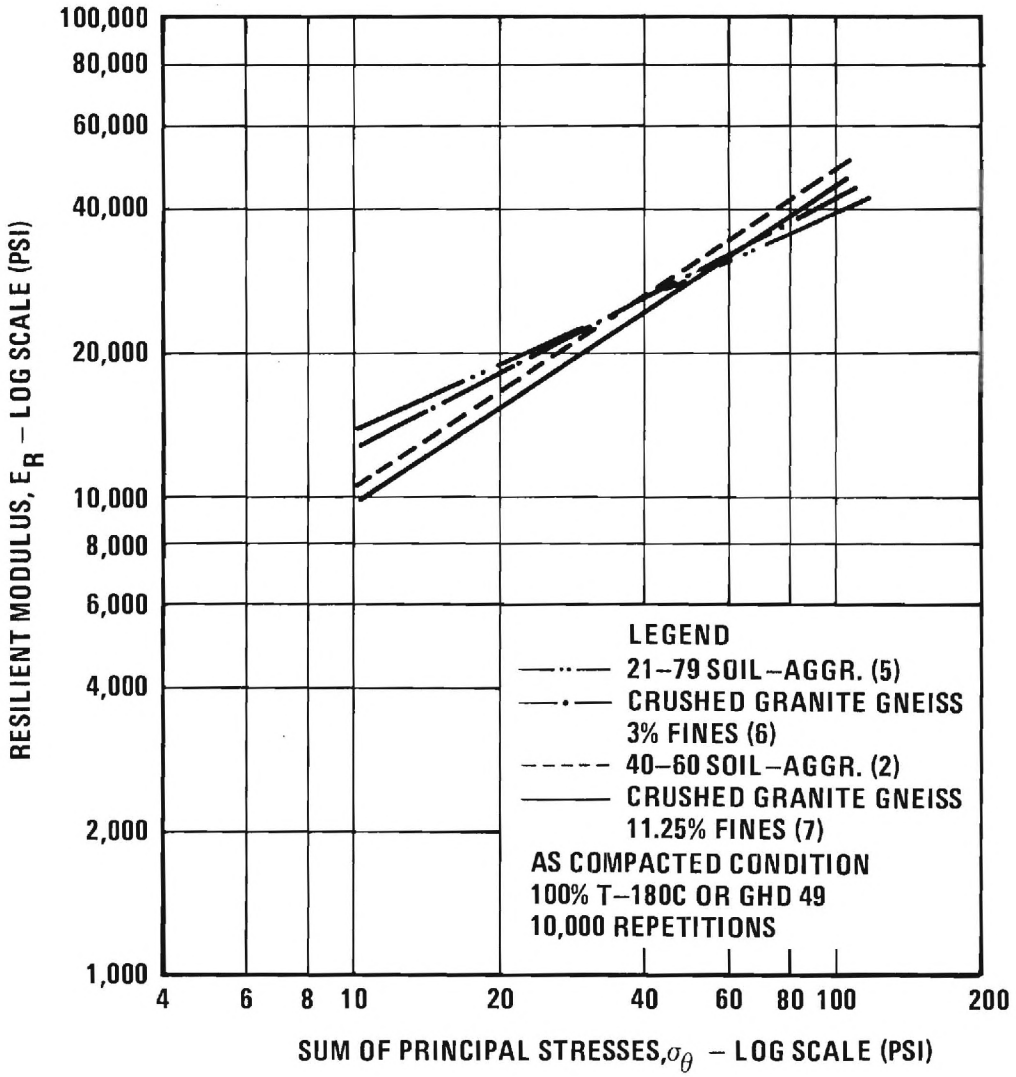

FIGURE 20. COMPARISON OF RESILIENT MODULUS FOR SELECTED SOIL-AGGREGATE AND CRUSHED STONE BASES

specified, the prophyritic granite gneiss apparently broke in the crusher so as to give a larger size of stone between each set of sieves.

Stabilized Base Materials

A comparison is shown in Figure 21 of the resilient modulus relationship determined for the soil-cement (Base 11) and the cement stabilized, 40-60 soil-aggregate (Base 12). The resilient modulus of the cement stabilized soil-aggregate base is about the same as that of the soil-cement base at a principal stress sum of about 10 psi. As the principal stress sum becomes greater, however, the two lines diverge with the resilient modulus of the cement stabilized soil-aggregate gradually becoming considerably larger than that of the soil-cement base. The laboratory evaluated moduli of the cement stabilized bases is approximately 10 to 100 times greater than the moduli of the unstabilized materials. The fact that the repeated load test does not simulate effects of gradual deterioration in the field of stabilized materials should be subjectively considered in interpreting the test results. The resilient moduli of the asphalt concrete base for 72 and 89° F are compared in Figure 22 with the moduli for the soil-cement and cement stabilized soil-aggregate bases. The asphalt concrete is seen to have a modulus for both temperatures considerably less than that of the cement stabilized bases.

Discussion

The moduli given for both the unstabilized and stabilized granular materials will be used in Chapter 8 to evaluate the fatigue life of pavement sections utilizing these base materials. The resilient moduli by themselves are hard to interpret in terms of quantitative effect on performance. When this data however is used together with a nonlinear layered system theory, the effect of changes in the resilient modulus on the fatigue life of a pavement structure can be readily evaluated.

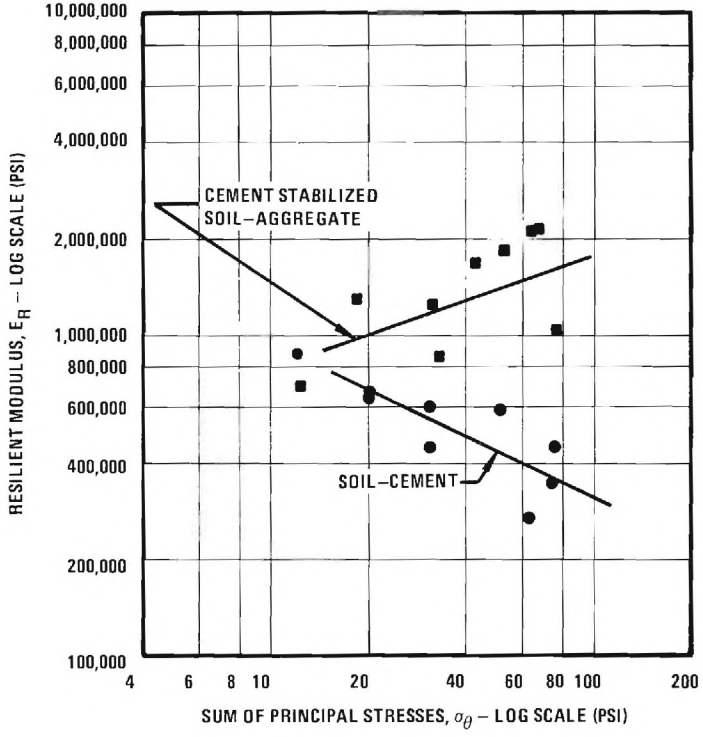

FIGURE 21. INFLUENCE OF STRESS STATE ON RESILIENT MODULI OF SOIL–CEMENT (BASE 11) AND CEMENT STABILIZED SOIL–AGGREGATE (BASE 12)

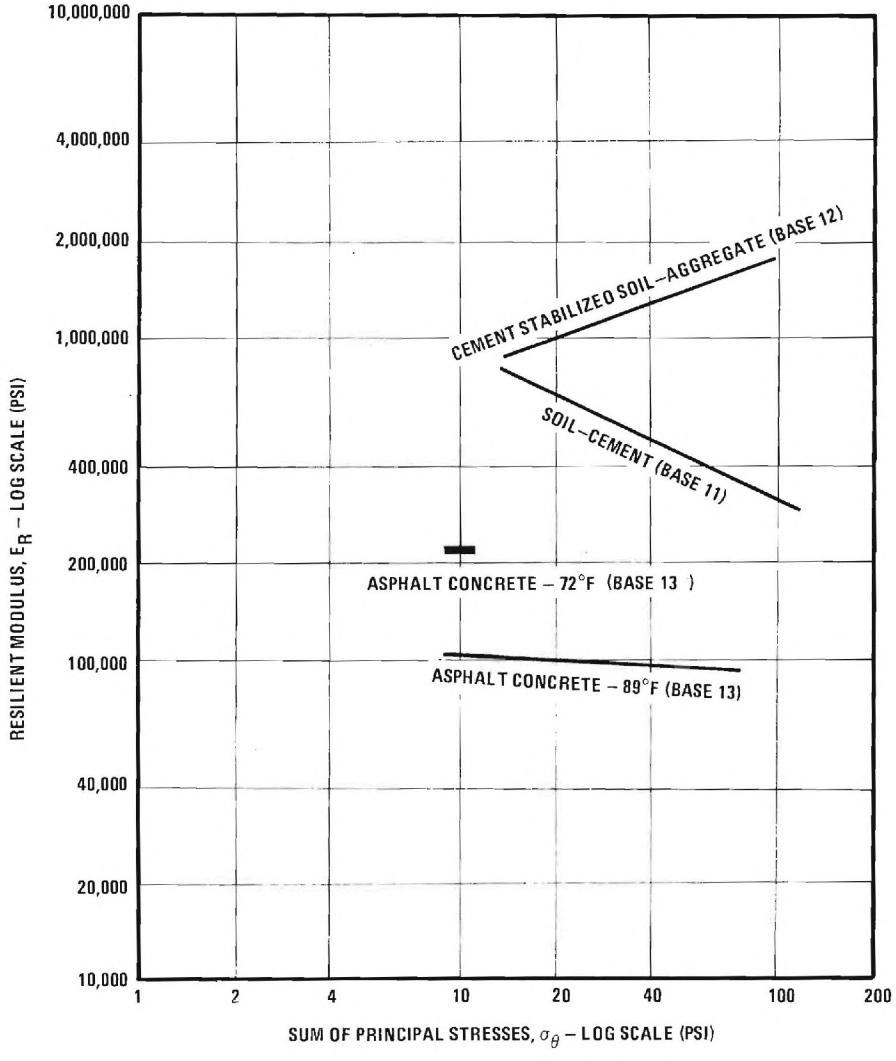

FIGURE 22. COMPARISON OF RESILIENT MODULUS FOR STABILIZED BASE MATERIALS

CHAPTER VI

PLASTIC STRAIN TEST RESULTS

Summary of Test Results

A typical relationship between the axial plastic strain occurring in the cylindrical specimens and the number of load applications for varying deviator stresses is shown in Figure 23. The plastic strain accumulates approximately logarithmically with the number of load applications. For very low deviator stresses, the rate of accumulation of plastic strain tends to decrease as the number of load applications increase. As the deviator stress increases a critical value is reached beyond which the rate of strain development tends to increase with increasing numbers of load repetitions. Furthermore, after a relatively large number of load repetitions the specimen may undergo an unexpected increase in the rate of plastic strain accumulation.

To study rutting in pavement systems in a rational manner the results given in Figure 23 can be plotted as plastic stress-strain curves (Figure 24). These curves are analogous to the stress-strain curves obtained from a series of static tests performed at varying confining pressures. For an arbitrarily selected number of load applications (in this instance 100,000 repetitions), a plot is made of the plastic strain as a function of deviator stress and confining pressure. Comparison of the plastic stress-strain response for different densities, water contents and materials permits an evaluation of the rutting characteristics for different materials when subjected to a given number of load applications.

Figures 24 through 45 show the plastic stress-strain response at 100,000 load repetitions for each base material tested in this investigation; these results are also summarized

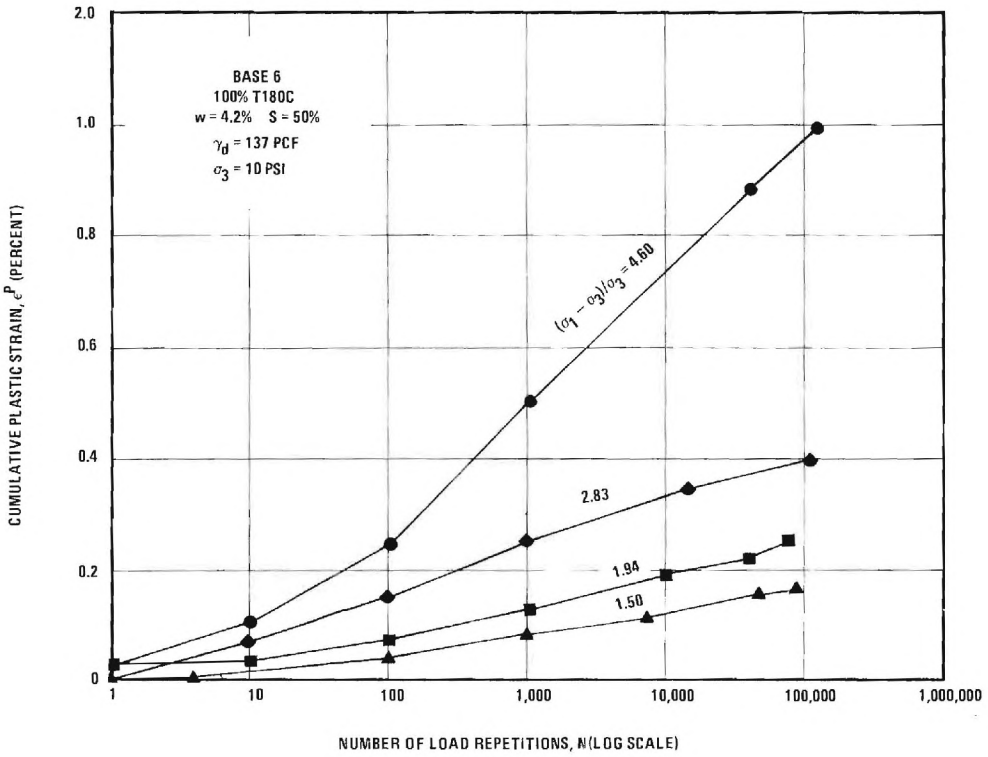

FIGURE 23. INFLUENCE OF NUMBER OF LOAD REPETITIONS AND DEVIATOR STRESS RATIO ON PLASTIC STRAIN IN A PORPHYRITE GRANITE GNEISS-THREE PERCENT FINES

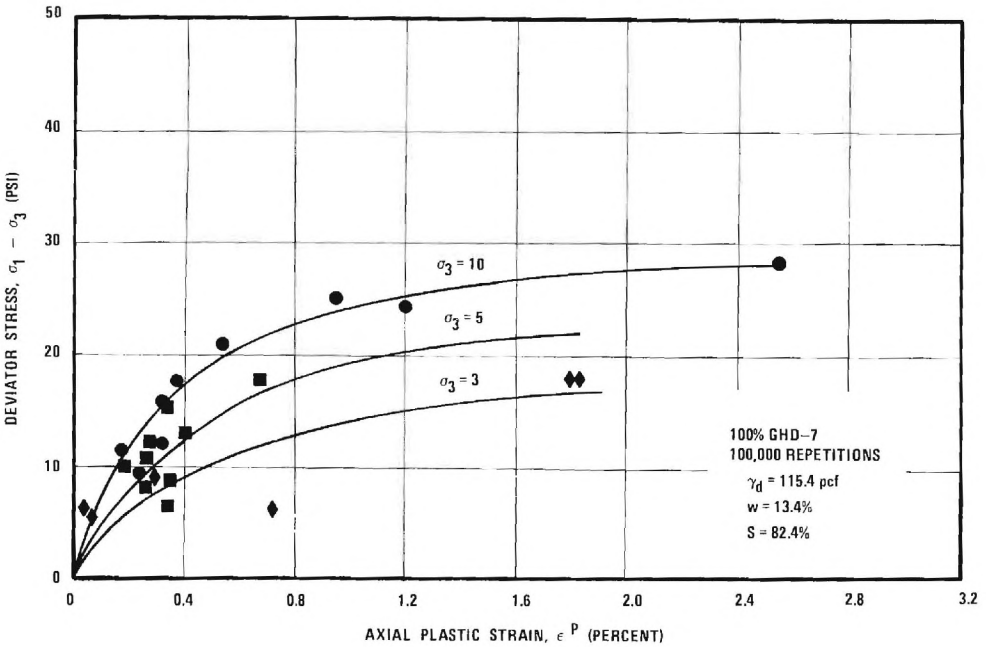

FIGURE 24. INFLUENCE OF DEVIATOR STRESS AND CONFINING PRESSURE ON PLASTIC STRAIN AFTER 100,000 REPETITIONS IN A FINE SILTY SAND-BASE 1

in Table 6. The plastic stress-strain curves shown in the figures exhibit a typical nonlinear response. At a given confining pressure and at small values of deviator stress, plastic strain is almost proportional to the deviator stress. As the deviator stress increases, the development of plastic strain increases at an increasing rate until the plastic strains become very large as the apparent yield stress of the material is reached for the number of repetitions under consideration. Plastic strain is also strongly dependent upon the confining pressure, undergoing a significant decrease as the confining pressure increases.

A summary comparison of the plastic stress-strain characteristics of the unstabilized and stabilized base course materials investigated is given in Figures 40 and 45, respectively, for a confining pressure of 10 psi. Although the average confining pressure in a typical pavement structure is probably less than 10 psi, the comparisons are shown for this value since these stress-strain curves were more well defined. The materials compared in Figure 40 were compacted to 100 percent of AASHO T-180 density or its approximate equivalent (GHD-49) except for the silty sand which was compacted to 100 percent of GHD-7 density which is approximately equivalent to T-99 density.

Effect of Unstabilized Base Type

The base materials exhibiting by far the greatest plastic strains were Base No. 1, a fine silty sand and Base No. 2 which was a 40-60 blend soil-aggregate. For deviator stress ratios greater than 2.5[1] the measured plastic strains in the silty sand were larger than those in the 40-60 blend soil-aggregate. Base 3, also a 40-60 soil-aggregate base, exhibited approximately one-half the plastic strains occurring in the first 40-60 soil-aggregate base due apparently to slight

1. The deviator stress ratio, $(\sigma_1 - \sigma_2)/\sigma_3$ is defined as the ratio of the deviator stress, $\sigma_1 - \sigma_3$ to the confining pressure, σ_3

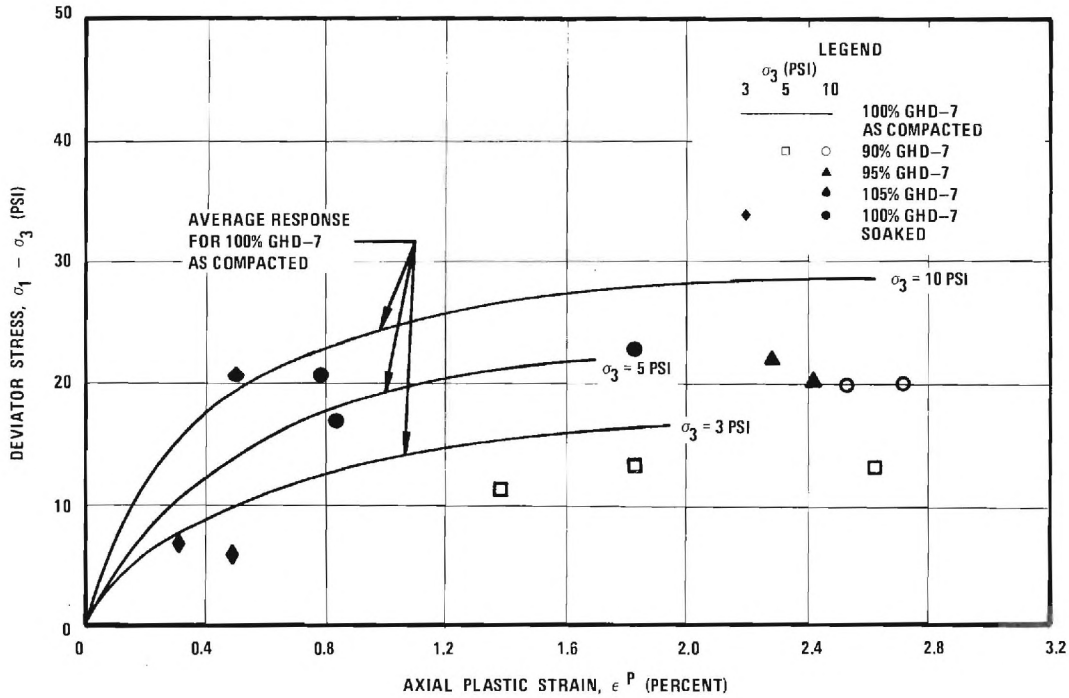

FIGURE 25. EFFECT OF SOAKING AND DEGREE OF COMPACTION ON PLASTIC STRAIN IN A SILTY SAND-BASE 1

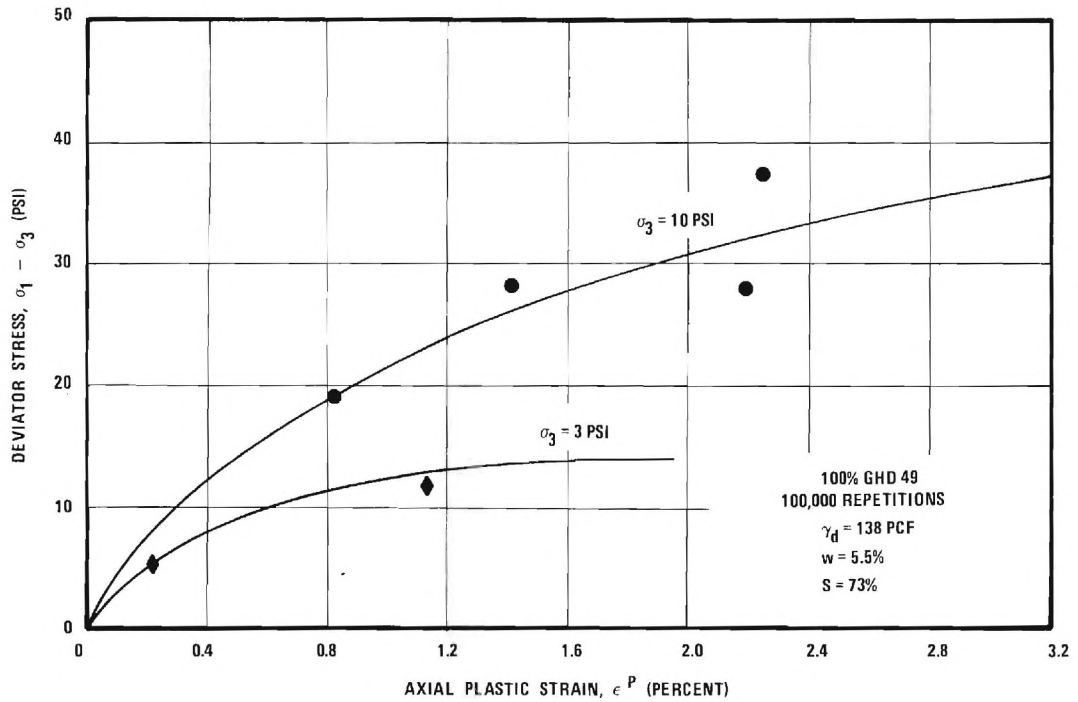

FIGURE 26. INFLUENCE OF DEVIATOR STRESS AND CONFINING PRESSURE ON PLASTIC STRAIN AFTER 100,000 REPETITIONS IN A 40-60 BLEND SOIL AGGREGATE-BASE 2

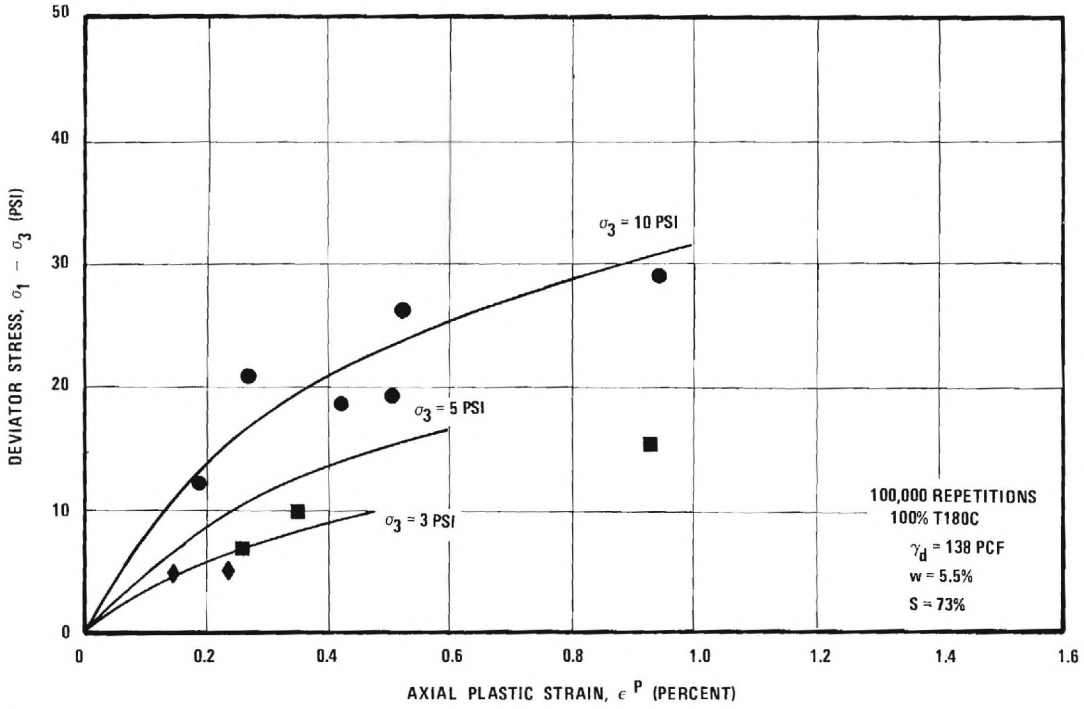

FIGURE 27. INFLUENCE OF DEVIATOR STRESS AND CONFINING PRESSURE ON PLASTIC STRAIN AFTER 1,000,000 REPETITIONS IN A 40-60 BLEND SOIL AGGREGATE-BASE 3

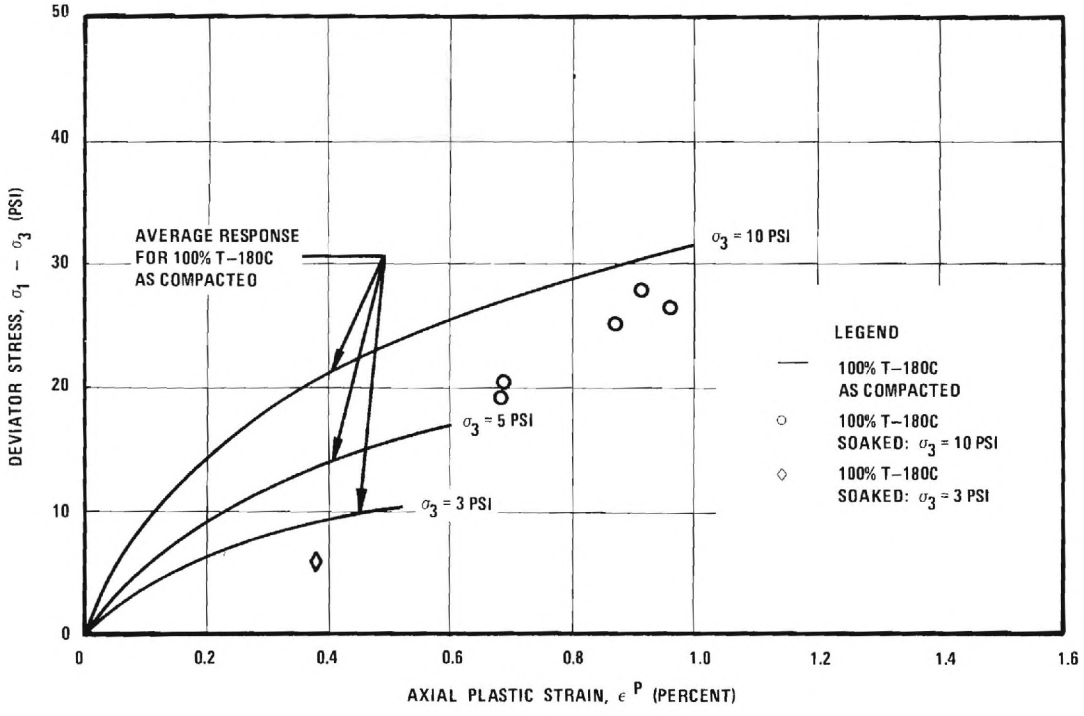

FIGURE 28. INFLUENCE OF SOAKING ON PLASTIC STRAIN IN A 40-60 BLEND SOIL AGGREGATE-BASE 3

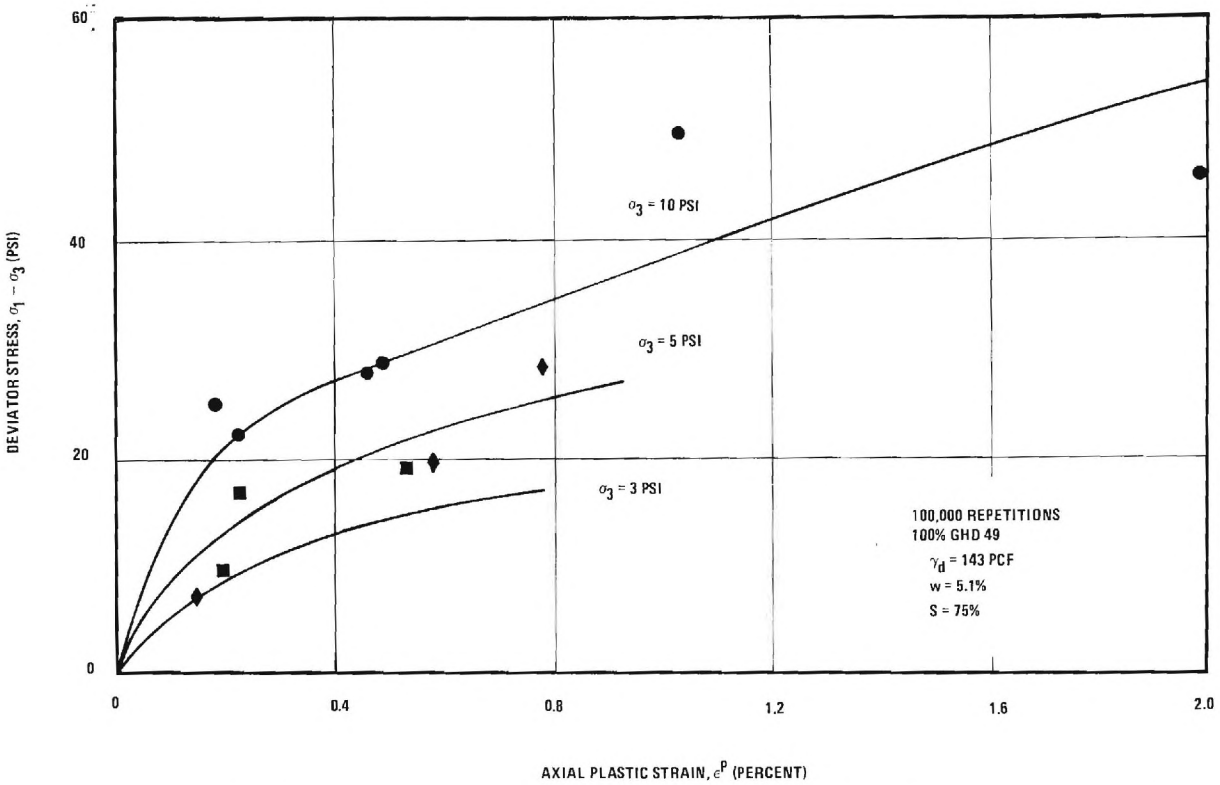

FIGURE 29. INFLUENCE OF DEVIATOR STRESS AND CONFINING PRESSURE ON PLASTIC STRAIN AFTER 100,000 REPETITIONS IN A 17-83 BLEND SOIL AGGREGATE-BASE 4

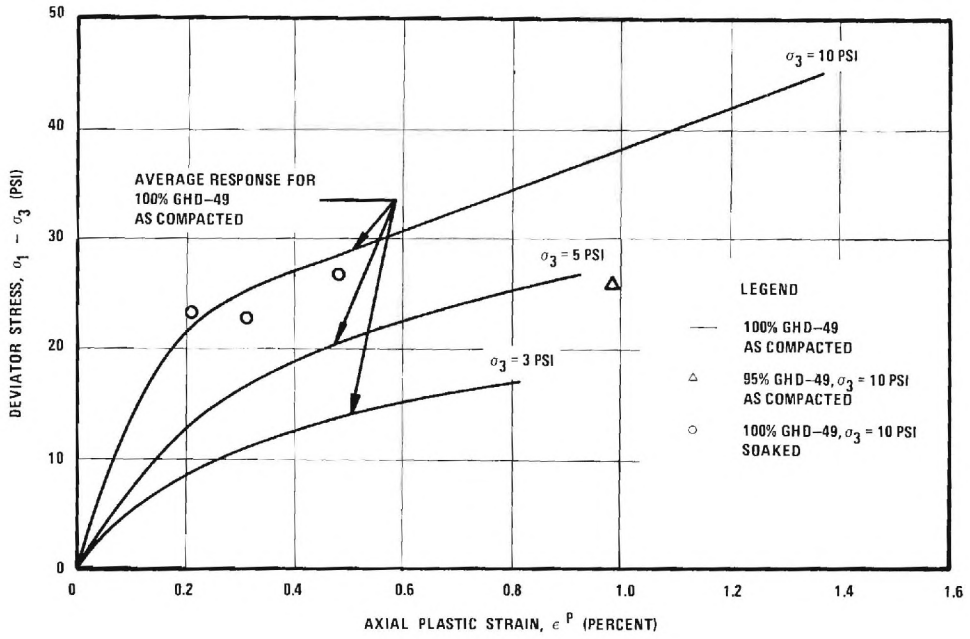

FIGURE 30. INFLUENCE OF SOAKING AND 95 PERCENT COMPACTION ON PLASTIC STRAIN IN A 17-83 BLEND SOIL AGGREGATE-BASE 4

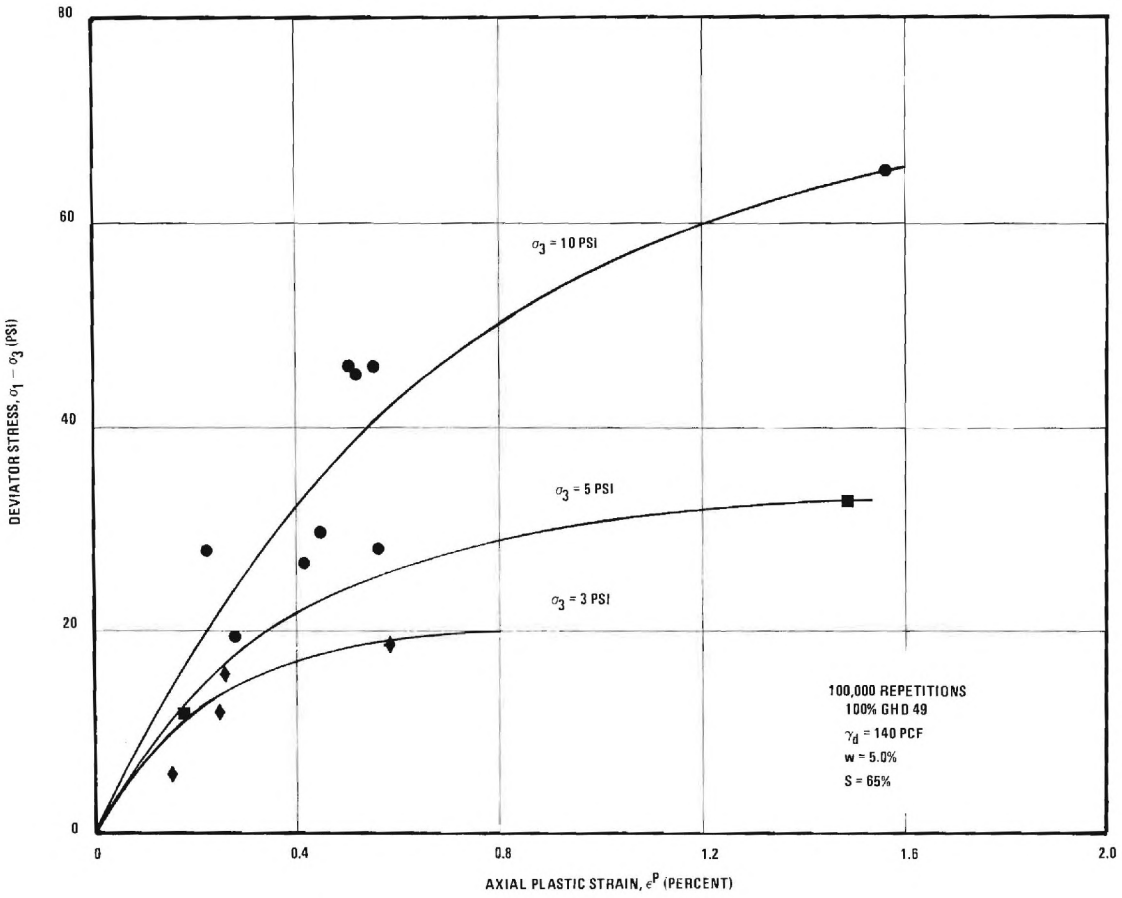

FIGURE 31. INFLUENCE OF DEVIATOR STRESS AND CONFINING PRESSURE ON PLASTIC STRAIN AFTER 100,000 REPETITIONS IN A 21-79 BLEND SOIL AGGREGATE-BASE 5

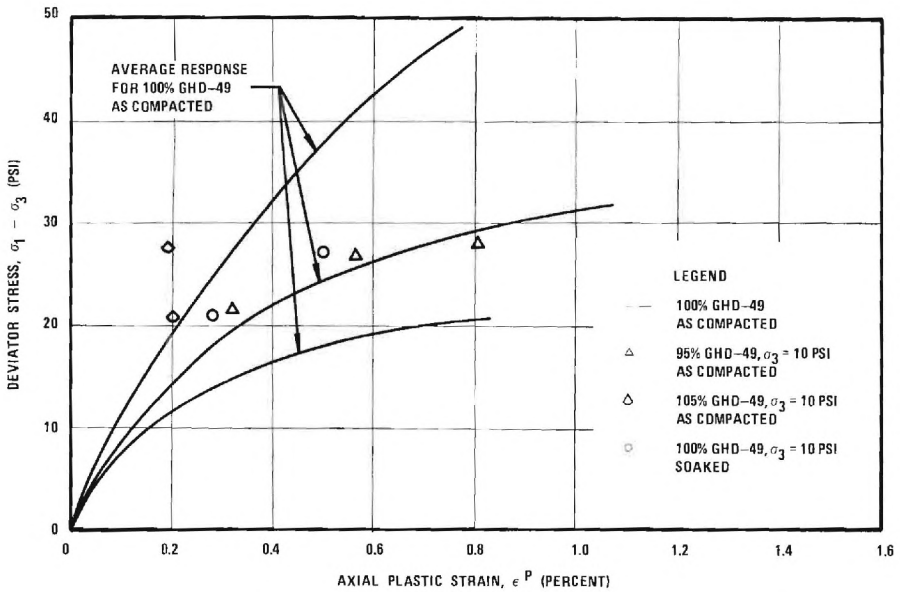

FIGURE 32. INFLUENCE OF SOAKING AND DEGREE OF COMPACTION ON PLASTIC STRAIN IN A 21-79 BLEND SOIL AGGREGATE-BASE 5

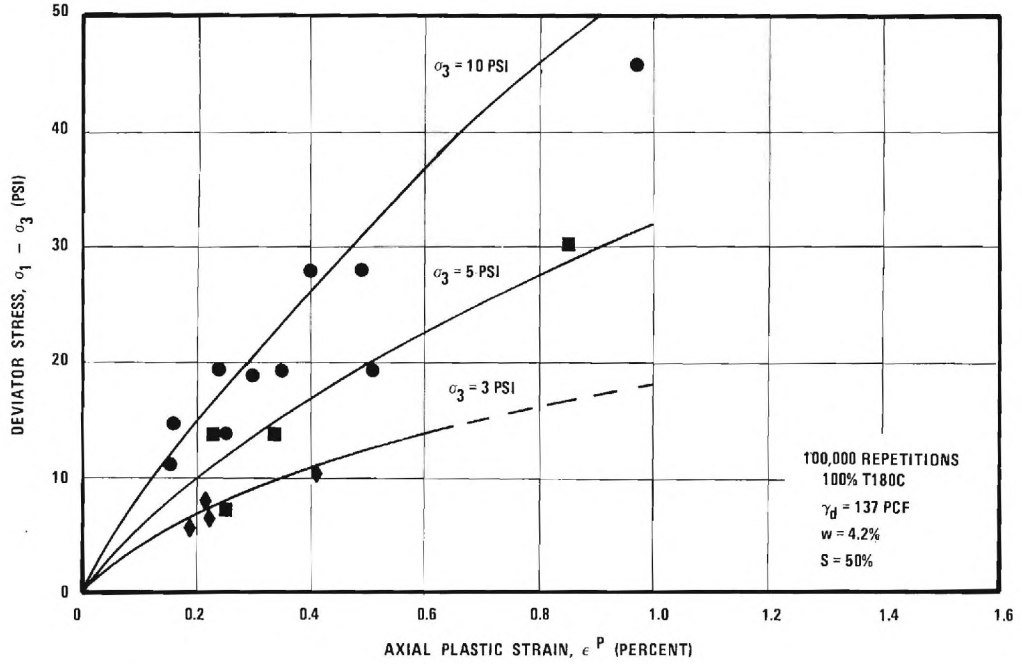

FIGURE 33. INFLUENCE OF DEVIATOR STRESS AND CONFINING PRESSURE ON PLASTIC STRAIN AFTER 100,000 REPETITIONS IN A CRUSHED PORPHYRITE GRANITE GNEISS WITH 3 PERCENT FINES-BASE 6

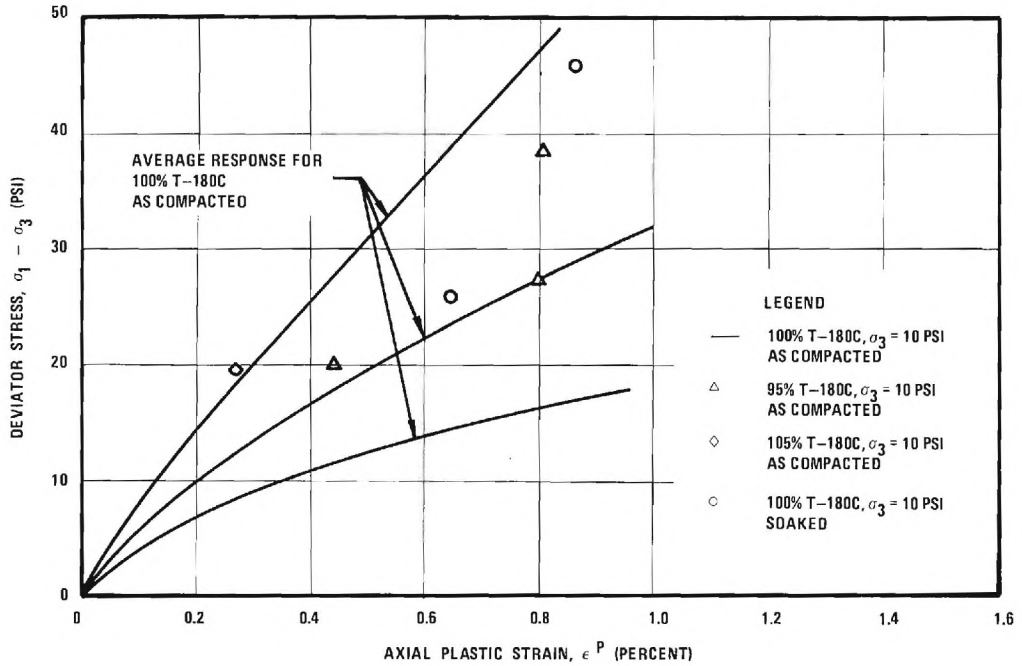

FIGURE 34. INFLUENCE OF SOAKING AND DEGREE OF COMPACTION ON PLASTIC STRAINS IN A CRUSHED PORPHYRITIC GRANITE GNEISS WITH 3 PERCENT FINES-BASE 6

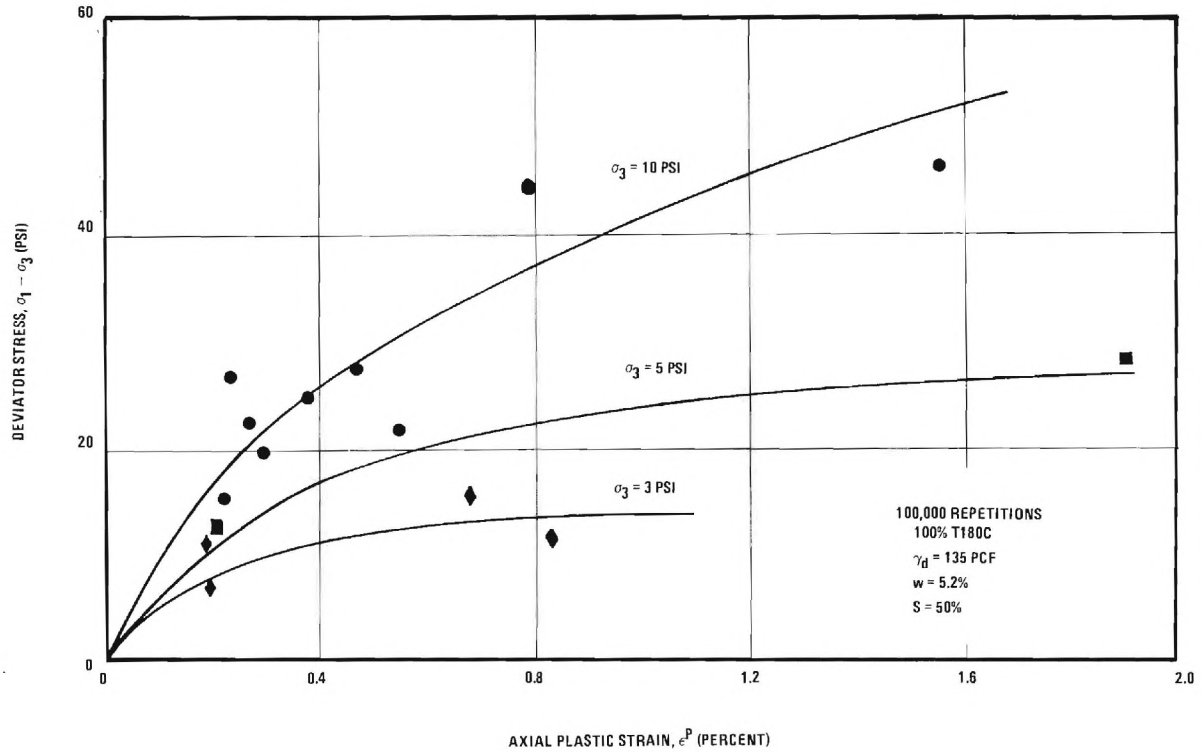

FIGURE 35. INFLUENCE OF DEVIATOR STRESS AND CONFINING PRESSURE ON PLASTIC STRAIN AFTER 100,000 REPETITIONS IN A PORPHYRITIC GRANITE GNEISS WITH 11.25 PERCENT FINES-BASE 7

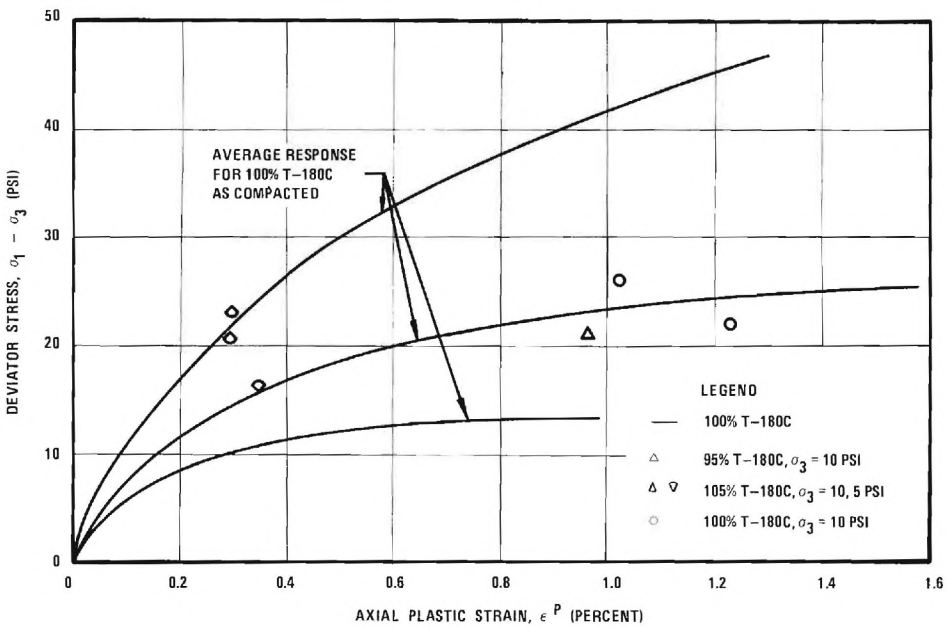

FIGURE 36. INFLUENCE OF SOAKING AND DEGREE OF COMPACTION ON PLASTIC STRAIN IN A PORPHYRITIC GRANITE GNEISS WITH 11.25 PERCENT FINES-BASE 7

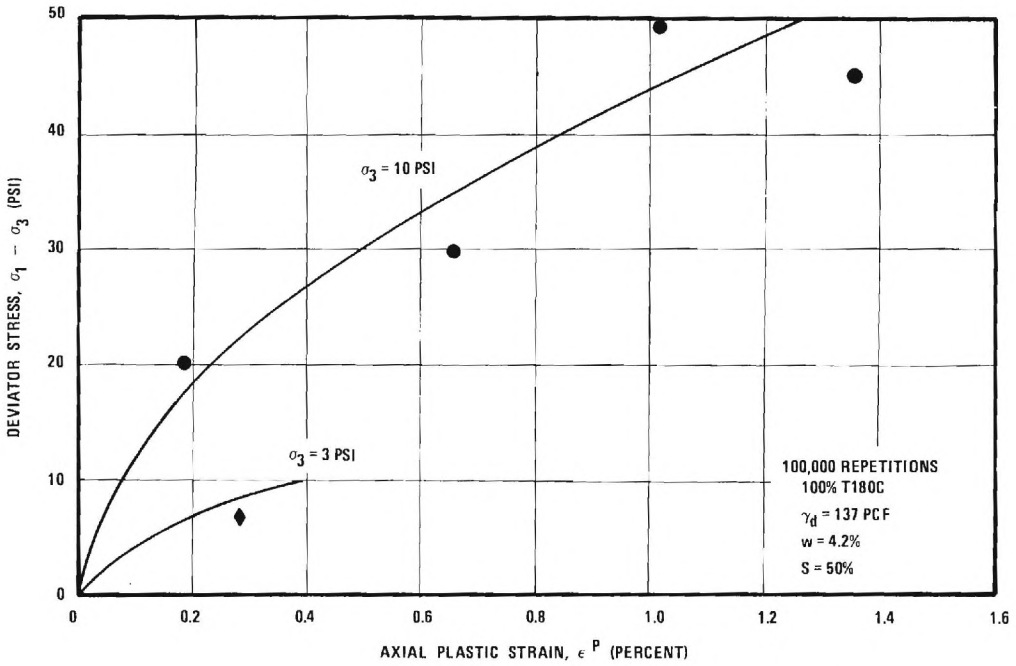

FIGURE 37. INFLUENCE OF DEVIATOR STRESS AND CONFINING PRESSURE ON PLASTIC STRAIN AFTER 100,000 REPETITIONS IN A CRUSHED BIOTITE GRANITE GNEISS WITH 3 PERCENT FINES-BASE 8

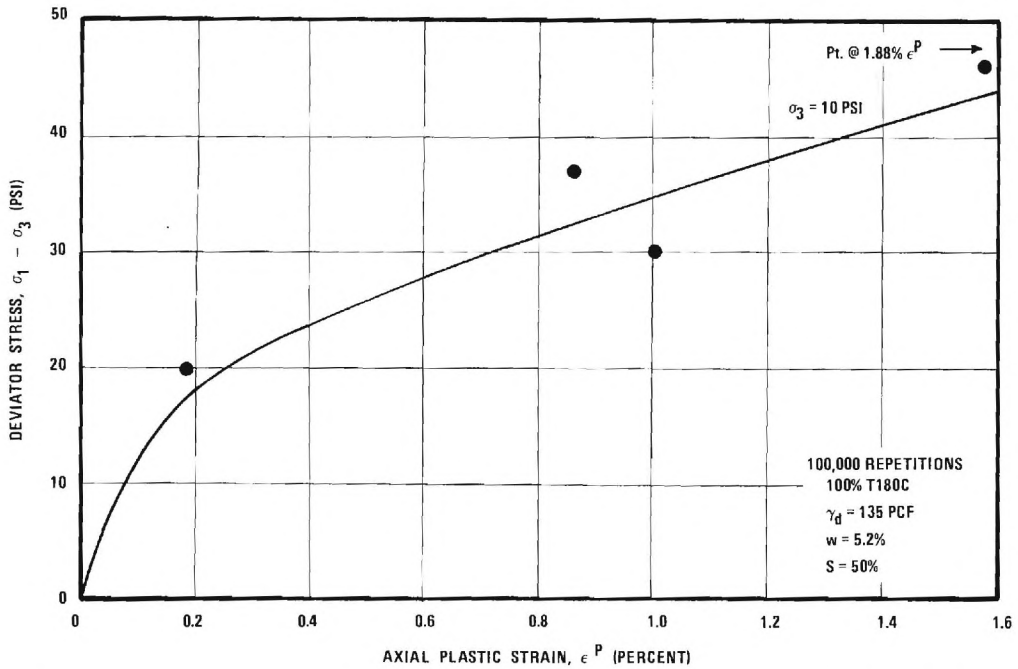

FIGURE 38. INFLUENCE OF DEVIATOR STRESS AND CONFINING PRESSURE ON PLASTIC STRAIN AFTER 100,000 REPETITIONS IN A CRUSHED BIOTITE GRANITE GNEISS WITH 11.25 PERCENT FINES-BASE 9

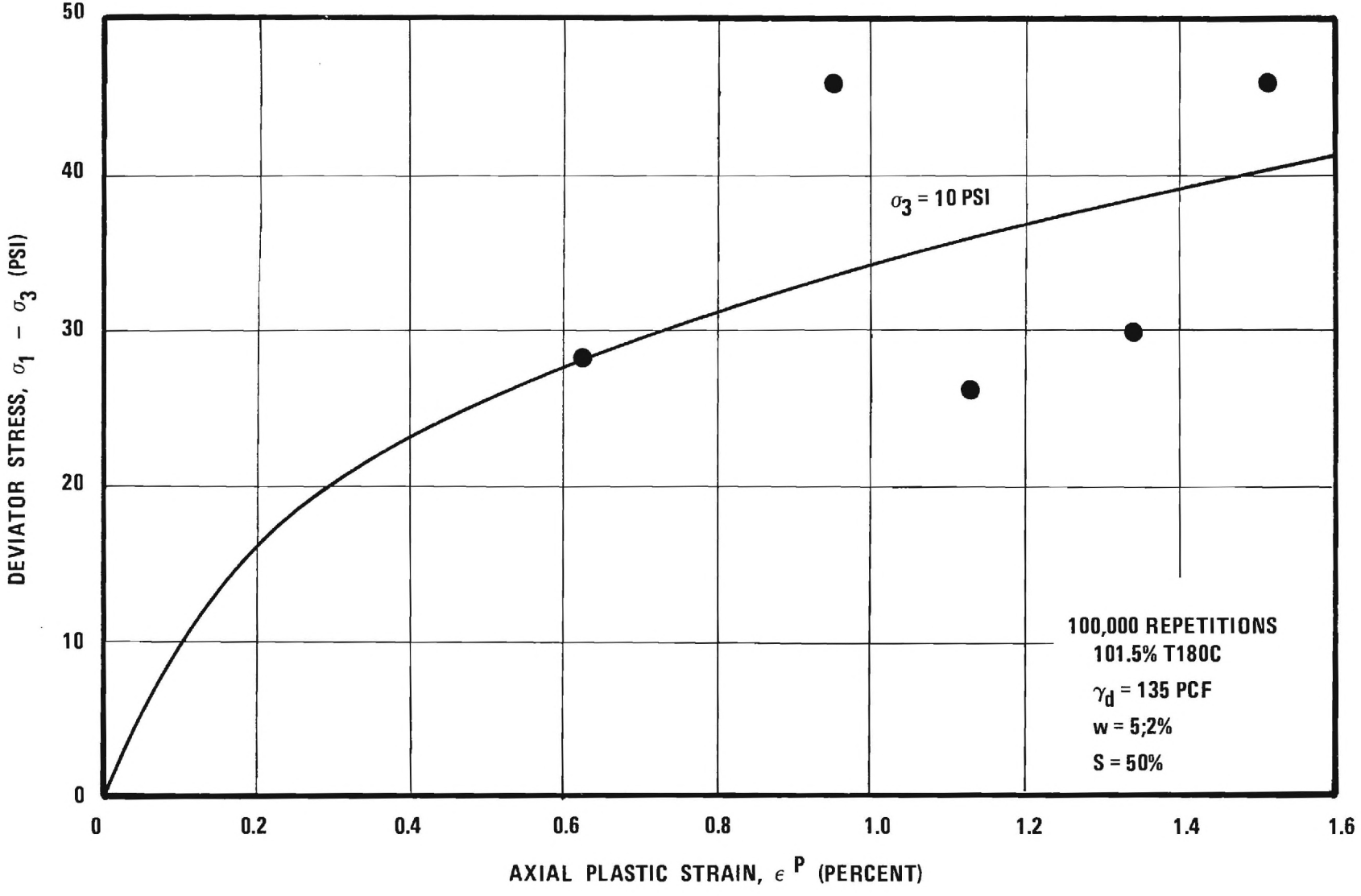

FIGURE 39. INFLUENCE OF DEVIATOR STRESS AND CONFINING PRESSURE ON PLASTIC STRAIN AFTER 100,000 REPETITIONS IN A CRUSHED BIOTITE GRANITE GNEISS WITH 22 PERCENT FINES-BASE 10

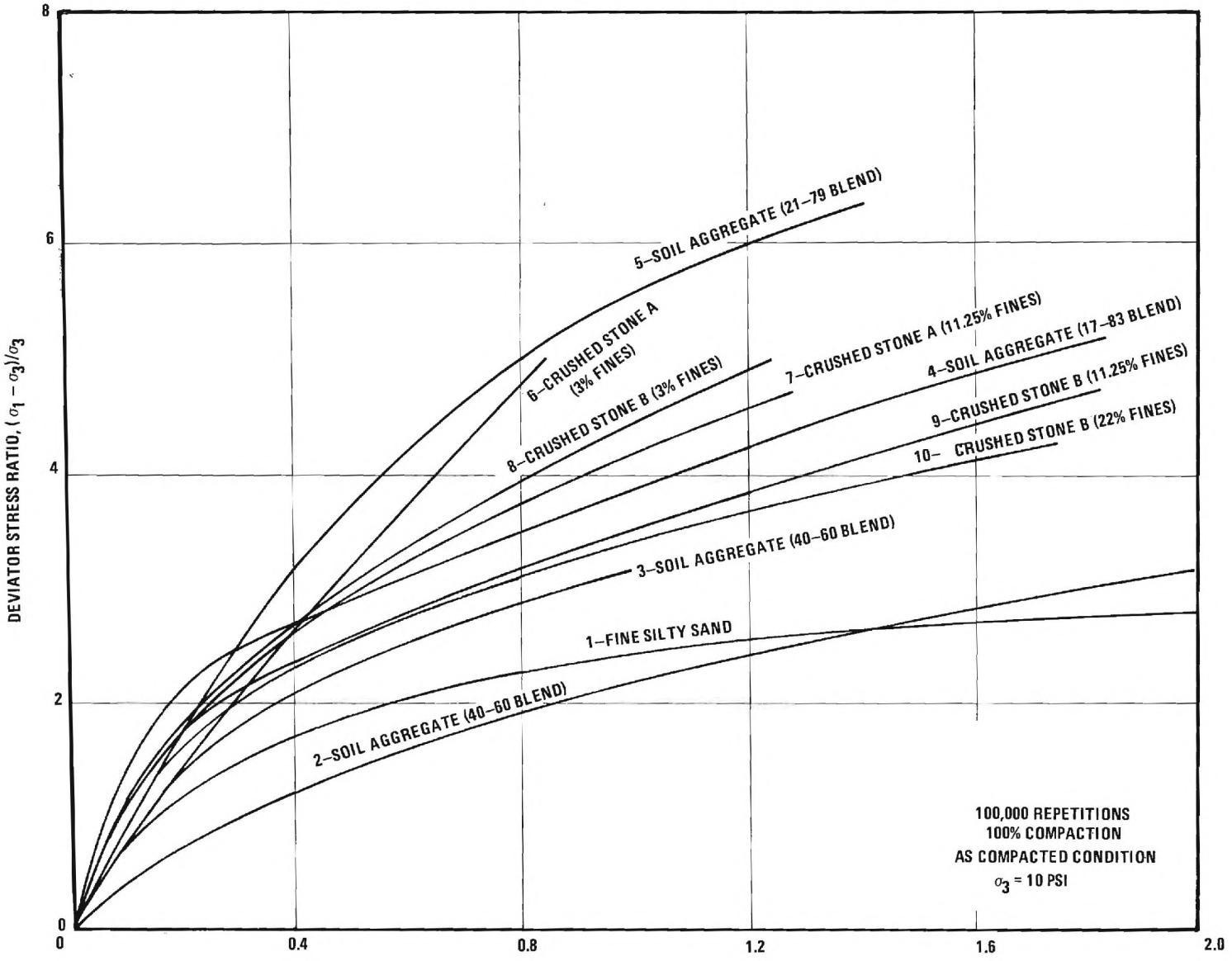

FIGURE 40. SUMMARY OF PLASTIC STRESS-STRAIN CHARACTERISTICS AT 100,000 LOAD REPETITIONS AND A CONFINING PRESSURE OF 10 PSI

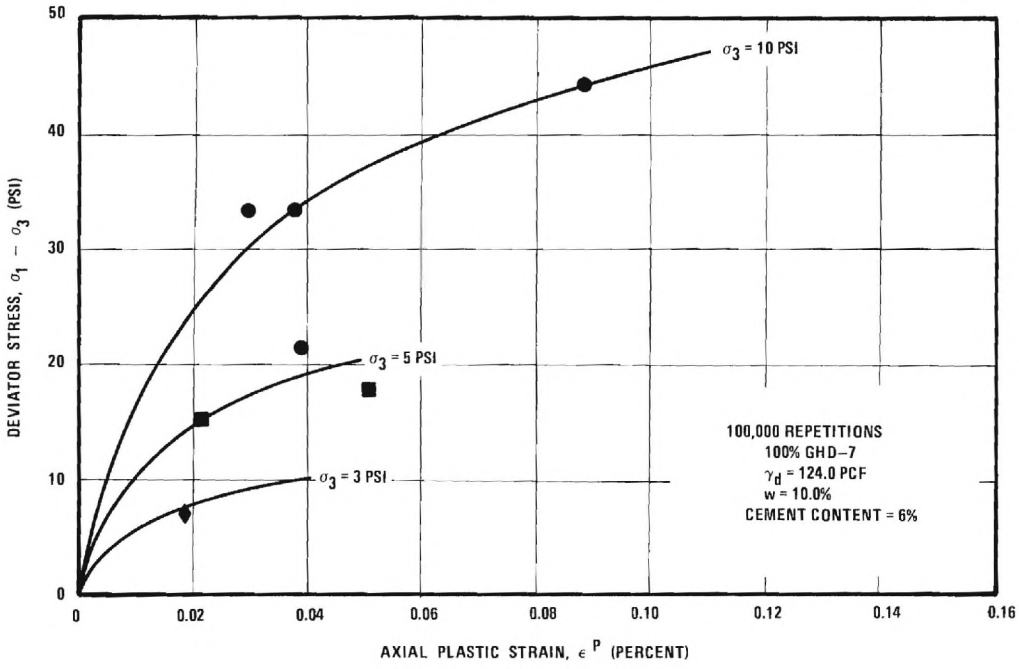

FIGURE 41. INFLUENCE OF DEVIATOR STRESS AND CONFINING PRESSURE ON PLASTIC STRAIN AFTER 100,000 REPETITIONS IN A SILTY SAND STABILIZED WITH 6 PERCENT CEMENT-BASE 11

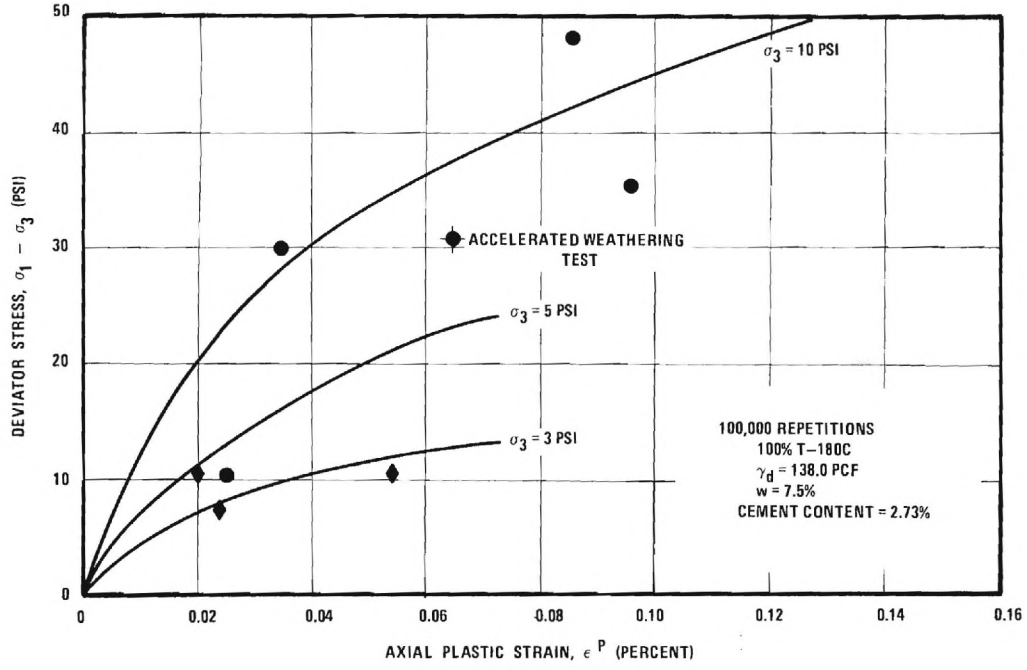

FIGURE 42. INFLUENCE OF DEVIATOR STRESS AND CONFINING PRESSURE ON PLASTIC STRAIN IN A 40-60 BLEND SOIL AGGREGATE STABILIZED WITH 2.73 PERCENT CEMENT-BASE 12

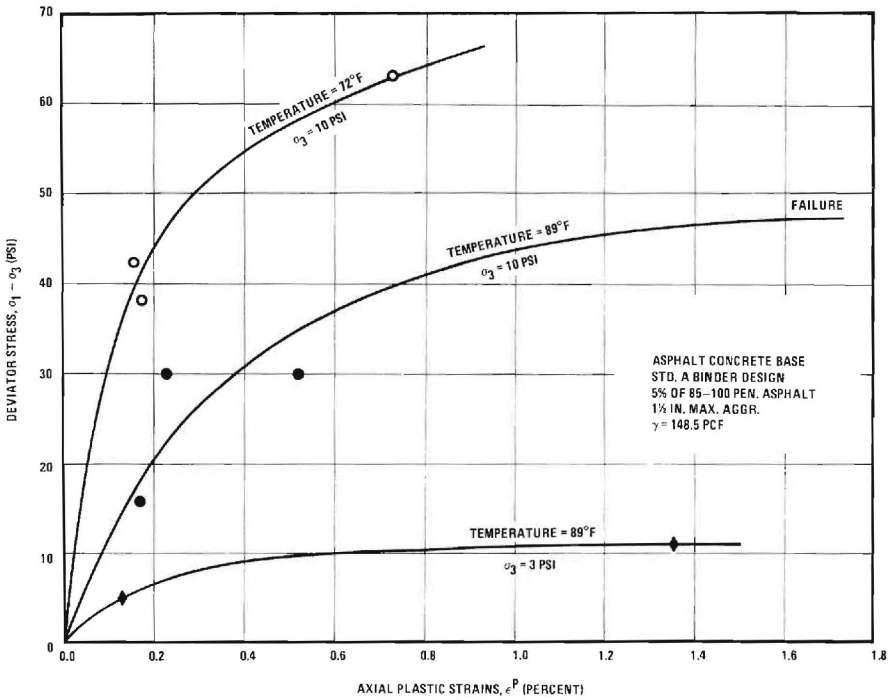

FIGURE 43. EFFECT OF STRESS STATE AND TEMPERATURE ON PLASTIC STRAINS IN AN ASPHALT CONCRETE-BASE 13

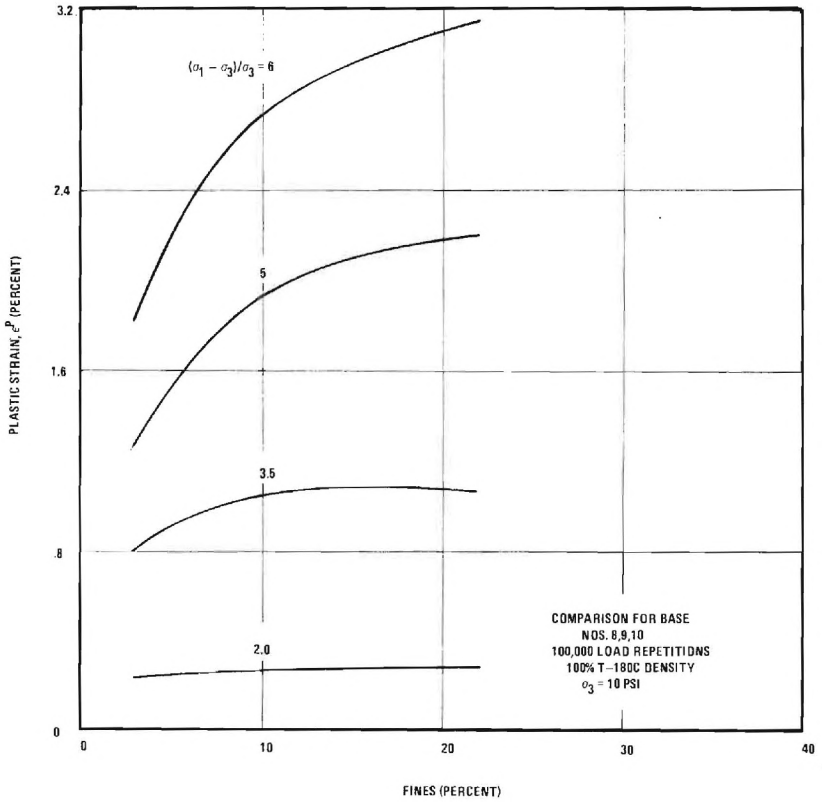

FIGURE 44. INFLUENCE OF FINES AND DEVIATOR STRESS RATIO ON THE PLASTIC STRAINS IN A CRUSHED GRANITE GNEISS BASE AFTER 100,000 LOAD REPETITIONS

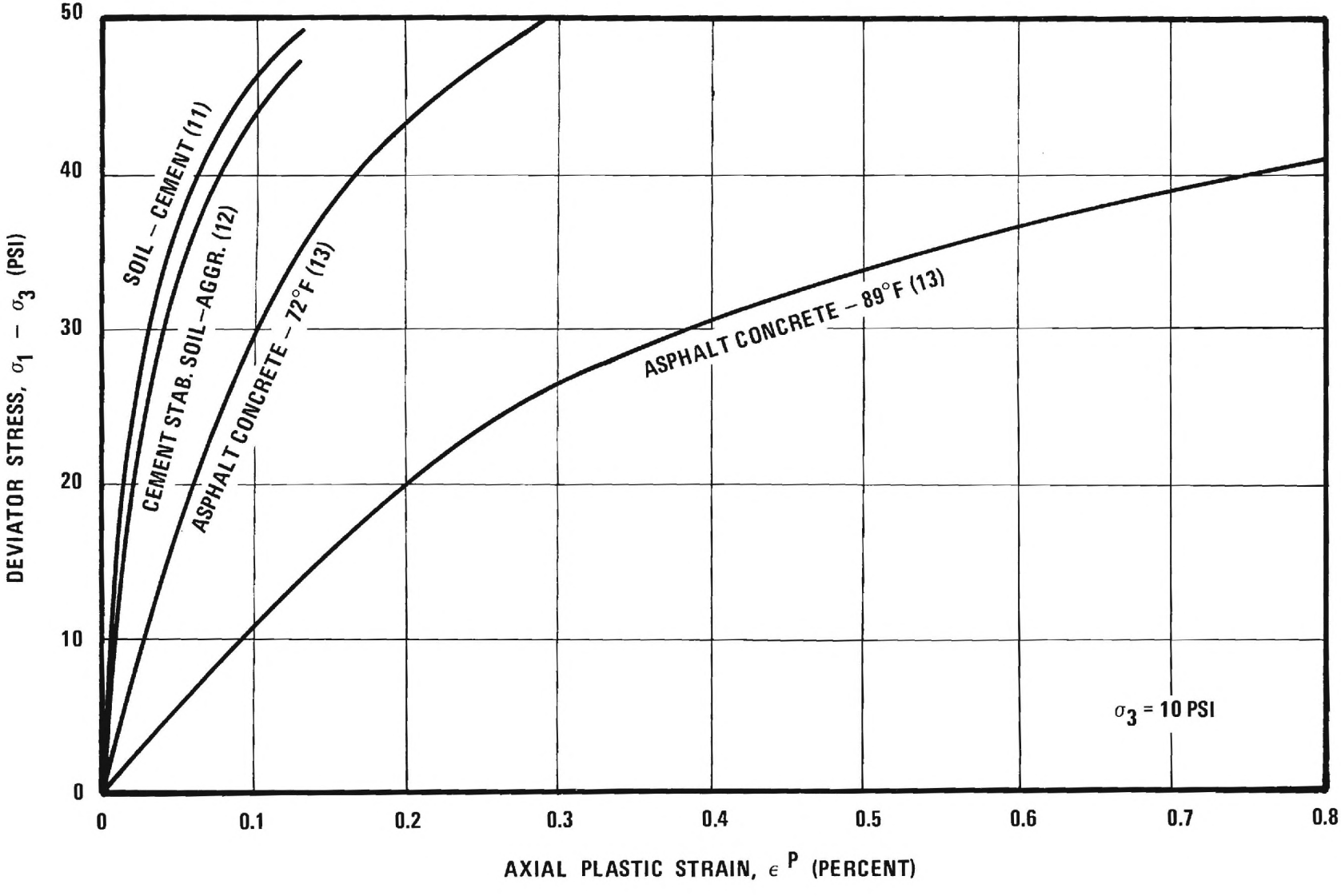

FIGURE 45. COMPARISON OF PLASTIC STRAIN RESPONSE OF STABILIZED BASE MATERIALS

differences in the soil properties. For deviator stress ratios greater than 2.5, the average plastic strains in this soil-aggregate base were, however, still almost twice those occurring in Bases 4 and 5 which had approximately 20 percent soil. Figure 40 shows that both soil-aggregate bases tested having nominally 20-80 blends had significantly lower plastic strains (and hence better performance) than did the two 40-60 bases. The plastic strain characteristics of the soil aggregate bases tested in the as compacted condition were thus found to vary from very poor to quite good depending apparently on the soil characteristics, the percent of soil used in the base and the degree of saturation.

For deviator stress ratios greater than about 2.5, the 17 to 83% blend of soil and aggregate (Base 4) exhibited significantly more plastic strain than did the best performing crushed stone (Base 6) which had 3 percent fines. For deviator stress ratios less than 5, the plastic strains occurring in the 21-79 blend soil-aggregate (Base 5) were on the average about 20 percent less than those occurring in the best crushed stone; at greater stress ratios, however, the trend was apparently reversed. Typical stress ratios in a pavement structure would vary between about 2 and 6.

Effect of Aggregate Type and Fines

The curves shown on Figure 40 for the crushed stone bases indicate that the plastic strain occurring in the biotite granite gneiss (Bases 8 and 9) are greater than those in a porphyritic granite gneiss (Bases 6 and 7) for the same specified gradations. The significant influence of an increase in percent fines and deviator stress on the plastic strains occurring in a crushed biotite granite gneiss is illustrated in Figure 41. The plastic strains increased significantly as the percent fines increased, with greater differences occurring at the larger deviator stress levels.

Effect of Density

A limited number of repeated load triaxial tests were

performed on specimens at 90, 95, and 105 percent of maximum density and the results are shown in Figures 25, 28, 30, 32, 34 and 36 and summarized in Table 6. Sufficient data was not obtained from the limited number of tests performed to make detailed comparisons of how these factors change with type of base material. The results did, however, indicate for all of the materials studied, an average of 185 percent increase in plastic strain occurs if the base is compacted at 95 instead of 100 percent of maximum compaction density the corresponding average reduction in plastic strain was only about 10 percent, although more extensive testing may show the effect to be somewhat greater. This result indicates for the conditions of the test that a base constructed at 100% of T-180 density should perform almost as good as one constructed to 105% density.

Effect of Soaking

The experimental results also indicate that for all of the materials tested an average increase in plastic strain of 68 percent occurs when the test is performed on specimens that are soaked, as compared with the results obtained from tests performed on specimens in the as compacted condition. In interpreting the effects of soaking on the plastic response of the base, it should be remembered that the "soaked" specimens had a high degree of saturation but may not have been completely saturated. These specimens furthermore were tested in a manner which permitted a free flow of water into and out of the specimen so that a significant build-up of pore pressure was not likely to have occurred during application of the 100,000 repetitions. Therefore, if a large build-up of pore pressure should occur in the field in any of these materials due to poor drainage conditions, the laboratory test results would probably under predict the effects of soaking the base on the actual amount of rutting. Materials having the lower permeabilities such as the silty sand and graded aggregate bases would be more susceptible to such a pore pressure build-up in the field.

Hyperbolic Plastic Stress-Strain Law

Only a limited number of plastic stress-strain curves from a practical standpoint can be obtained by laboratory testing since each test point on each curve represents the results of an individual repeated load triaxial test. To obtain data for 100,000 load repetitions or more using pneumatic testing equipment would in general require two or more days. The plastic stress-strain properties in general are needed for a wide range in stress states for predicting rutting in a pavement structure. An important advantage would therefore be gained if the results from two or three experimentally derived plastic stress-strain curves could be extended by means of an appropriate plastic stress-strain law to include a wide range in stress states.

Kondner and his co-workers [4-7] have shown that for a single confining pressure the stress-strain curves obtained from conventional, static triaxial tests performed on both sands and clays can be quite accurately approximated by a hyperbola. Duncan and Chang [8] extended this work and have shown that a general hyperbolic expression can be derived expressing the strain as measured in the static triaxial test as a function of the deviator stress and confining pressure as given in the following expression:

$$\varepsilon_a = \frac{(\sigma_1 - \sigma_3) \,/\, (K\,\sigma_3^n)}{1 - \dfrac{(\sigma_1 - \sigma_3)\,R_f}{\dfrac{2(C.\cos\phi + \sigma_3 \sin\phi)}{(1 - \sin\phi)}}} \qquad \ldots\ldots\ldots (2)$$

where ε_a = axial strain

$K\,\sigma_3^n$ = relationship defining the initial tangent modulus as a function of confining pressure, σ_3 (K and n are constants)

C = cohesion

ϕ = angle of internal friction

R_f = ratio of measured strength to ultimate hyperbolic strength

Of considerable practical significance is the fact that a hyperbolic expression analogous to Eqn. 2 has been found to closely fit the plastic stress-strain curves obtained from the repeated load triaxial test results for 100,000 load repetitions. The hyperbolic relationship would also be expected to fit the experimental data for other materials and numbers of load repetitions.

The procedure for evaluating the constants in the hyperbolic stress-strain law for conventional, static stress-strain data has been given by Duncan and Chang [8]. The analogous constants required for a hyperbolic curve fit of the plastic stress-strain response data obtained from the repeated load triaxial test can be evaluated from Eqn. 2 in a similar manner to that described by Duncan and Chang [8]. Plastic strain is considered to be analogous to elastic strain and the repeated deviator stress analogous to static deviator stress. An example of a hyperbolic fit of the plastic stress-strain curve obtained from the repeated load triaxial test is shown in Figure 46. The theoretical curves are almost identical to the laboratory curves at confining pressures of 3 and 5 psi; at a confining pressure of 10 psi the calculated plastic strains are slightly greater than the laboratory values. The constants required in Eqn. 2 to calculate the curves are given on the figure.

Rut Depth Prediction

The plastic stress-strain relationships shown in Figures 24 through 45 for 100,000 load repetitions can be only used in a general way to establish trends of the relative performance of different bases with respect to rutting. This data does not, however, give directly an estimate of the probable rut depth

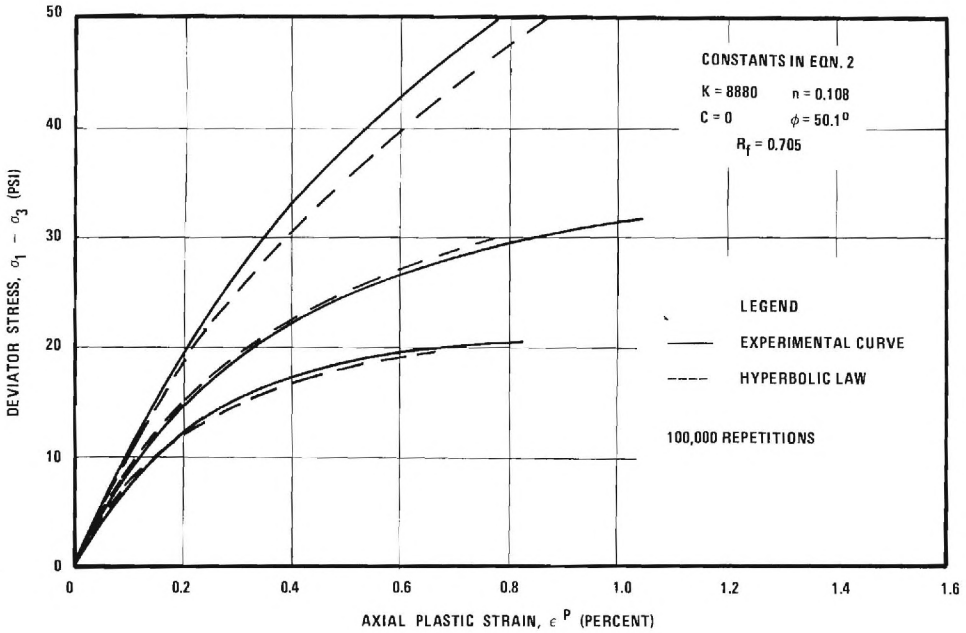

FIGURE 46. COMPARISON OF CALCULATED HYPERBOLIC PLASTIC STRAIN WITH EXPERIMENTAL CURVES FOR A 21-79 SOIL AGGREGATE-BASE 5

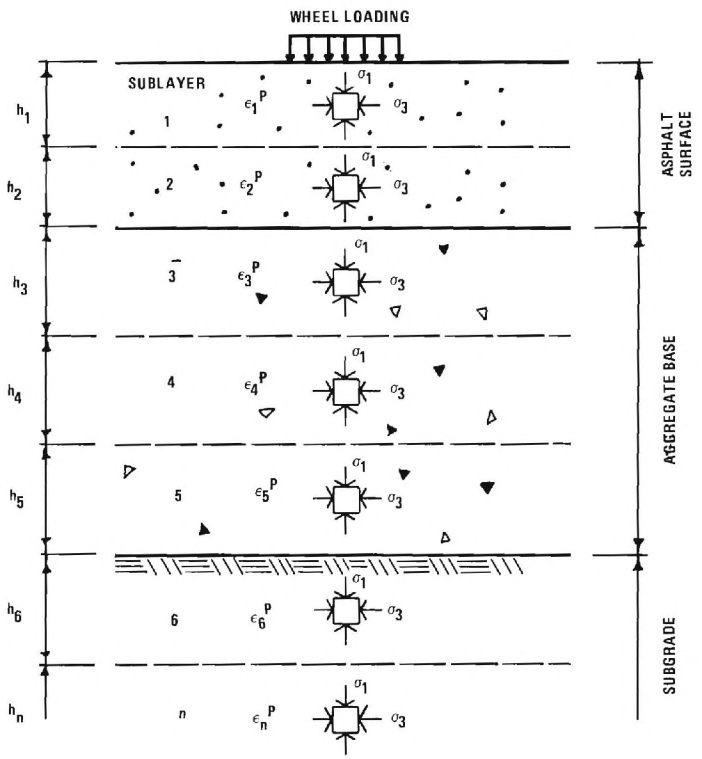

FIGURE 47. IDEALIZATION OF LAYERED PAVEMENT STRUCTURE FOR CALCULATING RUT DEPTH

although considerable insight can be gained from these curves concerning the probable relative behavior of the materials. A method for predicting rut depth using linear, viscoelastic layered theory and the results from repeated load triaxial tests has been proposed by Barksdale and Leonards [9]. More recently Elliott and Moavenzadeh [10] have also presented a linear viscoelastic approach for predicting permanent deformations using the results from creep tests. However, unstabilized granular base and subgrade materials perform in a very complicated, nonlinear manner. Therefore, a serious disadvantage of these two methods is that they can not adequately consider the nonlinear behavior of the materials used in the pavement structure.

The characterization of the base using nonlinear theory becomes particularly important when estimating the rut depth which occurs in the base. The following discussion presents a simplified engineering approach for predicting rutting in a pavement structure which makes use of nonlinear layered theory, the plastic stress-strain properties obtained from the repeated load triaxial tests, and the hyperbolic, plastic stress-strain law proposed in this report. The method proposed is somewhat similar to the general approach taken by Romain [11].

The amount of rutting that would occur after a certain number of repetitions is predicted by first dividing each layer of the pavement structure into several sublayers. The major principal stress, σ_1 and average confining pressure, σ_3 is then calculated at the center of each layer beneath the wheel load as illustrated in Figure 47. To obtain satisfactory results in unstabilized bases, the stress should be calculated using a nonlinear elastic [2] or nonlinear viscoelastic theory which gives special attention to the nonlinear, anisotropic behavior of the base. The plastic strains can then be readily calculated at the center of each sublayer by using for the desired number of load repetitions the appropriate hyperbolic, plastic stress-strain law, or else interpolating directly from

the laboratory plastic stress-strain curves. The total rut depth is then obtained by summing up all of the products of the average plastic strains occurring at the center of each layer and the corresponding sublayer thickness. This step can be mathematically expressed as

$$\delta^{P}_{Total} = \sum_{n=1}^{n} (\bar{\varepsilon}^{P}_{i} \cdot h_i) \quad \ldots\ldots\ldots\ldots\ldots\ldots \quad (3)$$

where δ^{P}_{Total} = total rut depth beneath the wheel load

$\bar{\varepsilon}^{P}_{i}$ = average plastic strain in the i^{th} sublayer

h_i = thickness of the i^{th} sublayer

n = total number of sublayers

Of course this summation can be applied if desired to only one pavement component at a time to determine the change in thickness that will occur in each component. Furthermore, the method can be applied to both stabilized and nonstabilized layers.

In order to consider the effects of changes in material properties with time and load repetitions, the above procedure can be applied at a number of selected load applications. The difference in plastic deformations occurring between the successive load applications at which deformations are calculated can be summed to give the total permanent deformation that will occur in the pavement structure. To increase the accuracy of this approximate procedure, all that has to be done is to increase the number of increments used in the analysis.

The hyperbolic, plastic stress-strain law was found during this investigation to hold true for several quite different, unstabilized base materials. This law has not at the present time been verified for asphalt concrete or subgrade soils, although it is postulated that a similar hyperbolic relationship also holds true for these materials. Although the experimental plastic stress-strain curves can always be used directly to estimate the average plastic strain in each layer, the hyperbolic

stress-strain law offers a considerable refinement to the approach.

The simplified engineering approach proposed for estimating rut depth in pavements is analogous in basic philosophy to the method used by Monismith and Deacon [12], Monismith and Kasianchuk [13] and others for predicting fatigue failure of the asphalt concrete surfacing in flexible pavements. Although the proposed method has certain shortcomings from an engineering mechanics viewpoint, it offers a practical, engineering approach for estimating the permanent deformations that will occur in a pavement structure under a large number of repetitions, or for evaluating the relative performance of different materials and different structural configurations.

Rut Index and Rut Potential

Quite frequently when evaluating rutting characteristics of base materials a simple procedure is needed which permits a qualitative evaluation of how one base material compares with another without having to use layered system theory. To meet this requirement an index is proposed which is easy to calculate and at the same time reflects the general susceptibility of a base to rutting.

If the base course is divided into two sublayers of equal thickness, the permanent deformation in the base can be calculated from Eqn. 2 by multiplying the average plastic strain in each sublayer by the sublayer thickness. Since the sublayer thicknesses are the same in the top and bottom, the rut depth is also proportional to the sum of the average plastic strains in each sublayer. To therefore simplify the comparison of the rutting tendencies of different base materials, a Rut Index can be defined as the sum of the average plastic strain in each equal sublayer multiplied by 10,000. From this definition it follows that the Rut Index is approximately proportional to the rut depth that would occur in the base with an increase in Rut Index indicating a larger rut depth.

To evaluate the plastic strain for use in calculating the Rut Index, repeated load tests are performed using appropriate stress states for the desired number of load repetitions. To keep from performing a nonlinear stress analysis for each base material evaluated, the same two confining pressures and deviator stresses can be used in testing each material to obtain the average plastic strain in each sublayer. These stress states should, therefore, be determined for a typical flexible pavement structure.

For a comparison of Rut Indices to remain valid, the structural section used and the material properties should not change significantly with the different base materials being compared. If more refinement is needed due to variation in geometry or materials, the procedure (Eqn. 3) given in the previous section can be used to predict the change in thickness of the base for each set of conditions. Since the average confining pressure changes with depth in the base, the average plastic strains in each sublayer used in calculating the Rut Index should, where possible, be obtained from stress-strain curves for different confining pressures.

A detailed study using a realistic nonlinear layered theory needs to be performed to evaluate the stress states from which to obtain the plastic strains used in the Rut Index. Preliminary studies conducted during this investigation indicate for a typical flexible pavement having a non-unstabilized base the average deviator stress ratio is probably 5 to 7 in the upper half of the base and about 2 to 3-1/2 in the lower half. For this investigation a number of the base materials were tested at only a confining pressure of 10 psi. Therefore, the plastic strains for deviator stress ratios of 3.5 and 6 used to calculate the Rut Index were obtained from the stress-strain curves corresponding to a confining pressure of 10 psi. Admittedly this confining pressure may be higher than the average confinement that actually exists in the base.

For normal highway traffic conditions, an evaluation of the performance of base materials is desirable for numbers of load repetitions varying from 100,000 to 1,000,000 or more. To perform repeated load triaxial tests on a large number of specimens to 500,000 or 1,000,000 load repetitions would in general be too costly and time consuming for extensive practical application. Therefore, to approximately extend the results of the repeated load triaxial tests to greater numbers of repetitions, the plastic strain-logarithm of the number of load applications relationship (Figure 23) for each test can be extrapolated through one log cycle of load repetitions. These results can be used to construct plastic stress-strain curves from which the Rut Potential can be estimated using the same procedure as described for the Rut Index. The Rut Potential is defined as a Rut Index calculated using data that has been extrapolated to a desired number of load applications. The Rut Potential was calculated in this investigation for 1,000,000 repetitions.

The Rut Potential approach for extending test results incorporates into it both the cumulative plastic strain at the end of the testing period and also the effect of the rate-of-change of the plastic strain at that time. Since the rate-of-change of plastic strain development may increase suddenly after a large number of repetitions, extrapolation of the data to 1,000,000 repetitions should certainly be considered as only an approximation. Furthermore, the Rut Potential should only be used when it is not for some reason practical to perform repeated load tests to the required number of load repetitions.

In applying the Rut Index and Rut Potential concepts, it should be remembered that the thickness of each layer and the materials used in the other components of the pavement structure would all influence to varying degrees the average stress ratios and confining pressures in the base and hence the permanent

change in thickness which would occur in that layer. To correctly consider these variables nonlinear elastic layered theory would have to be employed to calculate the correct stress ratios to use in each layer. As long as only the type material in the base is changed and not layer thickness, the Rut Index and Rut Potential concepts offer a rapid and reasonably valid approach for comparing the rutting characteristics of most unstabilized base materials.

Discussion of Plastic Response of Base Materials

The Rut Indices and Rut Potentials for the base materials investigated are summarized in Table 6. In general these indices tend to reinforce the previous discussion of the performance of the bases as summarized from the plastic stress-strain curves. The silty sand base exhibited extremely large plastic strains and an infinitely large Rut Index. These results indicate this base needs to be either stabilized or else a thick surfacing must be used to prevent excessive rutting from occurring on a heavily trafficked pavement. The design of pavement systems using this and all other bases studied will be considered in detail in Chapter 8.

The soil-aggregate bases tested at the as compacted water content exhibited Rut Indices and Rut Potentials varying between the two extremes of the test data. As would be expected, the average Rut Potentials of the 40-60 soil-aggregate bases were almost twice those of the nominal 20-80 mixtures. Probably most of the difference was due to the use of varying amounts of different soils, although the slightly different degrees of saturation at which the bases were tested undoubtedly had some effect. Large differences in Rut Index and Rut Potential occurred within each group of soil-aggregate bases. For example the 17-83 soil-aggregate exhibited a Rut Index about twice as large as did the 21-79 mixture. The fines (material passing the No. 200 sieve) in the 17-83 base was composed entirely of soil. Although the total amount of fines used in the 21-79

base was greater, only a small additional amount of soil was used in this base since a portion of the fines were stone screenings. Also the degree of saturation in the 21-79 base was somewhat lower than the 17-83 base. These differences help to account for the significant variation in performance of the two bases. Additional testing of soil-aggregate blends is necessary to evaluate the specific effects of type and amount of soil.

After 100,000 load repetitions the tendency to rut in the crushed stone which performed best (Base 5, Rut Index = 176) was found to be approximately the same as that of the best soil-aggregate (Base 5, Rut Index = 164) even though the degree of saturation in the crushed stone was lower. After 1,000,000 repetitions, however, the Rut Potential of the crushed stone had become equal to 254 while that of the soil-aggregate was only 202. Apparently this difference was due to the beneficial effects of the cohesion and the use of a more dense soil-aggregate mixture.

The test results indicate that very carefully selected 20-80 soil-aggregate mixtures should result in satisfactorily performing bases, provided that the degree of saturation in the base does not exceed about 65-75 percent. This would require good field conditions including proper surface maintenance and exceptionally good drainage conditions, or else a low amount of rainfall distributed approximately evenly throughout the year. Even under these conditions, which may or may not actually be achieved in the field, larger variations in rut depth would be expected to occur in soil-aggregate bases than in a properly controlled crushed stone base. The results of this study indicate that 40-60 soil-aggregate bases having properties similar to the two bases tested should in general exhibit significantly more rutting than either a 20-80 blend or pure crushed stone. Therefore, these materials should not be used in a heavily trafficked pavement structure as long as

other suitable alternatives exist unless a sufficiently thick asphalt concrete cover is placed over this material. Furthermore, it is recommended that neither 20-80 or 40-60 soil-aggregate blends should probably be used under poor conditions of drainage until more sophisticated laboratory studies or preferably full scale field investigations can be conducted to determine if a significant amount of rutting will occur due to the detrimental effects of water including a possible build-up in pore pressure.

Increasing the fines from 3 to 11.25 percent in two different crushed stone bases compacted for each gradation to 100 percent of AASHO T-180 density resulted in an average 60 percent increase in the Rut Index as illustrated in Figure 48. This means that even though 100 percent AASHO T-180 (or GHD-49) density might be specified, two bases both meeting this requirement might perform quite differently if different amounts of fines or different aggregate sources were used. This undesirable end result indicates a need for improved methods of specifying density requirements or suitable specifications that will insure approximately equal Rut Indices or Rut Potentials. Methods based on relative density concepts may be found to meet this need and certainly merit further study.

In order to apply the proposed Rut Index and Rut Potential to different materials, criteria need to be set to limit the amount of rutting that will occur in the base. To limit rutting in the base, a limiting Rut Index and Rut Potential of 260 and 300, respectively, for a confining pressure of 10 psi would appear based on laboratory data to be reasonable tentative limits. An alternative would be to use limiting plastic stress-strain curves rather than the Rut Index or Rut Potential. In either case, further theoretical work needs to be performed to better define the appropriate stress states upon which to base the interpretation, and field studies are needed to verify the overall approach.

The results of this investigation have shown that density,

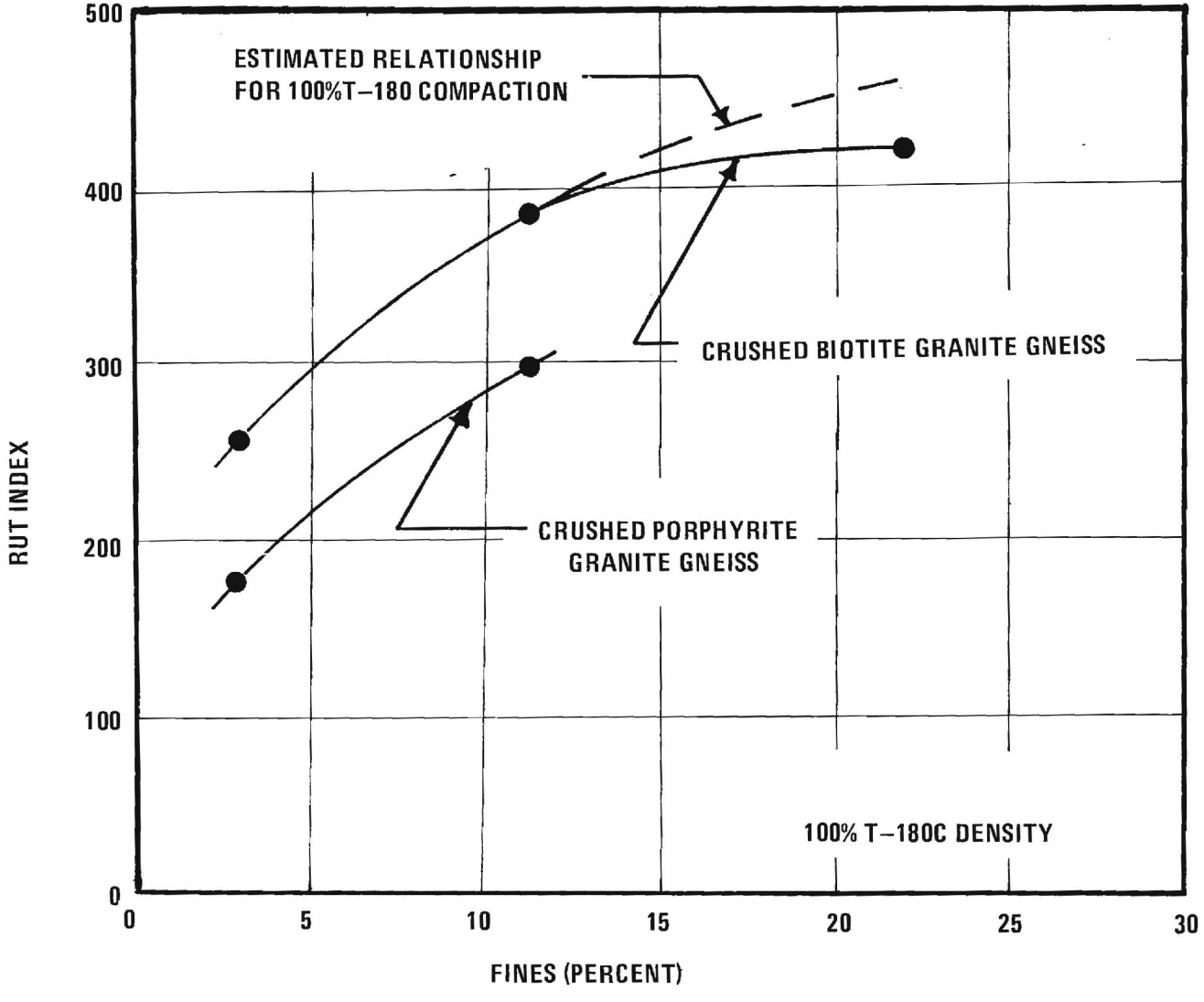

FIGURE 48. VARIATION OF RUT INDEX WITH PERCENT FINES FOR CRUSHED GRANITE GNEISS BASES AFTER 100,000 LOAD REPETITIONS

degree of saturation and amount and type of fines all effect the plastic strain and hence rutting in base materials. In addition it was shown that both the confining pressure and deviator stress also have significant effects on the magnitude of plastic strain occurring in a specimen. Any factor affecting the stress state in the base has an effect on the magnitude of rutting that will occur in that layer and throughout the pavement structure. This means that the thickness of the surfacing and underlying layers, the material properties of each layer, and the magnitude and configuration of the loading all effect the amount of rutting that would occur in the base. Since the rate of loading significantly effects some material properties, the speed at which the vehicle moves over the pavement also affects rutting.

In a flexible pavement structure rutting and fatigue of the surfacing are the two most important failure mechanisms that are usually considered in a mechanistic, structural design [9]. It should therefore be pointed out that rutting can also contribute to fatigue failure of a pavement due to the tensile strains in the surfacing resulting from bending caused by rutting of the surfacing, base and subgrade. Frequently, a flexible pavement which has undergone longitudinal rutting over a long distance will show cracks in the longitudinal direction in the vicinity of either/or the edge or center of the rut. In at least some instances, these cracks are probably caused by a fatigue failure which has been accelerated by tensile strains caused by varying magnitudes of rutting in the base and/or subgrade.

CHAPTER VII

MECHANISTIC ANALYSIS OF AASHO ROAD TEST RESULTS

A correlation of the material properties measured in the laboratory with actual field behavior was considered to be necessary in order to determine the base course coefficients. To obtain the desired correlation with field behavior a theoretical study was made of the performance of selected sections from the AASHO Road Test [14]. Fatigue relationships and a limiting subgrade stress criterion were developed from this study. The relationships developed are used later in performing an analytical study of the pavement sections selected for use in the Piedmont Province of Georgia.

Pavement Temperatures and Traffic Loading

In order to perform a realistic fatigue analysis of a flexible pavement structure an estimation must be made of the variation of the temperature with depth and time in the asphalt concrete surfacing. Fortunately, temperature measurements using thermocouples were made for each hour of the day throughout the duration of the AASHO Road Test at the top, middle and bottom of a four inch thick asphalt concrete pavement section. This quite extensive set of data is given in AASHO Road Test Data Set 3303-S.

In order to integrate this tremendous quantity of data into a fatigue analysis using a reasonable amount of computer time, certain compromises had to be made in analyzing this data and using it in the theoretical study of the test sections. A study of the average monthly air temperatures throughout the traffic loading period indicates that the variation of temperature with depth in the pavements would be similar in 1958-1959 to that occurring during 1959-1960. Therefore, only the

temperature data for the 1959-1960 loading period was analyzed. The second assumption made was that the modulus of elasticity of the asphalt concrete corresponding to the temperature at the center of the asphalt concrete layer could be used in a fatigue analysis. This assumption makes possible considering the hourly temperature variation throughout the entire year without having to analyze an excessive number of layered pavement systems. An alternative, considered to be less desirable since accurate temperature data was available, would have been to consider for possibly one day each month the variation of temperature with depth. Since fatigue life is sensitive to temperature changes, a realistic treatment of the problem of temperature variation with time was considered to be more important than considering accurately, for a few selected days, the variation of temperature with depth. Certainly further study needs to be made of the effects of temperature variations on fatigue life.

The axle loadings at the AASHO Road Test were not applied uniformly throughout the day. To approximately consider the nonuniform traffic loading, each day was divided into three time intervals which had approximately a uniform traffic loading throughout the interval. The time intervals used based on a 24 hour clock were 0500 to 1600, 1600 to 2100, and 2100 to 0500 hours. The axle loadings applied during these time intervals approximately correspond to 37, 19, and 44 percent,respectively, of the total applied axle loads. The temperature at each depth was then averaged over the time interval given above and tabulated in three degree increments by month. A table was prepared for each month giving the temperature increment and the corresponding estimated number of wheel loads applied.

The temperature variations were tabulated in this way at the center and bottom of the four inch asphalt concrete section in which the temperatures were monitored. A comparison of the difference between the percent of wheel loadings and the

temperature intervals for the center and bottom of the layer is shown in Figure 49 for the months of April, July and October of 1960. The average temperature in the asphalt concrete surfacing of the flexible pavement sections having 3 and 4 inches of asphalt concrete was assumed to correspond to the measured temperature variation at a two inch depth. The average temperature in the asphalt concrete base sections studied which had a total asphalt thickness of 9.8 and 12.6 inches was obtained by approximately correcting the tabulated temperature data to correspond to the average depth of the asphalt concrete.

Nonlinear Layered System Analysis

Nonlinear layered system theory was used throughout this study to calculate the theoretical displacements, stresses, and strains occurring in the AASHO Road Test sections studied, and also in developing the base course coefficients for use in Georgia.

The computer program used in the analysis approximates the pavement system as five layers [15] which extend to infinity in the lateral directions. Two uniform, circular loads are applied on the surface to approximate a single axle, dual wheel loading. The response of the pavement is initially calculated using assumed moduli for each layer. The calculated stresses are then used to estimate a stress dependent modulus from experimentally measured material properties. New stresses are calculated and the process is repeated until convergence of this iterative procedure occurs. This iterative technique makes possible the use of a modulus which is dependent on the average stress state which exists in each layer in the vicinity beneath the wheel loadings. This simiplified nonlinear approach makes possible the analysis of a large number of pavement sections at a reasonable computer cost. The use of more refined finite element techniques presently available would have been prohibitive for this study due to the excessive computer

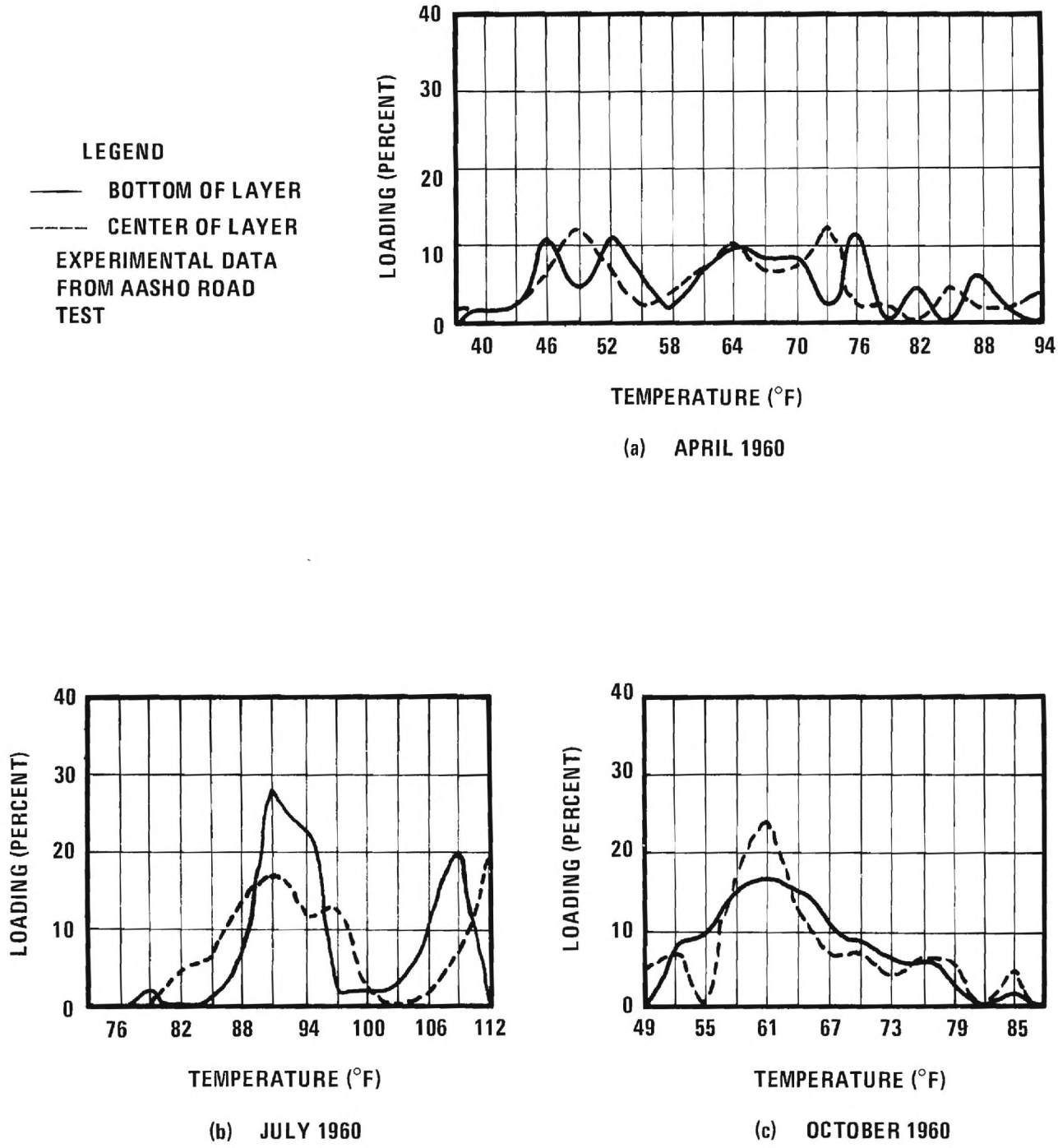

FIGURE 49. RELATIONSHIP BETWEEN APPLIED LOADING AND TEMPERATURE IN THE ASPHALT CONCRETE FOR THREE SELECTED MONTHS-EXPERIMENTAL DATA FROM THE AASHO ROAD TEST

time that would have been required to analyze the number of sections studied in this investigation.

In order to perform a theoretical analysis of the response of the pavement structure dynamic moduli had to be determined for each pavement component. Repeated load tests were run on simulated AASHO base and subbase materials to obtain the resilient modulus as a function of confining pressure.

The limestone base material that was tested was obtained from the same quarry that supplied limestone for the AASHO Road Test [16]. Specimens were prepared using a gradation and density corresponding to that measured in the field at AASHO. The sand gravel subbase material tested was composed of the same mixture of soil, sand, and gravel materials and came from the same general location as did the subbase material used at AASHO. The modulus of elasticity of the base and subbase was modeled using Eqn. 1. The modulus of elasticity of the cement stabilized gravel base was assumed to be 700,000 psi. This value is lower than that measured using the repeated load triaxial test apparatus for the cement stabilized Georgia base materials but appears to correlate reasonably well with the observed field response. The resilient properties of the subgrade used in the analysis were obtained from the literature [17]. In the analysis the resilient modulus of the subgrade was taken to vary linearly with deviator stress and be essentially independent of confining stress at low pressures [18].

Each year was divided into four time periods corresponding to spring, summer, fall and winter. The dynamic moduli of the base, subbase, and subgrade evaluated from laboratory tests and used in the theoretical analysis are given in Table 7 for all seasons except winter. The resilient properties of the materials were assumed to be the same for the corresponding season of each year throughout the duration of the Road Test. The relationship between modulus of elasticity of the asphalt concrete and temperature selected for use in the analysis corresponds to

TABLE 7. SUMMARY OF MATERIAL CHARACTERISTICS USED IN THE ANALYSIS OF THE AASHO ROAD TEST

Season	Crushed Limestone Base		Sand-Gravel Subbase		Silty Clay Subgrade		
	$\bar{K}$	$\bar{n}$	$\bar{K}$	$\bar{n}$	E_R $\sigma_1-\sigma_3=0$ (psi)	E_R $\sigma_1-\sigma_3=12$ (psi)	E_R $\sigma_1-\sigma_3=55$ (psi)
Spring	3631	0.560	1479	0.777	13,700	2300	3310
Summer	4000	0.545	1595	0.771	26,200	4430	6560
Fall	4467	0.534	1710	0.766	29,900	5050	7480

a speed of approximately 30 mph and was derived from the experimental test results given by Kallas and Riley [19] and Coffman et al [20] and is shown in Figure 50.

A comparison is shown in Figure 51 of the pavement surface deflections calculated using the layered theory and the material properties given in Table 7 and Figure 50. Using the same material properties the calculated vertical subgrade stress in Section 581 was found to be 3.75 psi while the average measured value for a speed of 30 mph was 4.31 psi [14, Report 6, p 40]. This comparison is reasonable considering that an uncertainty existed as to the exact temperature of the pavement to use in the theoretical calculations.

The two comparisons given of predicted and measured response indicate that the nonlinear theory and the material properties used to analyze the performance of the test sections give reasonably good results. The material properties could have been adjusted to compare more favorably with the observed deflections and stresses at the AASHO Road Test. Rather than doing this, it was believed to be more important to use unadjusted, experimentally measured material properties which could be directly translated to the measurement of properties of the pavement material used in Georgia. Although certainly highly desirable, an exact correlation with the measured deflections and stresses is not altogether necessary since the computed values are correlated directly with field performance.

In order to perform a fatigue analysis of selected sections from the AASHO Road Test a relationship was needed for each section studied between the maximum tensile strain in the stabilized layers, the temperature, and the season of the year. Typical relationships obtained using layered theory are shown in Figures 52-54 for sections having bases of crushed stone, asphalt concrete, and cement stabilized gravel. These figures readily show the very significant effect that temperature and type of section has on the resulting maximum tensile strains

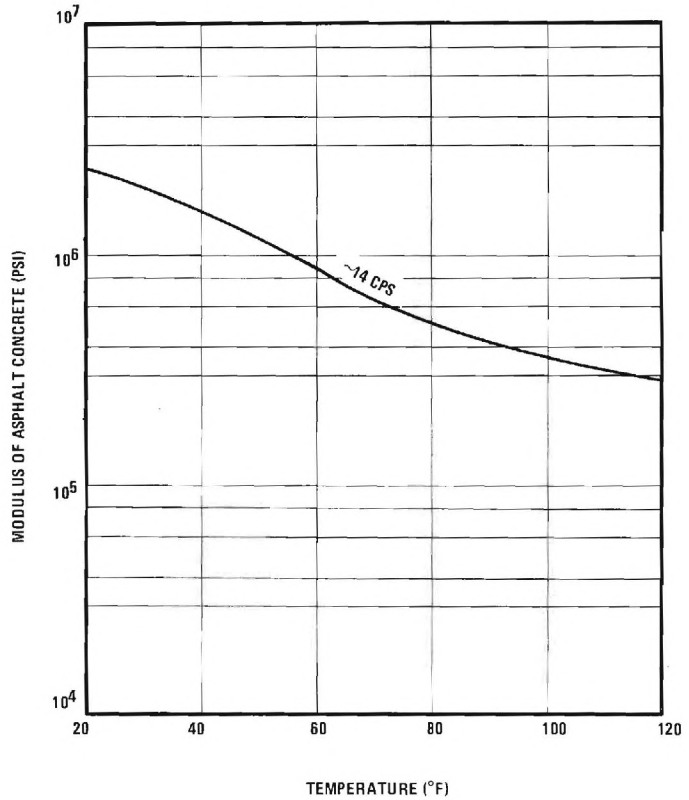

FIGURE 50. VARIATION OF MODULUS OF ELASTICITY OF ASPHALT CONCRETE WITH TEMPERATURE FOR A LOADING FREQUENCY OF 14 CPS

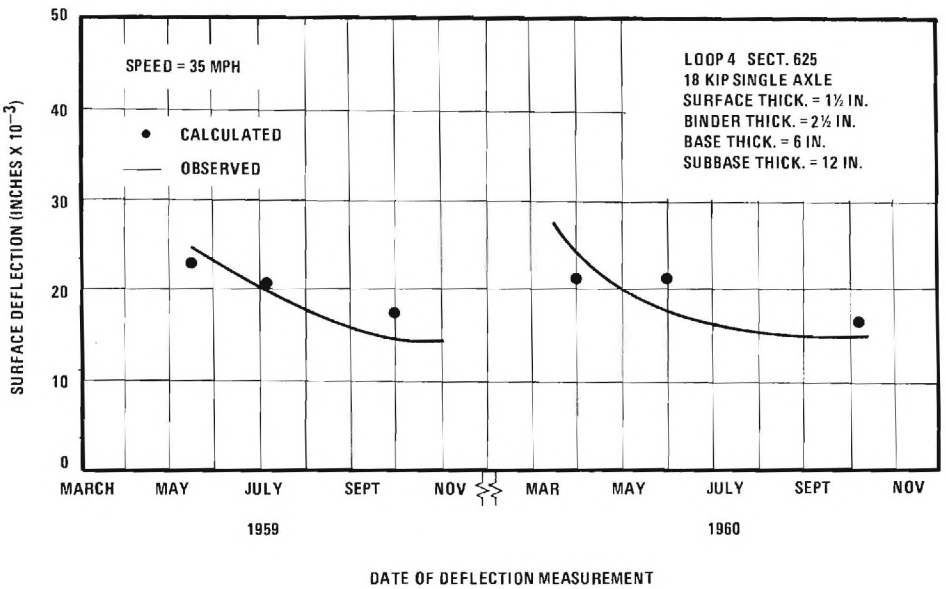

FIGURE 51. COMPARISON OF MEASURED AND CALCULATED SURFACE DEFLECTIONS-LOOP 4, SECTION 625, AASHO ROAD TEST

in the stabilized layers. The "S" shape response between tensile strain and temperature shown in Figures 52 and 53 was found to be typical for all of the crushed stone and asphalt concrete base sections studied.

Strains were also predicted for winter conditions when the base and in some sections the subbase and part of the subgrade had become frozen. A modulus of 1,500,000 psi was used in the analysis which corresponds to a representative value measured during this investigation for a frozen base course material. This analysis indicated that the strain levels associated with the deep depths of frost penetration which occurred during the winter months were so small that, considering the fatigue relationship for the appropriate temperature (Figures 55 through 57), no appreciable damage would have been caused to the pavement during this period. The fact that relatively little fatigue damage apparently occurs during the winter months is indirectly indicated since the Present Serviceability Index (PSI) remained for most sections relatively constant during this period. Kingham [21] has also independently reached a similar conclusion from a theoretical analysis of the AASHO Road Test results.

Development of Fatigue Curves

Laboratory fatigue test results on asphalt concrete and cement stabilized bases indicate that an approximately straight line relationship on a log-plot exists between the tensile strain and the corresponding number of load applications to failure [12, 13, 22]. Furthermore, a fatigue type of failure can be predicted using Minor's failure hypothesis for loading conditions which result in the occurence of different levels of tensile strain in the stabilized layers. According to Minor's failure hypothesis a state of failure is reached when

$$\sum_{i=1}^{m} \frac{n}{N} = 1.0 \quad \ldots \ldots \ldots \ldots \ldots \quad (4)$$

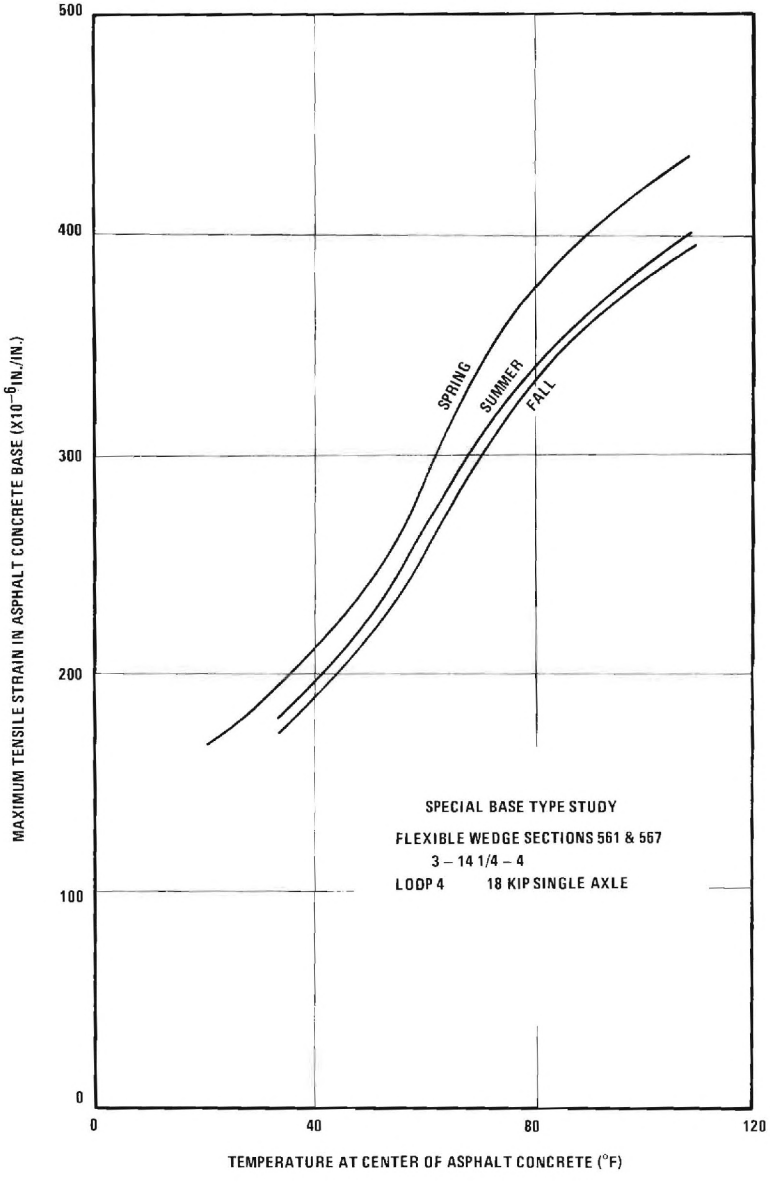

FIGURE 52. VARIATION OF MAXIMUM TENSILE STRAIN IN ASPHALT CONCRETE WITH TEMPERATURE AND SEASON.

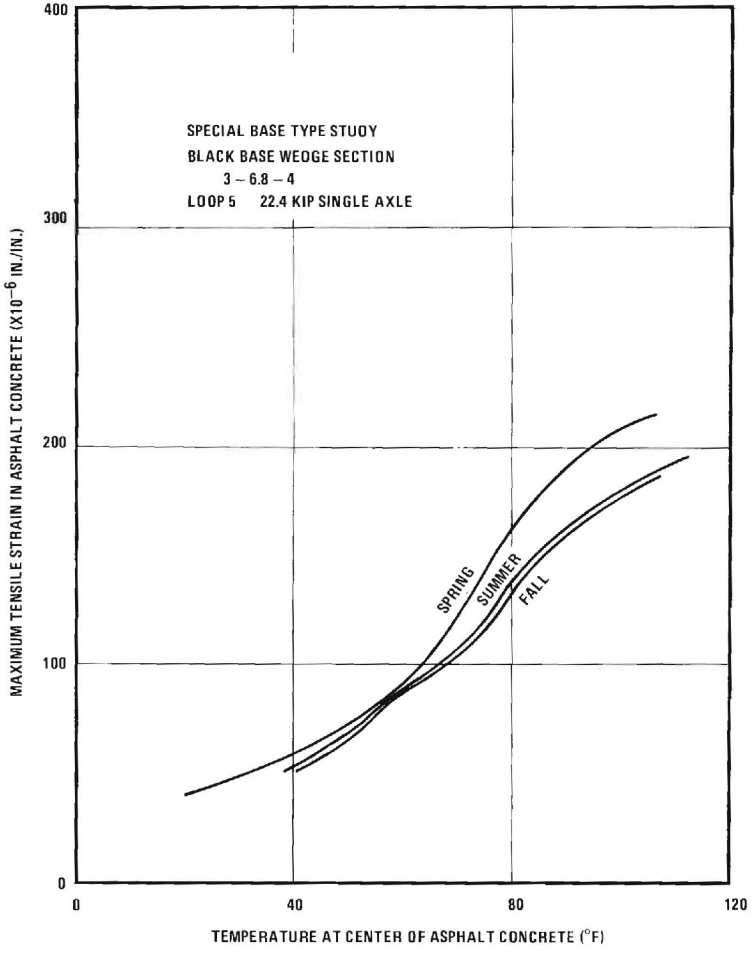

FIGURE 53. VARIATION OF MAXIMUM TENSILE STRAIN IN ASPHALT CONCRETE WITH TEMPERATURE AND SEASON.

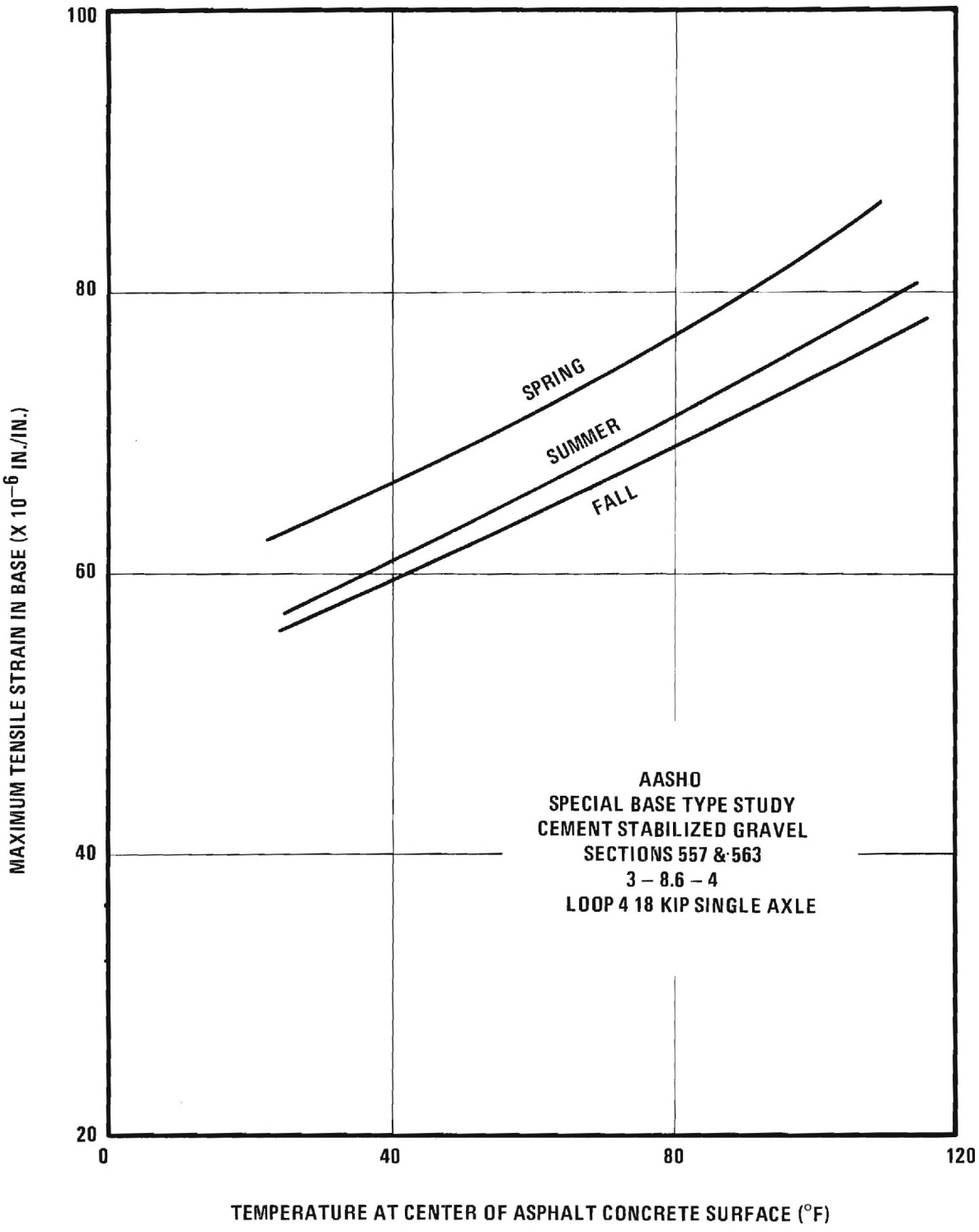

FIGURE 54. VARIATION OF MAXIMUM TENSILE STRAIN IN CEMENT STABILIZED GRAVEL WITH TEMPERATURE AND SEASON

Where n = number of load applications applied at a given strain level

N = number of load applications required to cause failure for the strain level corresponding to n

m = number of different strain levels at which loads are applied

For different temperatures the corresponding log-log relationship between strain and the number of repetitions to failure has been found in the laboratory to be approximately parallel for asphalt concrete. An increase in temperature results in a larger strain being required to cause failure for the same number of load repetitions. At the same time an increase in temperature also results in a lower modulus of the asphalt concrete and hence results in larger tensile strains. As a result the interaction between the fatigue life and the tensile strain is quite complicated.

Fatigue curves have been experimentally determined by a number of investigators [cf. 23, 24]. Of great practical significance is the fact that the method of loading the specimen (stress or strain controlled loading) has been found to greatly affect the fatigue life of asphalt concrete specimens [25]. Since the thickness of the asphalt layer is apparently related to the effective type of loading, the fatigue relationship would be expected to vary with the thickness of the stabilized layer. Furthermore, most laboratory fatigue tests have in the past been performed using primarily a uniaxial type of bending stress whereas the loading which occurs in the field actually causes a biaxial stress state in the layer. Finally, the effects that rutting, aging of the material and environmental factors have on fatigue life are certainly not clear at the present time. Because of these and other uncertainties, laboratory fatigue curves were not used directly to predict the fatigue response of the pavement structure. To overcome the limitations associated with the laboratory fatigue test results, a direct correla-

tion between fatigue life and actual field performance was considered to be necessary at this time in order to obtain reliable comparisons between the various pavement sections.

To establish a fatigue relationship for flexible pavement sections having both unstabilized and asphalt concrete stabilized bases, the results of laboratory fatigue tests [23, 24] were used to establish the slope and relative position of the fatigue curves corresponding to the range in temperatures occurring at the AASHO Road Test. Fatigue analyses of selected AASHO Road Test sections were then performed using a computer program to apply Minor's failure hypothesis. Failure of the pavement section was defined as occurring when the Present Serviceability Index of the pavement reached 2.5. The fatigue curves were shifted up or down as required in the direction of the strain axis (Figures 55 through 57) until Equation 4 was satisfied. Using this iterative approach a direct correspondence was obtained between the theoretical fatigue curves and actual field performance. The theoretical fatigue curves derived thus exhibited similar slopes and effects of temperature to those measured in the laboratory, but were adjusted to coincide with the observed behavior of selected AASHO Road Test pavement sections. Using this approach most of the good features of the laboratory tests were incorporated into the fatigue curves. Furthermore, the factors which at the present time are not thoroughly understood were also considered by using observed field performance results.

The fatigue relationship for the cement stabilized gravel base was found in a similar way to that used for the asphalt concrete. The fatigue response of this base was assumed to be independent of temperature, and therefore only a single fatigue curve was derived which was used for all temperatures.

The fatigue curves found in this way for selected pavement sections studied are shown in Figures 55 through 57. Figure 58 shows the relationship obtained from the asphalt

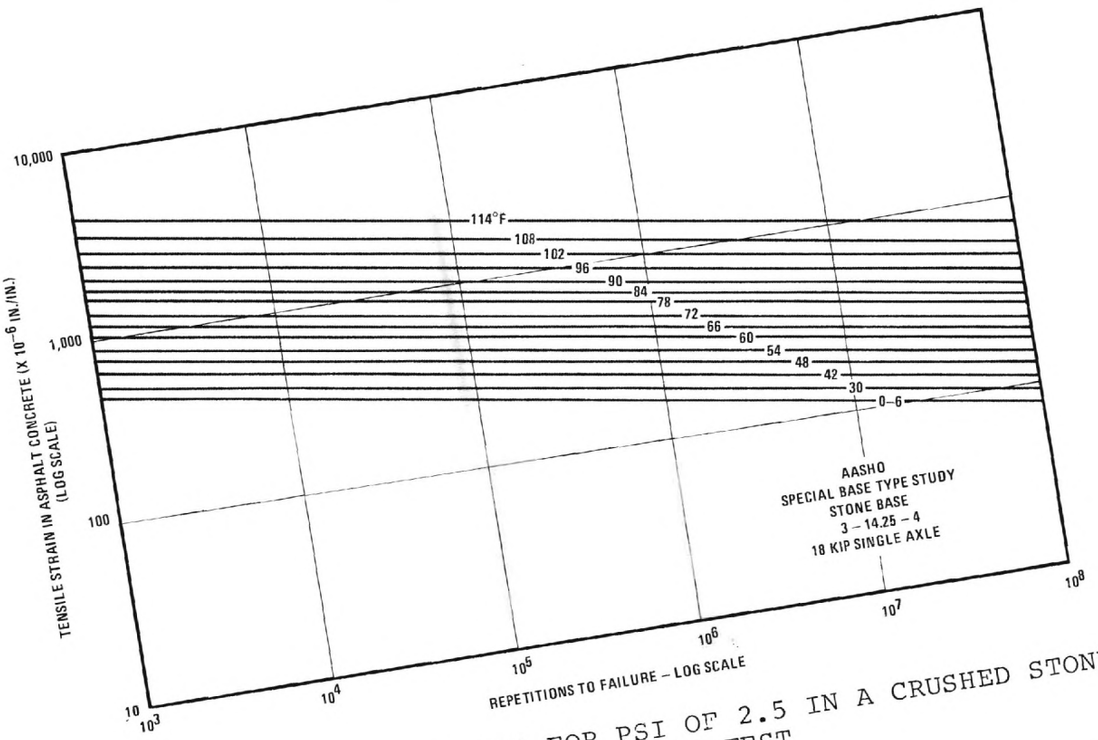

FIGURE 55. FATIGUE CURVES FOR PSI OF 2.5 IN A CRUSHED STONE BASE PAVEMENT-AASHO ROAD TEST

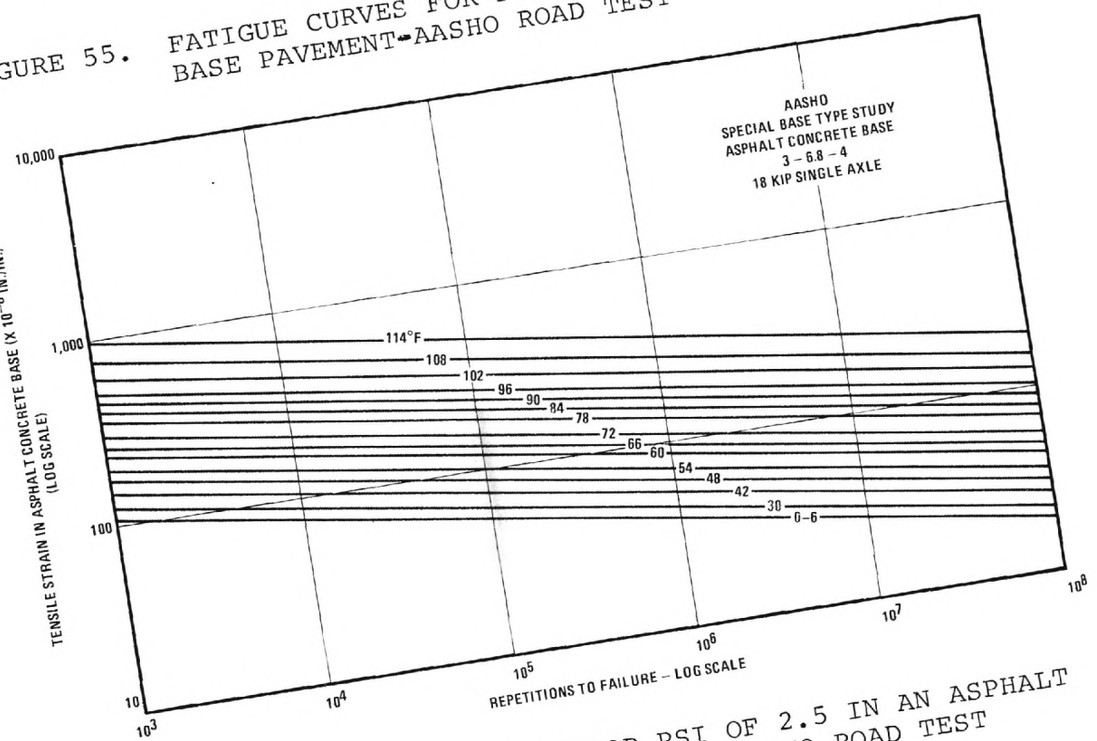

FIGURE 56. FATIGUE CURVES FOR PSI OF 2.5 IN AN ASPHALT CONCRETE BASE PAVEMENT-AASHO ROAD TEST

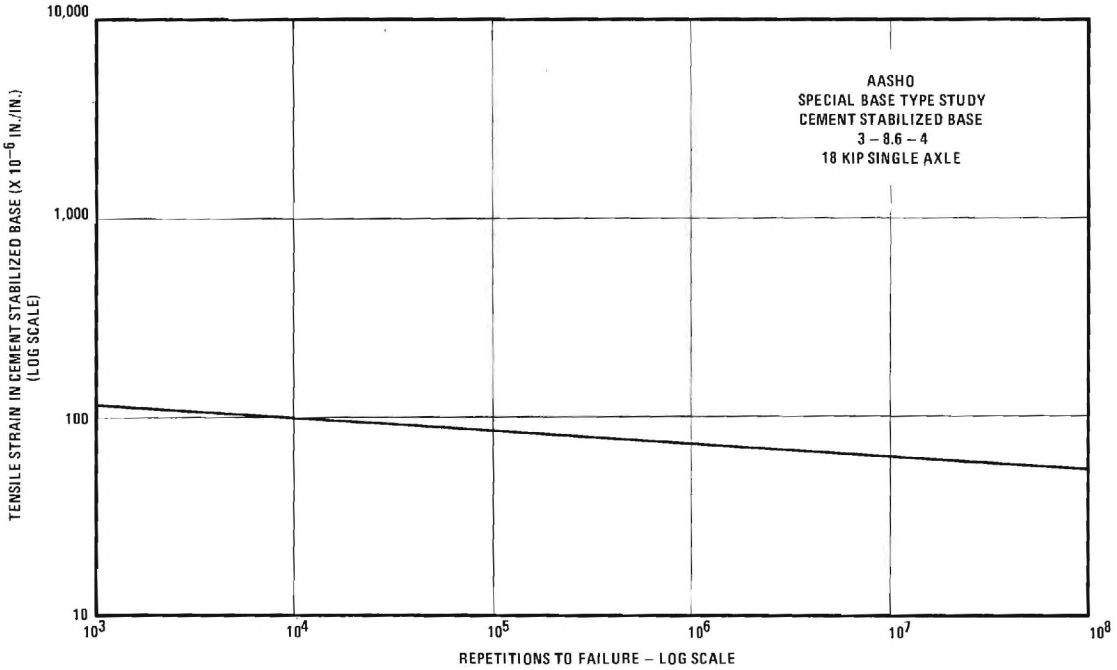

FIGURE 57. FATIGUE CURVE FOR PSI OF 2.5 IN A CEMENT STABILIZED BASE PAVEMENT-AASHO ROAD TEST

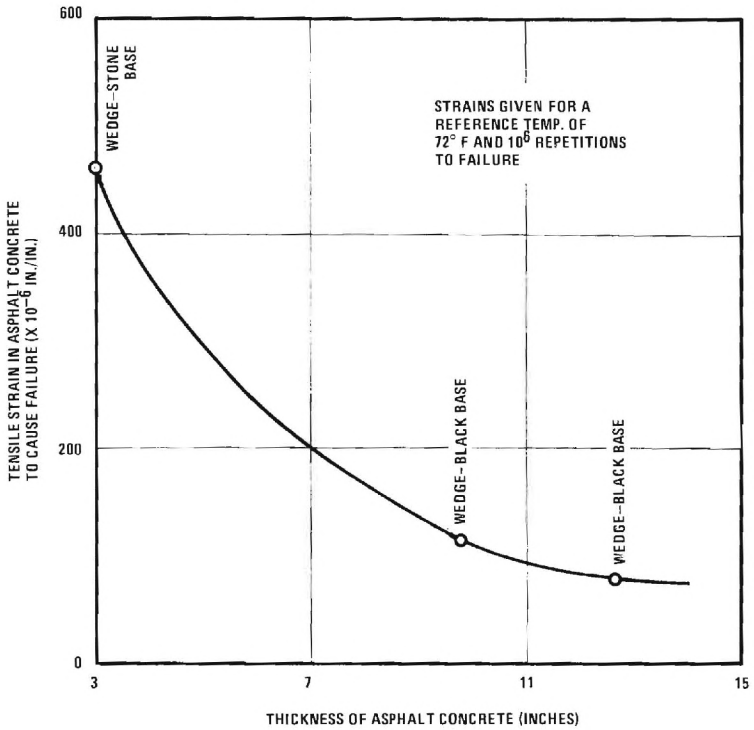

FIGURE 58. INFLUENCE OF ASPHALT CONCRETE SURFACING THICKNESS ON TENSILE STRAIN REQUIRED TO CAUSE FAILURE

concrete fatigue curves between the strain level required to cause failure at 10^6 repetitions and the asphalt concrete thickness for a reference temperature of 72° F. Failure of the AASHO pavement structures is defined as occurring at a Present Serviceability Index (PSI) value of 2.5. Figure 58 and also a comparison of the fatigue curves clearly shows that as the thickness of the asphalt concrete section increases, the allowable tensile strain in the base significantly decreases. In practical terms this means that each asphalt concrete thickness has a unique set of fatigue curves associated with that thickness. Due to the significant difference in these curves, the selection of the proper set of fatigue curves to match the asphalt concrete thickness is quite important in performing a reliable fatigue analysis.

CHAPTER VIII

DEVELOPMENT OF REQUIRED STRUCTURAL SECTIONS AND BASE COURSE COEFFICIENTS

In this section design coefficients for use in the AASHO Design Guide [30] are developed for base materials used on the micaceous silty sand and sandy silt subgrade soils found in the Piedmont Province of Georgia.

The design criterion developed using the results of the AASHO Road Test are used to predict fatigue life of the stabilized layers and to limit rutting in the subgrade to a tolerable level. Relative rutting in the base is considered using both the Rut Index concept and the more fundamental approach (Eqn. 3) which utilizes the theoretically calculated stress state in the base and the experimentally measured plastic strain properties of the base materials. The material properties used to evaluate the bases were obtained from the results of the repeated load triaxial tests, the fatigue tests performed on the stabilized base course materials, and the fatigue curves established from the study of the performance of the AASHO Road Test.

Design Parameters

The base course coefficients for all sections except the silty sand base were developed for 1,100,000 equivalent, 18,000 pound, single axle loads (one way) applied over a 20 year design life. The base course coefficient for the silty sand base was developed for 182,000 equivalent 18,000 pound single axle loads (one way) applied over a 20 year design period.

An examination of the long term rainfall data for the Atlanta area indicates that a dry season occurs during the summer and fall months with the rainfall during this period

being below the average for the year. To consider the seasonal effect of water content on the material properties, a wet season was considered to extend from December through May and a dry season to occur from June through November. The resilient modulus of the subgrade soil used for these two seasons is shown in Figure 61. The subgrade soil tested was randomly selected and is typical of the saprolitic, micaceous silty sands found in the Piedmont Province of Georgia. The results shown in Figure 61 indicate the resilient modulus decreases somewhat as the deviator stress increases. At a degree of saturation of 68% and a confining pressure of 3.5 psi the resilient modulus of the subgrade material was found to be 1920 psi at a deviator stress of 5.0 psi. The low modulus of these silty sands and sandy silt soils is partly due to their high resilience caused by a high mica content.

The elastic and plastic properties of the base materials previously presented in Chapters 4 and 5 were used in the analytical analysis. The asphalt concrete surfacing was assumed to have the same modulus-temperature relationship as that given in Figure 50.

Temperature Prediction

In order to perform a fatigue analysis on the structural pavement sections a prediction was made of the temperature variation with time in the asphalt concrete layers. For this study the method proposed by Barber [26] was selected to predict temperature variations with depth. This simplified solution assumes the pavement structure to conduct heat as a semi-infinite mass in contact with the air, and that the temperature variation within the mass varies as a sinusoid with time. The thermal properties of the asphalt concrete pavement layer are used in the analysis. Temperature distributions calculated using this method have been found to compare favorably with the actual measured temperature distribution in asphalt concrete pavement sections [15].

The climatogical information used to predict the temperature variation in the pavement sections studied in Georgia are the long term averages observed at the U. S. Weather Bureau Station in Atlanta, Georgia [27]. This climatogical data which is tabulated in Table 8 is representative of the long time average conditions found throughout the Piedmont Province of Georgia. Properties of the asphalt concrete used in the analysis are given in Table 9. Using these properties and the method proposed by Barber, the hourly temperatures were calculated with the aid of a computer program [51] using the long term weather data for each month of the year. Temperatures in the pavement structures were calculated from a depth of 0 to 12 inches in 2 inch increments for each hour of the day.

Table 9. Properties of the Asphalt Concrete Used In the Thermal Analysis

Unit Weight	148.0 pcf
Absorption of surface to solar radiation	0.95
Specific Heat	0.22 BTU/LB-°F
Thermal Conductivity	0.70 BTU-FT/FT^2-°F-HR

Criteria for Limiting Subgrade Rutting

The results from the Base Type Study conducted at the AASHO Road Test were used to develop subgrade stress criteria for limiting the amount of rutting which would occur in the subgrade. The results from the Base Type Study showed that for a constant thickness of the surfacing and subbase, a certain thickness of base existed for which little or no reduction in total surface rutting resulted for further increases in base thickness [14, Rpt. No. 5, p 79]. This significant finding indicates that for the sections studied and the AASHO subgrade soil, if the base thickness is made equal to or greater than

TABLE 8. LONG TERM CLIMATOGICAL WEATHER DATA FOR ATLANTA, GEORGIA

Month	Temperatures			Mean Wind Velocity (mph)	Solar Radiation (Langleys/day)	Cloud Cover
	Daily Max. (°F)	Daily Min. (°F)	Mean (°F)			
Jan.	52.0	37.3	44.7	10.7	215	0.48
Feb.	53.7	38.4	46.1	11.2	288	0.52
Mar.	60.3	42.5	51.4	11.1	386	0.57
April	70.1	50.2	60.2	10.2	477	0.65
May	78.9	59.2	69.1	8.6	535	0.69
June	85.7	67.5	76.6	7.9	545	0.67
July	87.0	70.7	78.9	7.4	525	0.62
Aug.	86.6	69.8	78.2	7.1	492	0.66
Sept.	81.8	64.3	73.1	8.0	414	0.64
Oct.	72.4	52.4	62.4	8.4	348	0.68
Nov.	60.9	41.5	51.2	9.1	260	0.59
Dec.	52.4	37.1	44.8	9.8	207	0.50

this limiting value, most of the rutting is contained within the pavement structure.

This limiting value of required base thickness to minimize subgrade rutting is summarized in Table 10 for pavements having a crushed stone base, cement stabilized gravel base, and asphalt concrete base; for each section the rest of the pavement structure is the same. The values of vertical subgrade stress calculated using layered theory which correspond to the limiting depths are also given in this table.

An analysis of rutting in selected unstabilized sections of the main factorial study at the AASHO Road Test indicates the total rut depth approached a constant value at a theoretical subgrade stress of about 4.0 psi for a 22.4 kip, single axle wheel loading. Since these sections used significantly thicker sand-gravel subbases and thinner crushed stone bases, the limiting value of vertical subgrade stress of 4.0 psi compares quite favorably with the corresponding value of 4.45 psi found for the thicker crushed stone base sections used in the Special Base Type Study.

The micaceous, silty sand subgrade soils of the Piedmont Province of Georgia, however, exhibit more plastic strain at the same stress level than the silty clay AASHO subgrade soil as illustrated in Figure 59. The calculated stress levels from the AASHO Base Type Study were therefore approximately corrected to Georgia subgrade conditions using the plastic stress-strain curves shown in Figure 59 so as to give the same amount of plastic subgrade strain in the micaceous silty sand as was determined for the AASHO silty clay subgrade. Due to the greater susceptibility of the micaceous silty sand to rutting, the allowable vertical subgrade stress on this soil was found to be less than on the AASHO subgrade. These subgrade stress criterion are summarized in Table 10 for each base type.

Table 10 shows that each type of base was found to have a different limiting subgrade stress. This can be partially

TABLE 10. REQUIRED BASE THICKNESS AND SUBGRADE STRESS TO MINIMIZE RUTTING IN THE AASHO SUBGRADE FOR A 22.4 KIP SINGLE AXLE LOADING(1)

Base Type	THICKNESS			Theoretical Subgrade Stress(3)	
	Surface (in.)	Base (in.)	Subbase (in.)	AASHO Silty Clay (psi)	Micaceous Silty Sand (psi)
Crushed Stone	3	14	4	4.45(2)	4.00
Asphalt Concrete	3	7	4	4.20	3.83
Cement Stabilized Gravel	3	10	4	2.81	2.53

1. Data From SPECIAL BASE TYPE STUDY, AASHO ROAD TEST.
2. An axle loading of 18 kips was found to be more critical for the unstabilized crushed stone base.
3. The subgrade stresses given are for an average asphalt concrete temperature of 75° F. The subgrade stresses given are the average of the spring and fall conditions.

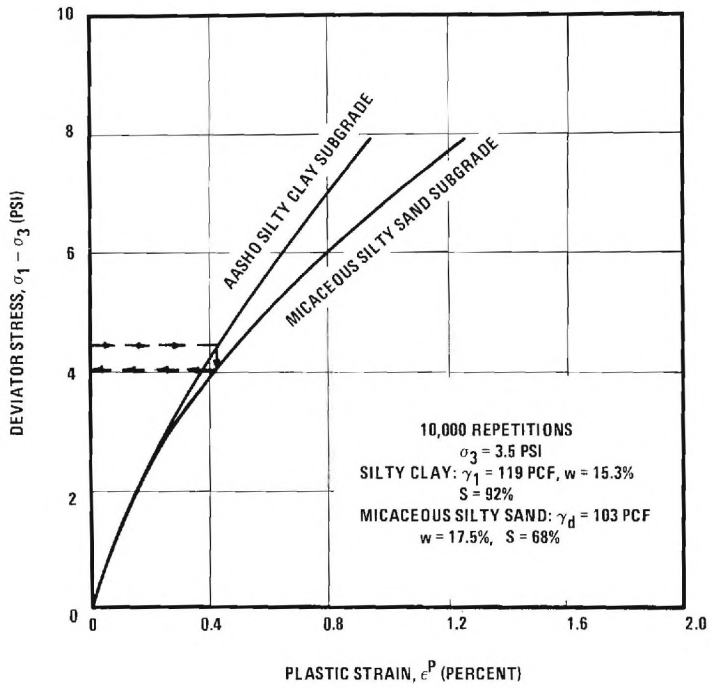

FIGURE 59. COMPARISON OF PLASTIC RESPONSE OF AASHO CLAY SUBGRADE AND A SILTY SAND SUBGRADE AFTER 10,000 REPETITIONS

explained since an unknown magnitude of error is associated with the theoretically calculated vertical subgrade stress. A gradual reduction in the stress distributing ability of the stabilized layers probably occurs with time. Since each pavement structure would undergo different amounts and types of deterioration with time, the actual stress distributing ability would also be expected to change with time differently for each base.

The criterion given in Table 10 are appropriate for use on pavement sections which are subjected to approximately 1,000,000 repetitions of an 18,000-22,400 pound, single axle load. Since the pavement sections used in Georgia having a silty sand base were to be designed for only 182,000 axle loadings, the subgrade stress should be increased to a value which would result in at least the same relative amount of rut depth in the subgrade at the end of its design life as occurs in the other structural sections.

Rut depth measurements made at the AASHO Road Test indicate that the rut depth after 1,000,000 repetitions is approximately twice the rut depth occurring after 180,000 repetitions [14, Rpt. 5, Figure 54]. Using this relationship and Figure 59, an approximate correction can be made to insure that equal rut depths in the subgrade would occur after any number of load applications. Similar correction factors were developed solely from the results of the repeated load triaxial tests performed on the micaceous silty sand subgrade soil. The resulting subgrade stress criterion obtained from these two approaches is summarized in Figure 60. A limiting vertical subgrade stress of 4.6 psi was selected from Figure 60 as being appropriate for design of sections subjected to 180,000 axle repetitions. This value of subgrade stress corresponds to the average of the field and laboratory criteria developed to yield a rut depth in the subgrade equal to that which should develop after 1,100,000 repetitions in the other type structural sections.

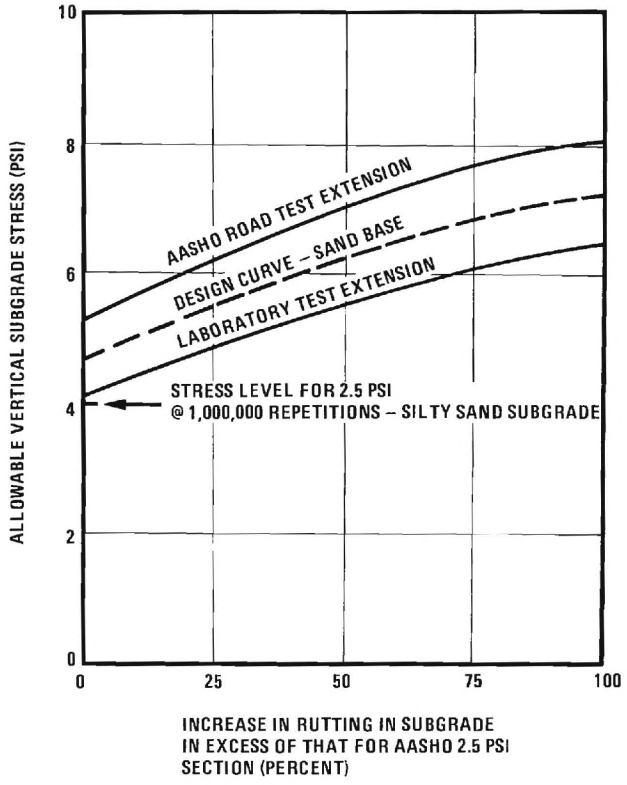

FIGURE 60. ALLOWABLE INCREASE IN VERTICAL SUBGRADE STRESS ON MICACEOUS SILTY SAND SUBGRADE FOR 180,000 REPETITIONS OF AN 18 KIP AXLE LOADING

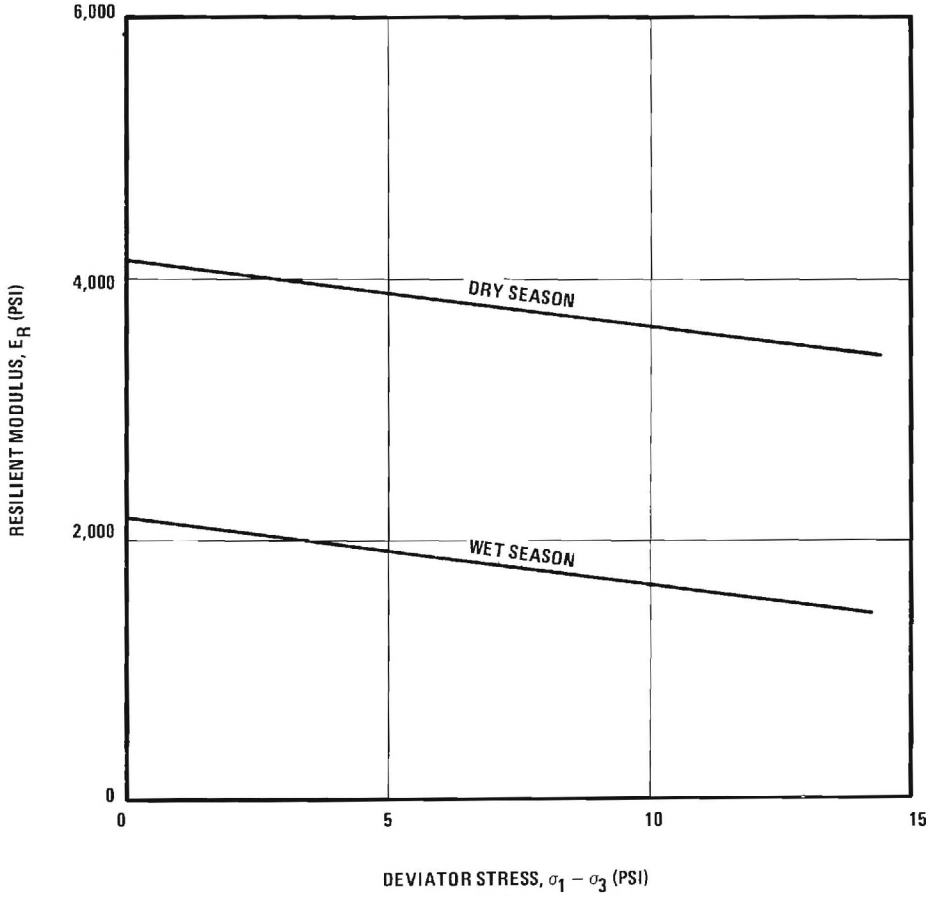

FIGURE 61. DESIGN RELATIONSHIP FOR RESILIENT MODULUS OF PIEDMONT MICACEOUS SILTY SAND SUBGRADE

Required Structural Sections

An asphalt concrete surfacing thickness was used in each structural section studied equivalent to that which would normally be selected following current State Highway Department of Georgia design practices. The thickness of the base was then varied until a structural section was found which was just sufficient to withstand the required number of equivalent 18 kip axle loads. The required base thickness for each of the seven base courses evaluated in this investigation were first determined using the SHELL 1963 DESIGN CHARTS FOR FLEXIBLE PAVEMENTS [31], the Asphalt Institute's design method [32], and the currently used State Highway Department of Georgia design method. The approximate average thickness of these sections was then used as a first trial for an analytical fatigue analysis. Failure in the structural sections corresponds to a Present Serviceability Index of 2.5. A subbase was not used in this analysis.

The set of fatigue curves used in this analysis were compatible with the asphalt concrete thickness and were generated using the relationship shown in Figure 58. After selecting a structural section based on fatigue, the vertical stress on the subgrade was then compared with the criterion given in Table 10 to insure that excessive rutting did not occur in the subgrade. Rutting in the base was considered separately for each material. The required structural sections calculated using this approach are summarized in Table 11 together with the controlling failure mode. The resilient moduli relationship used in the analysis for the subgrade is shown in Figure 61.

The theoretically required and recommended base course coefficients for use in the AASHO Design Guide are also given in Table 11. The base course coefficients given in Table 11 were calculated using a soil support value of 3.0, a regional factor of 1.85, and an asphalt concrete surface coefficient, a_1 of 0.44. These design parameters are typical values presently

used by the State Highway Department for flexible pavement design in the Piedmont Province of Georgia. Additional base course coefficients for assumed soil support values of 2.0 and 2.5 are given in Appendix B. In comparing the theoretical and recommended base course coefficients with the coefficients currently being used, it should be remembered that all the factors that account for differences in the required structural thickness were lumped into the theoretical and recommended base course coefficients.

The required base thicknesses for the crushed stone and soil-aggregate bases determined by the method developed in this report, the Shell method, and the Asphalt Institute method are all greater than the base thickness determined using the Georgia design approach. These results indicate that a need appears to exist for increasing the thickness of the base to more nearly equal the thicknesses determined by the method developed in this report in order to withstand the required number of axle loadings for Georgia environmental and subgrade conditions.

The required thickness of the structural section using the silty sand base was found to be 10 inches for 180,000 axle load applications. This thickness is slightly greater than the currently used value of 8 inches, but is less than that required by either the Shell or Asphalt Institute's methods. The controlling distress mode for this section was found to be rutting of the subgrade. The required thickness of 10 inches corresponds to a theoretical limiting vertical subgrade stress of 4.6 psi as obtained from Figure 60. If the allowable subgrade stress is increased to 5.3 psi which corresponds to the value indicated by the field test results the required base thickness would be 8 inches. The silty sand base section was found to be flexible enough so that the possibility is remote of fatigue distress occurring in the asphalt concrete surfacing. A comparative study indicates that the rutting in

the base of this section should be approximately 20 percent greater than that occurring in the crushed stone base sections after 1,100,000 axle loadings.

For the thickness of asphalt concrete surfacing used in the structural designs, the crushed stone and 20-80 soil-aggregate blend bases were assumed to have sufficient resistance to rutting when compacted to a minimum of 100 percent of GHD-49 or AASHO T-180 density. The laboratory results indicated that the 40-60 blend soil-aggregate bases, however, would exhibit appreciably more rutting. A comparison was made using Eqn. 3 of the relative rutting in a crushed stone base exhibiting average plastic strain properties and the 40-60 blend soil-aggregate bases. This study indicated that a minimum additional thickness of asphalt concrete of 2-1/2 to 3 inches would be required to reduce the amount of rutting in the 40-60 blend soil-aggregate bases to the same amount as would occur in the crushed stone base.

Although theory indicates that the rutting should not be excessive in this equivalent 40-60 blend base section, considerable caution should still be exercised in using 40-60 blends due to the effects of water, the wide variation in material properties observed for these materials, and other factors which at this time are neither well defined nor clearly understood.

The eight inch base thickness required for the full depth asphalt concrete section using the Georgia design method was found to be greater than both the Shell and Asphalt Institute's approach, but one inch less that that required by the new design method. Although the currently used asphalt concrete base thickness appears to be almost adequate, a small increase in base thickness may be necessary to prevent a premature fatigue failure.

This study indicated that 10 inches of cement stabilized gravel base material similar to that used at AASHO would be

required in Georgia to carry 1,100,000 18,000 pound, single axle loads. The AASHO cement stabilized base had an unconfined, 7 day field compressive strength of approximately 850 psi as compared to the design value of 500 psi currently being used in Georgia. As a result of this difference, the recommended base coefficients were adjusted downward so as to give a greater required base thickness.

The supplementary fatigue test results given in Table 12 and the repeated load tests results were used in adjusting the base coefficients to more nearly reflect the characteristics of the Georgia cement stabilized base materials. The base course coefficients for the cement stabilized materials were certainly the hardest to evaluate from the laboratory study and the extension of the AASHO Road Test results.

Table 11 shows that the theoretically required structural sections with the exception of the silty sand base are somewhat thicker than those predicted using the other design methods. The greater required thickness is at least partly a result of the very low dynamic modulus of elasticity observed for the micaceous silty subgrade soil. For the Shell Design method the required thicknesses were selected for a dynamic modulus of 4500 psi which corresponded to the worst subgrade conditions for which design curves were given. Had a lower dynamic modulus of elasticity been used in the Shell design which was closer to the value of moduli used in this investigation, undoubtedly a thicker structural section would have been required. Likewise, had a CBR value less than a value of 3.0 which was selected, the Asphalt Institute's method would also have required thicker structural sections. A lower support value would probably more accurately characterize the resilient behavior of these micaceous subgrade soils.

Discussion

The results of this investigation indicate that for the environmental and subgrade conditions the actual Soil Support

TABLE 11. SUMMARY OF REQUIRED STRUCTURAL SECTIONS AND BASE COURSE COEFFICIENTS FOR 18 KIP AXLE LOADING AND 20 YEAR DESIGN LIFE

Base No.	Base Type	A.C. Surface Thick. (in.)	Equiv. 18^k Axle Loads	Required Base Thickness[3] (in.)				Base Course Coefficients[1]			Primary Failure Mode
				Shell[2]	Asphalt[6] Inst.	Present GHD Design	Present[4] Study	Present GHD Design	Present Study	Recommended	
1	Silty Sand	3-1/2	0.182×10^6	15-1/2	12	9[7]	10	0.185[7]	0.165[8]	0.16[8]	Base/Subgrade Rutting
2	40-60 Soil-Aggregate	7	1.1×10^6	11	13	13 (4-1/2 in. surface)	14	0.18	0.088	.088[5]	Base Rutting/ Fatigue
3	Crushed Stone or 20-80 Soil-Aggregate	4-1/2	1.1×10^6	18	15	13	19	0.18	0.123	0.134	Fatigue
4	Full Depth Asphalt	4-1/2	1.1×10^6	5-1/2	7-1/2	8	9	0.30	0.267	0.267	Fatigue
5	Soil Cement	4-1/2	1.1×10^6	-	-	12	-	0.20	-	0.160	Fatigue
6	Cement Stabilized Soil-Aggregate	4-1/2	1.1×10^6	-	-	11	-	0.22	-	0.155	Fatigue
7	Cement Stabilized Crushed Stone	4-1/2	1.1×10^6	-	-	11	10[7]	0.22	0.242[7]	0.202	Fatigue

1. Base Course Coefficients for use in the AASHO Design Guide for Piedmont Province of Georgia are based on Soil Support Value of 3.0 and a Regional Factor of 1.85.
2. A dynamic resilient modulus of 4500 psi was used which is somewhat higher than the average value for the Piedmont subgrade soil tested.
3. A subbase was not used with any of these sections.
4. Theoretically required base course thicknesses or base course coefficients.
5. If 40-60 soil-aggregate bases are used a minimum of 7 to 7-1/2 in. of asphalt concrete should be placed over the base to prevent excessive rutting.
6. A CBR of 3.0 for the subgrade was assumed in the Asphalt Institute Design.
7. The 9 in. depth was determined by the GHD procedure; the GHD coefficient shown is backfigured for use in the AASHO method.
8. This coefficient compares favorably with the equivalent one presently used in the Georgia procedure; neither of these coefficients should be used for other wheel loads or directly compared with other materials.

Table 12. SUPPLEMENTARY FATIGUE TEST RESULTS FOR STABILIZED BASE MATERIALS

Base Description	Cement/Asphalt Content (%)	Age @ Testing	Applied Load (lbs) (1)	Repetitions to Failure
Cement Stabilized Silty Sand	6.0	13	1440	460
	6.0	14	1440	442
	6.0	90	1200	>660,000
40-60 Blend Soil-Aggregate	3.0	14	1200	1
	3.0	14	1200	1
Crushed Stone	3.9	14	1200	183
	3.9	14	1200	16
Standard A Binder Asphalt	5.0	14	1200	167,000
	5.0	14	1200	233,000 (2)

1. The load was applied by means of a 6 inch diameter, rigid loading plate.

2. This specimen had 0.75% (by weight of asphalt concrete) of KLING-BETA-LV anti-stripping additive produced by A. Z. Products, Inc., Carlstadt, New Jersey.

Value should probably be less than the currently used value of 3.0. Furthermore, the possibility also exists that the Regional Factor may not actually be 1.85. In order to be compatible with the proposed base course coefficients, the subbase and subgrade coefficients either need to be changed or else the Soil Support Value and/or Regional Factor should be adjusted. Probably an adjustment of the Soil Support Value and/or the Regional Factor with only minor relative changes in the base course coefficients themselves would constitute the most desirable and consistent approach.

Additional base course coefficients for Soil Support Values of 2.0 and 2.5 are given in Appendix B for a Regional Factor of 1.85. The Soil Support Values have been reduced so as to reflect more realistically the Piedmont Province micaceous subgrade soil characteristics. The base course coefficients given for each Soil Support Value all give the same required thickness and therefore are consistent with the environmental and subgrade conditions used to develop the required thicknesses given in Table 11.

The AASHO design method is based solely on statistical correlation studies of the observed field performance at the AASHO Road Test. This method has been extended to other environmental and subgrade conditions in a manner that is not entirely consistent with known mechanistic behavior and considerable subjective judgement is required to select both the regional factor and the Soil Support Value. The base course coefficients developed in this study on the other hand were derived by carefully considering the environmental and subgrade conditions in the Piedmont Province. In addition the observed pavement performance at the AASHO Road Test was incorporated directly into the procedure considering rationally the mechanistic behavior of the pavement under dynamic loading. This investigation has incorporated into the selection of the base course coefficients the good features of the AASHO Interim Design Method

(the observed performance of the AASHO Road Test) and also the specific effects on pavement performance of the environment and the resilient subgrade conditions of the Piedmont Province. Therefore, the adaptation of these coefficients for use in the Piedmont should improve the pavement design method.

Of considerable practical interest is the fact that the theoretical study indicated that 73 and 82 percent of the fatigue damage occurred to the full depth asphalt concrete and crushed stone sections, respectively, during the wet season of the year. This fact indicates the tremendous detrimental effect that water has on the performance of a flexible pavement structure, and emphasizes the need for properly controlling this water.

Due to the relatively spongy nature of the subgrade, rutting of the subgrade was found not to be a problem except in the section constructed with a silty sand base. Due to the resilient nature of the subgrade, stress at a given level tended to be spread out further than in a stiffer subgrade. For this reason, the stress level on top of the subgrade was low enough so that rutting in the subgrade in general should not be a problem in the proposed structural sections.

In selecting required structural thicknesses of layers it should be remembered that a relatively small increase in section thickness can result in a tremendous increase in the life of the section. As a result pavement life is very sensitive to base thickness as illustrated in Figure 62 for the crushed stone, asphalt concrete, and cement stabilized gravel bases used in the Special Base Type Study at the AASHO Road Test. To illustrate this point, an increase in thickness of the section with an asphalt concrete base shown in Figure 62 from 6 to 7 inches results in an increase in the required number of axle loads from 500,000 to 900,000 to result in a terminal Present Serviceability Index of 2.5. Similar relationships are shown on the figure to hold true for the other base types. Relatively small increases in thickness of both unstabilized bases shown

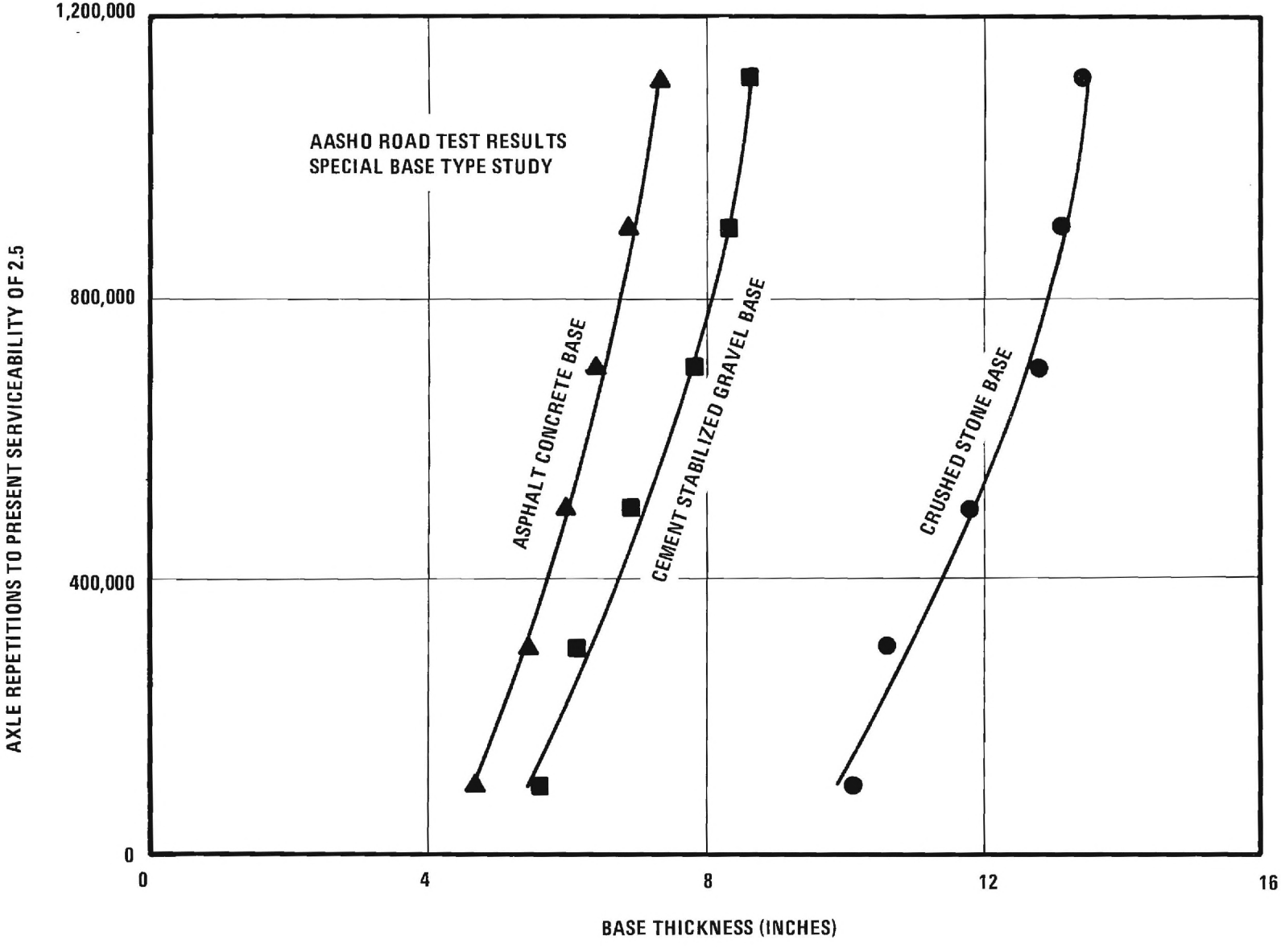

FIGURE 62. EFFECT OF BASE THICKNESS OF PAVEMENT LIFE FOR SELECTED BASE TYPES-3 IN. A.C. SURFACE AND 4 IN. SUBBASE

on the figure also result in very significant increases in useful life of the pavement structure before maintenance is required. In practical terms this means that if some of the presently used base layers are slightly on the thin side, as this study has indicated, the life of the pavement could be cut almost in half.

CHAPTER IX

RECOMMENDATIONS

The results of this investigation indicate a need for the modification and revision of several current specifications and design procedures involving base course materials. Consideration should be given to incorporating the following recommended changes into the specifications and design methods.

1. Serious consideration should be given to revising the presently used base course coefficients to more nearly reflect the environmental and subgrade conditions of the Piedmont Province as determined in this study. The somewhat thicker bases required for some sections using the recommended coefficients should significantly increase the life of the pavement. Consideration should be given to decreasing the presently used Soil Support Value of 3.0 to a lower value. If this is done the recommended base course coefficients should also be adjusted to reflect this change. Recommended base course coefficients are given in Table 11 and a discussion of the applicability of these coefficients are given in the latter two sections of Chapter 8.

2. The SPECIAL PROVISION dated November 18, 1970 and revised September 21, 1971 for the MODIFICATION OF ARTICLE 815.01 GRADED AGGREGATE allows up to 15 percent fines in a crushed stone base provided certain other requirements are satisfied. The results of this investigation indicate that the rut depth which will occur within an unstabilized crushed stone base is directly related to the percent of fines present. In order to reduce the amount of rutting which would occur in bases constructed of crushed stone the amount of fines used should be kept to the minimum amount which is practical. In order to keep the percent fines to a minimum, the contractor should not be permitted to blend appreciable amounts of pond screenings with the crushed stone in unstabilized bases.

   If the assumption is made that the base remains at

about the as compacted degree of saturation for all percent fines, a reduction of rutting in the base should be attained of approximately 20 percent if 10 rather than 15 percent fines is used as an upper limit in crushed stone bases. The permeability of the base, however, should increase by an estimated factor of probably 3 to 10 times if the reduction in fines is made. As a result of the considerably increased drainability of bases having the lower percent fines, the actual reduction in rutting should probably be even greater than 20 percent.

3. The results of this study and the AASHO Road Test indicate that for heavily trafficked pavements having a 4 to 5 inch asphalt concrete surfacing a minimum desirable thickness of top quality unstabilized base material is 12 to 14 inches above any subbase which might be used in the structural section.

4. The test results indicate that the use of an unstabilized 40-60 blend soil-aggregate in a base on the average would result in approximately 2.9 times greater rut depths in the base than for a 20-80 blend for approximately the same thickness of asphalt concrete surfacing.

   All base materials tested satisfied the STATE HIGHWAY DEPARTMENT OF GEORGIA STANDARD SPECIFICATIONS (January 1, 1966) and were designed using currently used methods. Therefore the presently used methods including the standard volume change test were apparently not effective in detecting the 40-60 blends which exhibited significant rutting characteristics. The repeated load triaxial test is recommended as an appropriate test method for evaluating these and other types of unstabilized base materials. Since these 40-60 soil-aggregate bases performed quite poorly, a revision of the specifications appears to be desirable to either exclude the use of these mixtures, or else appropriate tests should be performed which will detect undesirable blends which would result in excessive rutting. If blends are used which exhibit excessive rutting characteristics a thicker surfacing of asphalt concrete should be used to reduce the amount of rutting that will occur in the base. A detailed study of material and maintenance costs and anticipated traffic would be of tremendous benefit in selecting the optimum base design.

5. The two 20-80 blend soil aggregate bases exhibited good rutting characteristics when tested at the as compacted degree of saturation. Additional repeated load testing should probably be performed using several different soils to determine the variation in rutting characteristics with soil type. As previously discussed the effects of water on the soil-aggregate bases is probably greater than for a crushed stone base. The severity of this effect should be investigated further, and until this is done even 20-80 blends should probably not be used under conditions of poor drainage.

6. The very poor performance of the cement stabilized 40-60 blend soil-aggregate bases indicates a need exists for modifying the presently used procedure for selecting base materials for cement stabilization. Either a fatigue test using circular or beam specimens or else a simple bending test might be found to be suitable.

7. Pavement performance studies of cement stabilized bases [33] indicate that a minimum unconfined compressive strength in the field of 500 psi is required to insure a relatively maintenance free pavement life. Consideration should therefore be given to requiring a minimum laboratory design compressive strength of 600 to 650 psi to insure adequate field strength.

CHAPTER X

ADDITIONAL RESEARCH

Several areas which appear to warrant further study became apparent during the course of this investigation. The basic concepts were described in this report for a pavement design procedure which realistically considers both fatigue and rutting in the pavement structure. This method takes into account variations in traffic, climate and material properties. The approach described needs to be extended and developed into a formal, simplified design procedure. To do this evaluation studies would be desirable of existing pavements in Georgia to develop field performance criterion for local materials and environmental conditions. The criterion developed from the study could be related with experimentally measured material properties following a similar approach as was used in this investigation for the analysis of the AASHO Road Test results. The procedure for selecting required structural thickness then needs to be condensed into an engineering design approach which would be relatively simple to apply, but at the same time would adequately consider both fatigue and rutting of the pavement structure.

The State Highway Department of Georgia constructs a large number of asphalt concrete, soil-cement and cement stabilized soil-aggregate bases. Field performance and evaluation studies as well as extensive laboratory fatigue studies need to be performed on these materials to determine optimum designs.

This investigation readily demonstrated the important effects that degree of saturation has on the performance of unstabilized bases. Studies need to be conducted to determine the seasonal variation in the degree of saturation and its

and Displacements in Three Layer Viscoelastic Systems," Highway Research Board, HIGHWAY RESEARCH RECORD No. 345 (1971), pp. 45-57.

11. Romain, J. E., RUT DEPTH PREDICTION IN ASPHALT PAVEMENTS, Centre De Recherches Routieres, Research Report No. 150/JER/1969, Bruxelles.

12. Monismith, C. L., and Deacon, J. A., "Fatigue of Asphalt Paving Mixtures," PROCEEDINGS OF THE AMERICAN SOCIETY OF CIVIL ENGINEERS, Vol. 95, No. TE2, May (1969), pp. 317-346.

13. Monismith, C. L., and Kasianchuk, D. A., "Fatigue Consideration in the Design and Performance of Asphalt Pavements," Paper presented at the 1968 Canadian Technical Asphalt Association Conference, Ottawa, Canada (1968).

14. "The AASHO Road Test," Highway Research Board, SPECIAL REPORT 61, (1961).

15. Kasianchuk, D. A., FATIGUE CONSIDERATIONS IN THE DESIGN OF ASPHALT CONCRETE PAVEMENTS, Ph.D. Thesis, University of California, Berkeley (1966).

16. Busching, H. W., Roberts, F. L., Rostron, J. R., and Schwarts, A. E., AN EVALUATION OF THE RELATIVE STRENGTH OF FLEXIBLE PAVEMENT COMPONENTS, Clemson University, Research Project No. 522 (1971).

17. Seed, H. B., Chan, C. K., and Lee, C. E., "Resilience Characteristics of Subgrade Soils and Their Relation to Fatigue Failures in Asphalt Pavements," INTERNATIONAL CONFERENCE ON THE STRUCTURAL DESIGN OF ASPHALT PAVEMENTS PROCEEDINGS, University of Michigan, Ann Arbor (1962), pp. 611-636.

18. Duncan, J. M., Monismith, C. L., and Wilson, E. L., "Finite Element Method of Analysis of Pavements," Highway Research Board, HIGHWAY RESEARCH RECORD No. 228 (1968), pp. 18-33.

19. Kallas, B. F., and Riley, J. C., "Mechanical Properties of Asphalt Pavement Materials," SECOND INTERNATIONAL CONFERENCE ON THE DESIGN OF ASPHALT PAVEMENTS, University of Michigan, Ann Arbor (1967).

20. Coffman, B. S., Kraft, D. C., and Tamayo, J., "A Comparison of Calculated and Measured Deflections for the AASHO Road Test," PROCEEDINGS OF THE ASSOCIATION OF ASPHALT PAVING TECHNOLOGISTS, Vol. 33 (1964), pp. 54-90.

21. Kingham, I. N., Oral Communication, January (1971).

22. Pretorius, P. C., and Monismith, C. L., "Fatigue Crack Formation and Propagation in Pavements Containing Soil Cement Bases," Paper Prepared For Presentation at the 1972 Highway Research Board Meeting, Washington, D. C.

23. Finn, F. N., FACTORS INVOLVED IN THE DESIGN OF ASPHALTIC PAVEMENT SURFACES, NCHRP Report 39 (1967).

24. Pell, P. S., and Taylor, I. F., "Asphalt Road Materials In Fatigue," PROCEEDINGS OF THE ASSOCIATION OF ASPHALT PAVING TECHNOLOGISTS, Vol. 38 (1969), pp. 371-422.

25. Monismith, C. L., ASPHALT MIXTURE BEHAVIOR IN REPEATED FLEXURE, Soil Mechanics and Bituminous Materials Research Laboratory, Rpt. No. TE 66-6, University of California, Berkeley (1966).

26. Barber, E. S., "Calculation of Maximum Pavement Temperatures From Weather Reports," HIGHWAY RESEARCH BOARD, Bulletin No. 168 (1957).

27. LOCAL CLIMATOLOGICAL DATA ANNUAL SUMMARY WITH COMPARATIVE DATA, ATLANTA, GEORGIA, U. S. Department of Commerce, Washington, D. C. (1970).

28. MIX DESIGN METHODS FOR ASPHALT CONCRETE, The Asphalt Institute, Manual Series No. 2 (MS-2), (1963).

29. Sherman, G. B., In Situ Materials Variability, STRUCTURAL DESIGN OF ASPHALT CONCRETE PAVEMENT SYSTEMS, Proceedings of a Workshop Sponsored by the Federal Highway Administration, Austin, Texas, (1970).

30. AASHO Committee On Design, AASHO DESIGN GUIDE FOR THE DESIGN OF FLEXIBLE PAVEMENT STRUCTURES, (1961).

31. SHELL 1963 DESIGN CHARTS FOR FLEXIBLE PAVEMENTS, Shell International Petroleum Co., London, England (1965).

32. THICKNESS DESIGN, The Asphalt Institute, Manual Series No. 1 (MS-1), (1965).

33. Zube, E., Gates, C. G., Shirley, E. C., and Munday, H. A., "Service Performance of Cement Treated Bases As Used in Composite Pavements," HIGHWAY RESEARCH BOARD, Record 291 (1969), pp. 57-69.

APPENDIX A

GLOSSARY OF TERMS

GLOSSARY OF TERMS

1. Rutting - Rutting is the gradual accumulation of permanent deformations in the pavement structure due to the repeated application of wheel loadings. The pavement structure is assumed to be designed so that appreciable rutting (a bearing capacity failure) does not occur under the application of a single wheel load.

2. Nonlinear, Elastic Layered Theory - An analytical theory used to predict stresses, strains and displacements in layered pavement systems due to the application of a wheel load on the surface. Experimentally measured values of the resilient moduli, E_r of each layer are used in the analysis.

3. Fatigue Failure - The failure of a stabilized layer due to the repeated flexing of that layer resulting from the passage of a large number of wheel loads. At first fatigue failure shows up on the surface of the pavement in the form of cracks. As time progresses, the cracks become more noticeable, and the presence of these cracks can lead to rutting.

4. Fatigue Test - The fatigue test is performed on either a circular or beam specimen of stabilized material by repeatedly flexing it until failure occurs. Specimens may either be supported on a rubber or spring base, or else the specimens may be tested in an unsupported condition. Circular specimens and a rubber base were used in this investigation.

5. Fatigue Curves - A family of curves relating the number of repetitions of loading required to cause a fatigue failure in a stabilized layer with the tensile strain and temperature in that layer.

6. Minor's Law - Minor's Law was proposed many years ago in the aircraft industry for estimating the fractional part of the total fatigue life of a material which has been used up due to the application of a given number and magnitude of load repetitions. The applied load level need not be sufficient to cause total failure but some permanent damage is caused by each application of load. Minor's Law has been shown to be reasonably valid for predicting fatigue damage of asphalt concrete stabilized layers.

7. Repeated Load Triaxial Test - In this test a cylindrical shaped specimen of material is placed in a conventional triaxial cell. The specimen is subjected to a constant, all around confining pressure, σ_3. After the specimen has consolidated under this loading, a pulsating (repeated) deviator stress, $\sigma_1 - \sigma_3$ is applied axially to the specimen. The data obtained from this test is given below:

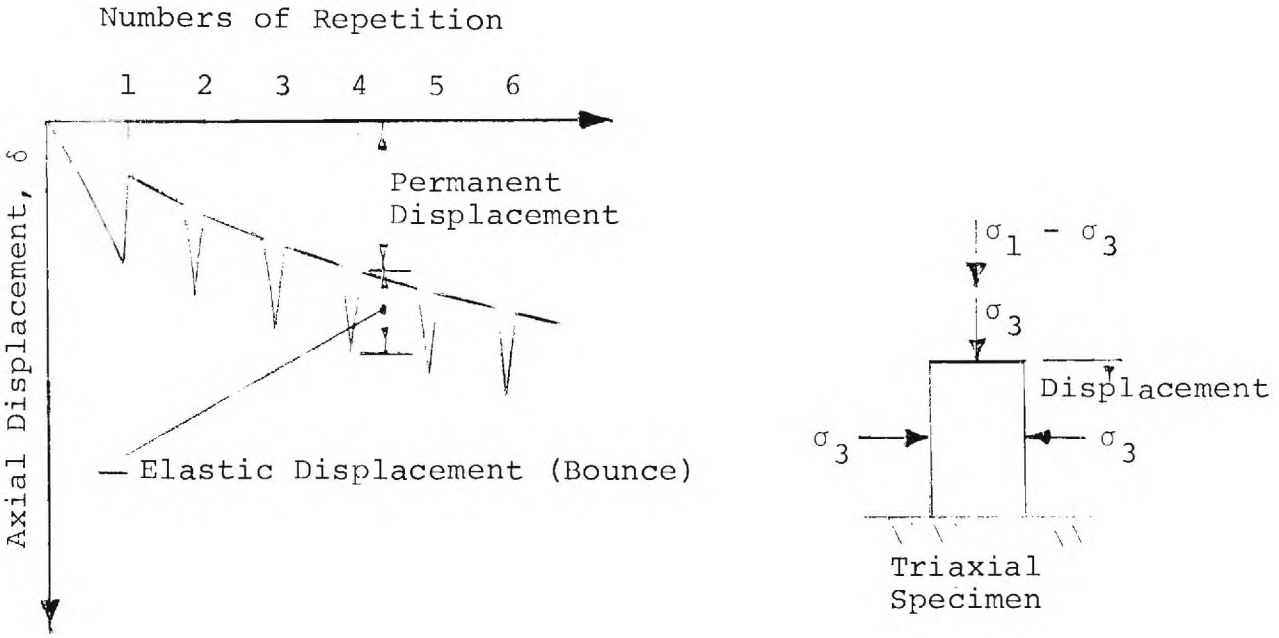

8. Resilient Strain, ε_r - The elastic deformation or "bounce" of a cylindrical specimen divided by the distance over which the bounce is measured. This test is performed in the triaxial cell for a selected number of load repetitions (10,000 in this investigation).

9. Resilient Modulus, E_r - The repeated deviator stress, $\sigma_1 - \sigma_3$ applied to a cylindrical triaxial specimen divided by the resilient strain, ε_r. From this definition it follows that the resilient modulus is a secant modulus.

10. Plastic Strain - The permanent deformation which has developed in the cylindrical triaxial specimen after a given number of load applications divided by the distance over which the deformation was measured.

11. Rut Index - A parameter developed in this report for estimating the relative rut depth which will develop in bases having the same thickness and reasonably similar material characteristics. The Rut Index is calculated from data

obtained from two specimens of material using the repeated load triaxial apparatus. As applied in this report, the Rut Index is evaluated in one test using a deviator stress ratio of 6.0 and in the other test using a stress ratio of 3.5. Both tests are performed at a confining pressure of 10 psi. The Rut Index is then defined as the sum of the two measured plastic strains at the end of 100,000 repetitions multiplied by 10,000. The Rut Index is approximately proportional to the rut depth which should develop in the layer.

12. Present Serviceability Index (PSI) - The Present Serviceability Index is a parameter developed at the AASHO Road Test to give a subjective rating of the present condition of a pavement from the users standpoint. The PSI ratings vary from 0 to 10 with a value of 10 indicating the best pavement condition theoretically possible.

13. Linear Variable Differential Transducer (LVDT) - A small, cylindrical shaped electronic device used for electrically measuring linear displacements in the repeated load triaxial test and the fatigue test.

APPENDIX B

BASE COURSE COEFFICIENTS

TABLE B-1. THEORETICALLY REQUIRED BASE COURSE COEFFICIENTS

	Base Type	Support Value (S)	Required Base Thickness (in.)	Theoretical Base Coefficient
1.	Silty Sand	2.0	10	0.213[1]
		2.5		0.188
		3.0		0.165
2.	40-60 Soil Aggregate	2.0	14	0.134
		2.5		0.111
		3.0		0.088
3.	Crushed Stone or 20-80 Soil Aggregate	2.0	19	0.156
		2.5		0.138
		3.0		0.123
4.	Full Depth Asphalt	2.0	9	0.340
		2.5		0.302
		3.0		0.267
5.	Cement Stabilized	2.0	10	0.298
		2.5		0.264
		3.0		0.242

1. This coefficient compares favorably with the equivalent one presently used in the Georgia procedure; neither of these coefficients should be used for other wheel loadings or directly compared with other materials.